République Algérienne Démocratique et Populaire
Ministère de l'Enseignement Supérieur et de la Recherche Scientifique

Ecole Nationale Polytechnique
Département d'Automatique
Laboratoire de Commande des Processus

Mémoire de Magister en Automatique

Option : **Informatique Industrielle et Robotique**

Présenté par :
KHODJA Mohammed Abdallah
Ingénieur d'état en Electronique de l'Université de M'sila

Thème

TYPE-2 FUZZY LOGIC CONTROLLER FOR ROBOT MANIPULATOR

Devant le jury suivant :

Président	:	M.S. BOUCHERIT,	Professeur à l'ENP.
Rapporteur	:	M.TADJINE,	Professeur à l'ENP.
Examinateurs	:	F.BOUDJEMA,	Professeur à l'ENP.
		H.CHEKIREB,	Professeur à l'ENP.

Dimanche 06 Février 2011

Mémoire préparée au sein du Laboratoire de Commande des Processus de l'ENP
10, avenue Hassen Badi BP 182 El-Harrach 16200 Alger

Dedication

إهداء

الْحَمْدُ لِلَّهِ الَّذِي أَرْسَلَ رَسُولَهُ بِالْهُدَى وَدِينِ الْحَقِّ؛ لِيُظْهِرَهُ عَلَى الدِّينِ كُلِّهِ وَكَفَى بِاللَّهِ شَهِيدًا. وَأَشْهَدُ أَنْ لَا إِلَهَ إِلَّا اللَّهُ وَحْدَهُ لَا شَرِيكَ لَهُ؛ إِقْرَارًا بِهِ وَتَوْحِيدًا. وَأَشْهَدُ أَنَّ مُحَمَّدًا عَبْدُهُ وَرَسُولُهُ. صَلَّى اللَّهُ عَلَيْهِ وَعَلَى آلِهِ وَسَلَّمَ تَسْلِيمًا مَزِيدًا.

أما بعد:

أهدي هذا العمل المتواضع إلى أبي وأمي إلى من سهرا وإجتهدا في تربيتي وتعليمي بفضل الله عز وجل

وإلى أخواتي مريم ، سمية و أخي زكرياء

وإلى زوجتي أم أميمة التي صبرت معي في كل المحن والصعاب وكانت بفضل الله عز وجل ثم بصبرها على غيابي وسفري بسبب الدراسة عونا لي في مرحلة ماجستير

كما أهديه إلى فلذتي كبدي ابنتي أميمة وابني سعد

وإلى كل العائلة حفظهم الله جميعا وإلى كل أصدقائي خصوصا صديقي وجاري و زميلي في المرحلة الدراسية من التحضيري إلى الدراسات العليا عادل عطوي.

سبحانك اللهم وبحمدك نشهد أن لا إله إلا أنت نستغفرك ونتوب إليك.

Acknowledgments

شكروعرفان

أَبْدَأُ بِاسْمِ اللَّــهِ مُسْــتَعِينَا راض بـــه مـــدبر مُعِينَـــا
وَالْحَمْدُ لِلَّهِ كَمَـا هَـدَانَا إِلَى سَـبِيلِ الْحَـقِّ وَاجْتَبَانَـا
أَحْمَدُهُ سُبْحَانَهُ وَأَشْـكُرُهْ وَمِنْ مَسَاوِي عَمَلِي أَسْـتَغْفِرُهْ
وَأَسْتَعِينُهُ عَلَى نَيْـلِ الرِّضَـا وَأَسْتَمِدُّ لُطْفَهُ فِي مَا قَضَـى
وَبَعْدُ : إِنِّي بِـالْيَقِينِ أَشْـهَدُ شَهَادَةَ الْإِخْلَاصِ أَنْ لَـا يُعْبَـدُ
بِالْحَقِّ مَأْلُوهٌ سِـوَى الـرَّحْمَنِ مَنْ جَلَّ عَنْ عَيْبٍ وَعَنْ نُقْصَانِ
وَأَنَّ خَيْرَ خَلْقِـهِ مُحَمَّـدَا مَنْ جَاءَنَا بِالْبَيِّنَـاتِ وَالْهُـدَى
رَسُولُهُ إِلَى جَمِيـعِ الْخَلْـقِ بِالنُّورِ وَالْهُدَى وَدِيـنِ الْحَـقِّ
صَلَّى عَلَيْهِ رَبُّنَا وَمَجَّدَا وَالْآلِ وَالصَّحْبِ دَوَامًا سَرْمَدَ

أما بعد:

عَنْ أَبِي هُرَيْرَةَ، عَنِ النَّبِيِّ صَلَّى اللهُ عَلَيْهِ وَسَلَّمَ قَالَ: «لَا يَشْكُرُ اللَّهَ مَنْ لَا يَشْكُرُ النَّاسَ» رواه أحمد.

عَنْ عَائِشَةَ، أَنَّ رَسُولَ اللَّهِ صَلَّى اللهُ عَلَيْهِ وَسَلَّمَ، قَالَ: «مَنْ أُتِيَ إِلَيْهِ مَعْرُوفٌ، فَلْيُكَافِئْ بِهِ، وَمَنْ لَمْ يَسْتَطِعْ، فَلْيَذْكُرْهُ، فَمَنْ ذَكَرَهُ، فَقَدْ شَكَرَهُ» رواه أحمد.

أشكر الله عز وجل وأحمده حمدا كثيرا طيبا مباركا أن وفقني لإتمام هذه المذكرة ثم أشكر من سخره الله عز وجل ليكون سببا في هذا الإنجاز وهو الأستاذ المشرف طجين محمد الذي كان موجها وناصحا ومرشدا طيبا

كما أتقدم بجزيل الشكر إلى الأستاذ بوشريط محمد الذي كان نعم الأستاذ فهو ذو مكانة خاصة وتقديركبير عند كل الطلبة، استفدنا منهم الكفاءة العلمية و الأخلاق الفاضلة والتواضع لله عز وجل فقد غرسوا في الطلبة حب البحث العلمي والاهتمام بما هو أنفع وكل أساتذة قسم الآليات يتصفون بهذه الميزات الحميدة، وهذا واقع عايناه معهم وسمعناه بشهادة كثير من الطلبة الذين التقينا بهم من مناطق متعدد من أنحاء الوطن أسأل الله عز وجل أن يثبتهم و يوفقهم لما فيه الخير والصلاح

، كما أتقدم بجزيل الشكر للأستاذ بركات سعيد بجامعة المسيلة الذي قدم لي يد العون، كما أتقدم بجزيل الشكر إلى مدير وحدة الإنتاج مصنع الأنابيب بالمسيلة، بعلي إبراهيم خريج المدرسة الوطنية العليا متعددة التقنيات تخصص هندسة مدنية، الذي كان محفزا معنويا وماديا و المشجع لربط الجامعة الجزائرية بالمصنع والإنتاج.

وفي الأخير أقول لهم جميعا بارك الله فيكم وادعوا الله عز وجل أن يجازيهم خير الجزاء.

سبحانك اللهم وبحمدك نشهد أن لا إله إلا أنت نستغفرك ونتوب إليك.

أَخِـيْ لَـنْ تَنَـالَ «الْعِلْـمَ» إِلاَّ بِـسِتَّةٍ سَـأُنْبِيْكَ عَـنْ تَفْـصِيْلِهَا بِبَيَـانِ:
ذَكَـاءٌ، وَحِـرْصٌ، وَاجْتِهَـادٌ، وَبُلْغَـةٌ وَصُـحْبَةُ أُسْـتَاذٍ، وَطُـوْلُ زَمَـانِ

Abstract

ملخص:

في هذه الأطروحة نستعمل نظرية المنطق المبهم من نوع 1 ونوع 2 من أجل التحكم في الذراع آلي، نهتم بدراسة التحكم بواسطة المنطق المبهم نوع 1 وتطبيق هذه التقنية على الذراع الآلي، ثم دراسة التحكم بواسطة المنطق المبهم من نوع 2 وتطبيق هذه التقنية على الذراع الآلي ثم عرض مقارن بين التقنيتين في حالتين للذراع الآلي الحالة المثالية والحالة الحقيقية للذراع الآلي باستعمال مسارين في كل حالة (مسار دائري، مسار ليهي).

كلمات مفتاحيه: الذراع الآلي PUMA560، المتحكم المبهم نوع 1، المتحكم المبهم نوع 2.

Abstract:

This memory describes a fuzzy type-1 and type-2 position control scheme designed for manipulator robot. The first is the fuzzy logic type-1 and the second is the fuzzy logic type-2. We focus our interest to study the performances of fuzzy logic controller type-1, and then the application of this control to the manipulator robot PUMA560 3DOF, the second controller type-2 will be studied and will be applied to the manipulator robot PUMA560 3DOF.Finally we present a comparative study between these strategies; the computer simulation results on three links robot manipulators, in two cases ideal and noisy system with two trajectory for each one (Circle trajectory, LEAHY trajectory).

Key word: Manipulator robot PUMA560, fuzzy logic controller type-1, fuzzy logic controller type-2.

Résumé:

Ce mémoire consiste à présenter deux types de commande floue d'un robot manipulateur PUMA, le premier est la commande floue type-1, et le deuxième est la commande floue type-2. Nous intéressons à l'évaluation des performances de la commande floue type-1, puis l'application de cette technique au robot manipulateur PUMA 3DDL, la deuxième technique de commande floue type-2 est appliquée au robot manipulateur PUMA 3DDL, enfin nous présentons une étude comparative des deux stratégies de commande, deux cas idéal et avec bruit avec deux trajectoires pour chaque cas (trajectoire cercle, trajectoire LEAHY).

Mot clé : robot manipulateur PUMA560, Régulateur flou Type-1, Régulateur flou Type-2.

TABLE OF CONTENTS

LIST OF FIGURES

LIST OF TABLES

General Introduction

The use of industrial robots became identifiable as a unique device in the 1960s. Since then, their field of application evolved from rather simple tasks like welding and painting to those requiring more precision, such as assembly tasks.

Control theory provides tools for designing and evaluating algorithms to realize desired motions or force application. The methods of linear control are not well suited for the control problem of robotic arms. This is due to the fact that robotic arms constantly move among widely separated regions of their workspace such that no linearization valid for all regions can be found. On the other hand, nonlinear control methods used in robot arms' applications should however face the major difficulty resulting from the dynamic modeling of robots, the indetermination of their parameters [3]. Preferred methods are those which reduce or eliminate the undesired effects generated by this indetermination. Another difficulty in robot arm control is the coupling effects of the coriolis and centrifugial forces that might be canceled in a single axis mode operation where the joints are activated sequentially. Existing methods of nonlinear control are also used in robotics in order to eliminate the above mentioned coupling effect like the Individual Joint PID control method [3] and the PD-plus-gravity control method [3].

Among the recent control methods, fuzzy control methods grab nowadays the attention of many researchers. In fact, these methods do not require the knowledge of the dynamic model of the controlled system. This feature becomes one of the major importances when dealing with complex nonlinear systems. Moreover, the dynamic modeling of robot arms shows a dependency on their mechanical parameters, subject to lifetime modifications (friction factors affected by the abuse of joints), and on their dynamical parameters that vary with the performed task (centers of gravity of the links affected by tool's replacements). These considerations also give advantage to fuzzy control methods on other nonlinear methods as a result of their robustness towards perturbations affecting the system.

The first fuzzy logic controller was introduced by Mamdani in 1974 [7]. It is equivalent to two-input fuzzy PI controllers, where error and change of error were used as the inputs of the inference system. Mamdani's work also introduced the most common and robust fuzzy reasoning method, called Zadeh–Mamdani min– max gravity reasoning. Different comparative studies, like [5], prove that Zadeh– Mamdani min–max gravity scheme is the best reasoning scheme if the nonlinearity variation is a main concern.

Although control methods, especially nonlinear control methods, had greatly evolved, the proportional-integral-derivative (PID) control method is still widely used in all domains [2]. The success of the PID control is attributed to its simplicity (in terms of design and tuning) and to its good performance in a wide range of operating conditions. However, the neccesity of retuning the PID controllers characterizes their major disadvantage when the controlled plant is subject to disturbances or when it presents complexities (non-linearities).

The main objective of this memory is to study and analyse the type-1 and type-2 fuzzy logic controller structures to the trajectory tracking control of a robotic arm containing high nonlinearities. Performance evaluation of the closed loop system will focus on the ability of the fuzzy controller's structures, in terms of tracking precision, to control the arm.

This memory is divided into 4 chapters. Chapter 1 introduces the three degrees of freedom robot arm PUMA560 and its dynamic model [1]. In chapter 2 the main ideas underlying type-1 fuzzy logic, and the application of this powerful computational theory to the problems of modeling, control. We discuss in some detail type-1 fuzzy set theory, fuzzy reasoning, and fuzzy inference systems. At the end, we also illustrate these concepts with PUMA560 3DOF that show the applicability of type-1 fuzzy logic. The importance of type-1 fuzzy logic as a basis for developing intelligent systems has been recognized in several areas of application. Chapter 3 the basic concepts, notation, and theory of type-2 fuzzy logic, which is a generalization of type-1 fuzzy logic, type-2 fuzzy logic enables the management of uncertainty in a more complete way, this is due to the fact that in type-2 membership functions we also consider that there is uncertainty in the form of the functions, unlike type-1 membership functions in which the functions are considered to be fixed and not uncertain. We describe type-2 fuzzy set theory, type-2 fuzzy reasoning, and type-2 fuzzy systems. At the end chapter 4 provides a comparative evaluation of the type-1 and type-2 fuzzy logic controller by using simulation result from chapter 2 and chapter3.

Chapter 1

Modeling rigid manipulator robot

1.1.1 Introduction

The control and simulation of robots requires the development of different mathematical models. Several levels of modeling –geometric, kinematic and dynamic- are needed depending on the objectives, the constraints of the task and the desired performance.

Obtaining these models is not an easy task. The difficulty varies according to the complexity of the kinematics of the mechanical structure and its degrees of freedom. For that we take the dynamic model of PUMA560 from [1].

In this memory we interested by fuzzy control of robot then this chapter show some mathematical tools witch using for modeling robot, the aim of modeling to simplifies and estimate the values of the geometric and dynamic parameters of the robot. Besides to find a control law on robot controller with reduced number of operations.

1.1.2 Description of the geometry of serial robots [4]

A serial robot is composed of a sequence of n+1 links and n joints. The links are assumed to be perfectly rigid. The joints are either revolute or prismatic and are assumed to be ideal (no backlash, no elasticity).

The links are numbered such that link 0 constitutes the base of the robot and link n is the terminal link (Figure 1.1). Joint j connects link j to link j – 1 and its variable is denoted q_j. In order to define the relationship between the location of links, we assign a frame R_j attached to each link j, such that:

- The z_j axis is along the axis of joint j.

- The x_j axis is aligned with the common normal between z_j and z_{j+1}. If z_j and z_{j+1} are parallel or collinear, the choice of x_j is not unique. The intersection of x_j and z_j defines the origin O_j. In the case of intersecting joint axes, the origin is at the point of intersection of the joint axes.
- The y_j axis is formed by the right-hand rule to complete the coordinate system (x_j, y_j, z_j).

The transformation matrix from frame R_{j-1} to frame R_j is expressed as a function of the following four geometric parameters (Figure 1.2):

• α_j : the angle between z_{j-1} and z_j about x_{j-1}.

• d_j : the distance between z_{j-1} and z_j along x_{j-1}.

• θ_j : the angle between x_{j-1} and x_j about z_j.

• r_j : the distance between x_{j-1} and x_j along z_j.

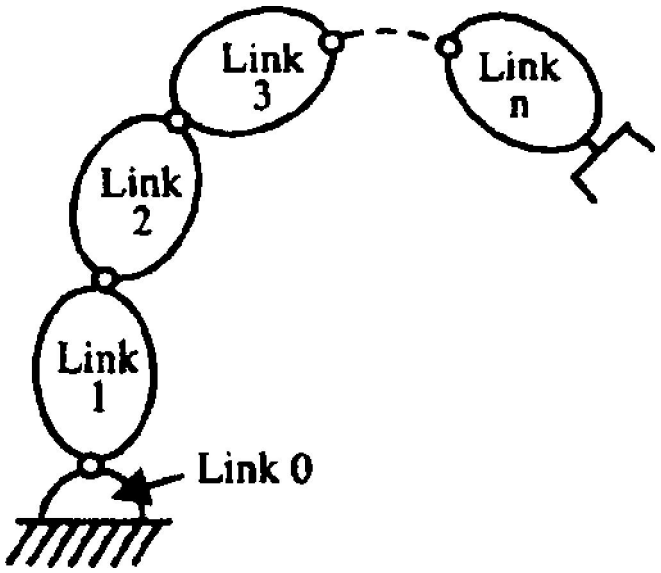

Figure 1.1. Robot with simple open structure.

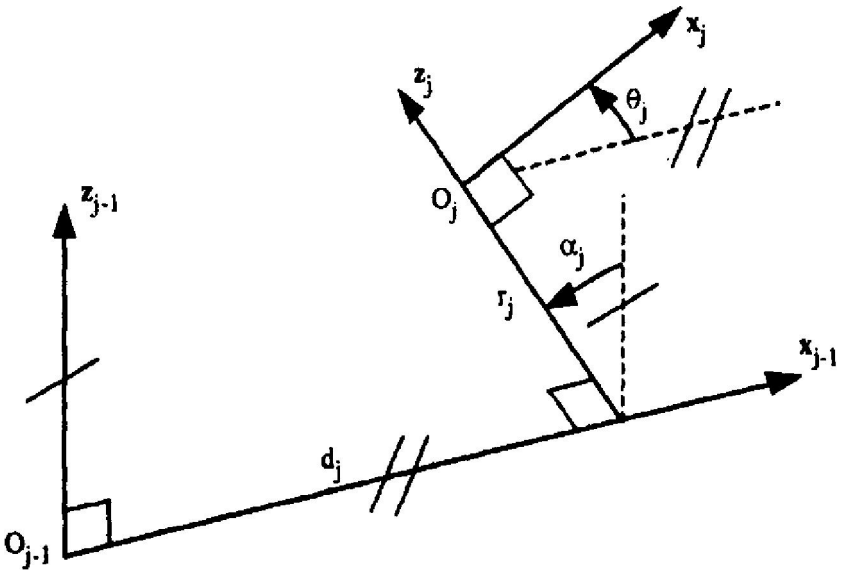

Figure 1.2. The geometric parameters in the case of a simple open structure.

The variable of joint j, defining the relative orientation or position between links j - 1 and j, is either θ_j or r_j, depending on whether the joint is revolute or prismatic respectively. This is defined by the relation:

$$q_j = \bar{\sigma}_j \theta_j + \sigma_j r_j \tag{1.1}$$

with:

- $\sigma_j = 0$ if joint j is revolute.
- $\sigma_j = 1$ if joint j is prismatic.
- $\bar{\sigma}_j = 1 - \sigma_j$.

The transformation matrix defining frame R_j relative to frame R_{j-1} is given as (Figure 1.2):

$$\begin{aligned} {}^{j-1}T_j &= Rot(x,\alpha_j)Trans(x,d_j)Rot(z,\theta_j)Trans(z,r_j) \\ &= \begin{bmatrix} C\theta_j & -S\theta_j & 0 & d_j \\ C\alpha_j S\theta_j & C\alpha_j C\theta_j & -S\alpha_j & -r_j S\alpha_j \\ S\alpha_j S\theta_j & S\alpha_j C\theta_j & C\alpha_j & r_j C\alpha_j \\ 0 & 0 & 0 & 1 \end{bmatrix} \end{aligned} \tag{1.2}$$

NOTES:

- The frame R_0 is chosen to be aligned with frame R_1 when $q_1 = 0$. This means that z_0 is aligned with z_1, whereas the origin O_0 is coincident with the origin O_1 if joint 1 is

revolute, and x_0 is parallel to x_1 if joint 1 is prismatic. This choice makes $\alpha_1 = 0, d_1 = 0$ and $\overline{q}_1 = 0$.

- In a similar way, the choice of the x_n axis to be aligned with x_{n_1} when $q_n = 0$ makes $\overline{q}_n = 0$.
- If joint j is prismatic, the z_j axis must be taken to be parallel to the joint axis but can have any position in space. So, we place it in such a way that $d_j = 0$ or $d_{j+1} = 0$.
- If z_j is parallel to z_{j+1}, we place x_j in such a way that $r_j = 0$ or $r_{j+1} = 0$.

In this memory we interesting by PUMA560 robot then we show example of geometric description for this robot.

Example1.1: Geometric description of the PUMA560 [1]

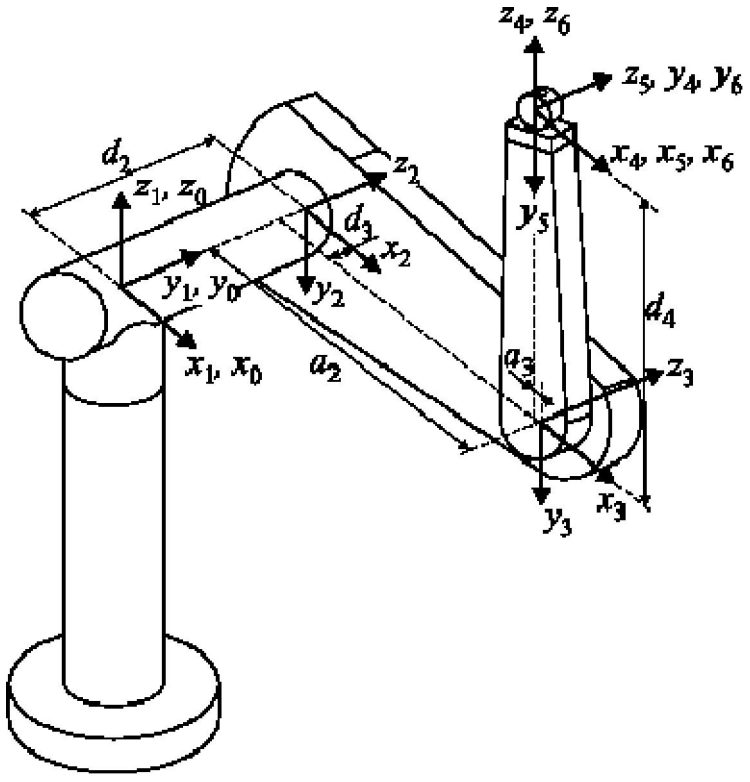

Figure 1.3: The Puma 560 is shown along with the DH parameters and body frames for each link in the chain.

Matrix	α_{i-1}	a_{i-1}	θ_i	d_i
$T_1(\theta_1)$	0	0	θ_1	0
$T_2(\theta_2)$	$-\pi/2$	0	θ_2	d_2
$T_3(\theta_3)$	0	a_2	θ_3	d_3
$T_4(\theta_4)$	$\pi/2$	a_3	θ_4	d_4
$T_5(\theta_5)$	$-\pi/2$	0	θ_5	0
$T_6(\theta_6)$	$\pi/2$	0	θ_6	0

Table 1.1: The DH parameters.

This example demonstrates the 3D chain kinematics on a classic robot manipulator, the PUMA 560, shown in Figure 1.3. The procedure is to determine appropriate body frames to represent each of the links. The first three links allow the hand (called an end-effector) to make large movements, and the last three enable the hand to achieve a desired orientation. There are six degrees of freedom, each of which arises from a revolute joint. The body frames are shown in Figure 1.3, and the corresponding DH parameters are given in Table 1.1. Each transformation matrix T_i is a function of θ_i. The other parameters are fixed for this example. Only $\theta_1, \ldots\ldots\theta_6$ are allowed to vary. The parameters from Table 1.1 may be substituted into the homogeneous transformation matrices to obtain:

$$T_1(\theta_1) = \begin{pmatrix} \cos\theta_1 & -\sin\theta_1 & 0 & 0 \\ \sin\theta_1 & \cos\theta_1 & 0 & 0 \\ 0 & 0 & 1 & 0 \\ 0 & 0 & 0 & 1 \end{pmatrix}, \tag{1.3}$$

$$T_2(\theta_2) = \begin{pmatrix} \cos\theta_2 & -\sin\theta_2 & 0 & 0 \\ 0 & 0 & 1 & d_2 \\ -\sin\theta_2 & -\cos\theta_2 & 0 & 0 \\ 0 & 0 & 0 & 1 \end{pmatrix}, \tag{1.4}$$

$$T_3(\theta_3) = \begin{pmatrix} \cos\theta_3 & -\sin\theta_3 & 0 & a_2 \\ \sin\theta_3 & \cos\theta_3 & 0 & 0 \\ 0 & 0 & 1 & d_3 \\ 0 & 0 & 0 & 1 \end{pmatrix}, \tag{1.5}$$

$$T_4(\theta_4) = \begin{pmatrix} \cos\theta_4 & -\sin\theta_4 & 0 & a_3 \\ 0 & 0 & -1 & -d_4 \\ \sin\theta_4 & \cos\theta_4 & 0 & 0 \\ 0 & 0 & 0 & 1 \end{pmatrix}, \tag{1.6}$$

$$T_5(\theta_5) = \begin{pmatrix} \cos\theta_5 & -\sin\theta_5 & 0 & 0 \\ 0 & 0 & 1 & 0 \\ -\sin\theta_5 & -\cos\theta_5 & 0 & 0 \\ 0 & 0 & 0 & 1 \end{pmatrix}, \tag{1.7}$$

$$T_6(\theta_6) = \begin{pmatrix} \cos\theta_6 & -\sin\theta_6 & 0 & 0 \\ 0 & 0 & -1 & 0 \\ \sin\theta_6 & \cos\theta_6 & 0 & 0 \\ 0 & 0 & 0 & 1 \end{pmatrix}. \tag{1.8}$$

Note that a_3 and d_3 are negative in this example (they are signed displacements, not distances).

1.2.1 Dynamic modeling of serial robots

The dynamics of robot manipulators whereas the kinematic equations describe the motion of the robot without consideration of the forces and torques producing the motion, the dynamic equations explicitly describe the relationship between force and motion [6]. The equations of motion are important to consider in the design of robots, in simulation and animation of robot motion, and in the design of control algorithms. We introduce the so-called Euler-Lagrange equations.

In order to determine the Euler-Lagrange equations in a specific situation, one has to form the Lagrangian of the system, which is the deference between the kinetic energy and the potential energy.

1.2.2 The EULER-LAGRANGE equations

In general, for any system of the type considered, an application of the Euler- Lagrange [6] equations leads to a system of n coupled, second order nonlinear ordinary deferential equations of the form:

$$\frac{d}{dt}\frac{\partial L}{\partial \dot{q}_i} - \frac{\partial L}{\partial q_i} = \tau_i \qquad i = 1, \cdots\cdots, n \tag{1.9}$$

The order, n, of the system is determined by the number of so-called gener- alized coordinates that are required to describe the evolution of the system. We shall see that the n Denavit-Hartenberg joint variables serve as a set of generalized coordinates for an n-link rigid robot.

1.2.3 Kinetic Energy for an n-Link Robot

Now consider a manipulator consisting of n links. The linear and angular velocities of any point on any link can be expressed in terms of the Jacobian matrix and the derivative of the joint variables. Since in our case the joint variables are indeed the generalized coordinates, it follows that, for appropriate Jacobian matrices J_{v_i} and J_{w_i} , we have that[6]:

$$v_i = J_{v_i}(q)\dot{q}\,, \quad w_i = J_{w_i}(q)\dot{q} \tag{1.10}$$

$$K = \frac{1}{2} m v^T v + \frac{1}{2} w^T \mathrm{I} w \tag{1.11}$$

$$\mathrm{I} = RIR^T \tag{1.12}$$

Where R is the orientation transformation between the body attached frame and the inertial frame.

Now suppose the mass of link i is m_i and that the inertia matrix of link i, evaluated around a coordinate frame parallel to frame i but whose origin is at the center of mass, equals I_i . Then from (1.15) it follows that the overall kinetic energy of the manipulator equals

$$K = \frac{1}{2}\dot{q}^T \sum_{i=1}^{n} \left[m_i J_{v_i}^T(q) J_{v_i}(q) + J_{w_i}(q)^T R_i(q) I_i R_i(q)^T J_{w_i}(q) \right] \dot{q} \tag{1.13}$$

In other words, the kinetic energy of the manipulator is of the form:

$$K = \frac{1}{2}\dot{q}^T D(q)\dot{q} \tag{1.14}$$

Where $D(q)$ is a symmetric positive definite matrix that is in general configuration dependent. The matrix D is called the inertia matrix.

1.2.4 Potential Energy for an n-Link Robot

Now consider the potential energy term. In the case of rigid dynamics, the only source of potential energy is gravity. The potential energy of the i-th link can be computed by assuming that the mass of the entire object is concentrated at its center of mass and is given by [6]:

$$P_i = g^T r_{ci} m_i \tag{1.15}$$

Where g is vector giving the direction of gravity in the inertial frame and the vector r_{ci} gives the coordinates of the center of mass of link i. The total potential energy of the n-link robot is therefore:

$$P = \sum_{i=1}^{n} P_i = \sum_{i=1}^{n} g^T r_{ci} m_i \tag{1.16}$$

1.3.1 PUMA 560 robot Dynamics:

The dynamic model used for PUMA560 it is[1]:

$$M(q).\ddot{q} + B(q).[\dot{q}.\dot{q}] + C(q).[\dot{q}^2] + G(q) = \Gamma \tag{1.17}$$

Where,

$B(q)$: nxn(n-1)/2 matrix of Coriolis torques

$C(q)$: nxn matrix of Centrifugal torques

$[\dot{q}\dot{q}]$: n(n-1)/2x1 vector of joint velocity products given by:

$$[\dot{q}_1.\dot{q}_2, \dot{q}_1.\dot{q}_3, ..., \dot{q}_1.\dot{q}_n, \dot{q}_2.\dot{q}_3, \dot{q}_2.\dot{q}_4, ..., \dot{q}_{n-2}.\dot{q}_n, \dot{q}_{n-1}.\dot{q}_n]^T$$

$[\dot{q}^2]$: nx1 vector given by: $[\dot{q}_1^{\,2}, \dot{q}_2^{\,2}, ..., \dot{q}_n^{\,2}]$

The position of zero joint angles and coordinate frame attachments to the PUMA arm are shown in Figure 1.3 above. The modified Denavit-Hartenberg parameters, assigned according to the method presented in [3] are listed in Table 1.2.

i	α_{i-1} $(\text{deg}rees)$	θ_i	a_{i-1} $(meters)$	d_i $(meters)$
1	0	q_1	0	0
2	-90	q_2	0	0.2435
3	0	q_3	0.4318	-0.0934

Table 1.2 Modified Denavit - Hartenberg Parameters

The mass of links 2 through 6 of the PUMA arm are reported in Table 1.3, the mass of link 1 in not included because that link was not removed from the base. Separately measured mass and inertia terms are not required for link one because that link rotates only about its own 2 axis.

Link	Mass
Link2	17.40
Link3	4.80

Table 1.3 Link Mass[1]

The positions of the centers of gravity are reported in Table 1.4 the dimensions $r_x, r_y and\ r_z$ refer to the x, y and z coordinate of the center of gravity in the coordinate frame attached to the link.

Link	r_x	r_y	r_z
Link 2	0.068	0.006	-0.016
Link 3	0	-0.070	0.014

Table 1.4 Centers of Gravity.

Link	I_{xx}	I_{yy}	I_{zz}	I_{motor}
Link 1	-	-	0.35	$1.14(\pm 0.27)$
Link 2	$0.130(\pm 3\%)$	$0.524(\pm 5\%)$	$0.539(\pm 3\%)$	$4.71(\pm 0.54)$
Link 3	0.066	0.0125	0.086	$0.83(\pm 0.09)$

Table 1.5 Diagonal Terms of the Inertia Dynamics and Effective Motor Inertia. [1]

	Joint 1	Joint 2	Joint 3
Gear Ration	62.61	107.36	53.69
Maximum Torque(N-m)	97.6	180.4	89.4
Break Away Torque (N-m)	6.3	5.5	2.6

Table 1.6 Motor and Drive Parameter[1]

1.3.2 Using PUMA Robot as 3-DOF Robot:

Recall that only three links of PUMA robot are used in this thesis, the configuration space equation same (1.17),

With,

Matrix A is a symmetric 6x6 matrix:

$$A(q) = \begin{bmatrix} a_{11} & a_{12} & a_{13} \\ a_{21} & a_{22} & a_{23} \\ a_{31} & a_{32} & a_{33} \end{bmatrix} \tag{1.18}$$

Where,

$a_{11} = I_{m1} + I_1 + I_3.CC2 + I_7.SS23 + I_{10}.SC23 + I_{11}.SC2 +$
$+ 2.[I_5.C2.S23]$

$a_{12} = I_4.S2 + I_8.C23 + I_9.C2$

$a_{13} = I_8.C23$

$a_{22} = I_{m2} + I_2 + I_6 + 2.[I_5.S3]$

$a_{23} = I_5.S3 + I_6$

$a_{33} = I_{m3} + I_6$

$a_{21} = a_{12}$, $a_{31} = a_{13}$ and $a_{32} = a_{23}$

While matrix B is:

$$B(q) = \begin{bmatrix} b_{112} & b_{113} & 0 & 0 & 0 & b_{123} & 0 \\ 0 & 0 & 0 & 0 & 0 & b_{223} & 0 \\ 0 & 0 & 0 & 0 & 0 & 0 & 0 \end{bmatrix} \tag{1.19}$$

Where,

$b_{112} = 2.[-I_3.SC2 + I_5.C223 + I_7.SC23] + I_{10}.(1 - 2.SS23) + I_{11}.(1 - 2.SS2)$

$b_{113} = 2.[I_5.C2.C23 + I_7.SC23 -] + I_{10}.(1 - 2.SS23)$

$b_{123} = 2.[-I_8.S23]$

Matrix C is:

$$C(q) = \begin{bmatrix} 0 & c_{12} & c_{13} \\ c_{21} & 0 & c_{23} \\ c_{31} & c_{32} & 0 \end{bmatrix} \tag{1.20}$$

Where,

$c_{12} = I_4.C2 - I_8.S23 - I_9.S2$

$c_{13} = 0.5.b_{123} = -I_8.S23$

$c_{21} = -0.5.b_{112} = I_3.SC2 - I_5.C223 - I_7.SC23 - 0.5.I_{10}.(1 - 2.SS23) - 0.5.I_{11}.(1 - 2.SS2)$

$c_{23} = 0.5.b_{223} = I_5.C3$

$c_{31} = -0.5.b_{113} = -I_5.C2.C23 - I_7.SC23 - 0.5.I_{10}.(1 - 2.SS23)$

$c_{32} = -c_{23} = -I_5.C3$

And matrix G is:

$$g(q) = \begin{bmatrix} 0 \\ g_2 \\ g_3 \end{bmatrix} \tag{1.21}$$

$g_2 = g_1.C2 + g_2.S23 + g_3.S2$

$g_3 = g_2.S23$

Where,

Si = sin(θi), Ci = cos(θi), Cij = cos(θi+ θj), Sijk = sin(θi +θj +θk),
CCi = cos(θi).cos(θi) and Csi = cos(θi).sin(θi)

Tables 1.7 and 1.8 contain the computed values for the constants appearing in the equations of forces of motion,

$I_1 = 1.43 \pm 0.05$	$I_2 = 1.75 \pm 0.07$
$I_3 = 1.38 \pm 0.05$	$I_4 = 0.69 \pm 0.02$
$I_5 = 0.372 \pm 0.031$	$I_6 = 0.333 \pm 0.016$
$I_7 = 0.298 \pm 0.029$	$I_8 = -0.134 \pm 0.014$
$I_9 = 0.0238 \pm 0.012$	$I_{10} = -0.0213 \pm 0.0022$
$I_{11} = -0.0142 \pm 0.0070$	$I_{m1} = 1.14 \pm 0.27$
$I_{m2} = 4.71 \pm 0.54$	$I_{m3} = 0.827 \pm 0.093$

Table 1.7 Inertiel Constants ($kg.m^2$)[1]

$g_1 = -37.2 \pm 0.5$	$g_2 = -8.44 \pm 0.20$
$g_3 = 1.02 \pm 0.50$	

Table 1.8 Gravitational Constants (N.m) [1]

The three degree of freedom PUMA robot has the same configuration space equation general form as its 6-DOF convenient. In this type, the last three joints are blocked so they keep their initial states while the robot is moving. Using the configuration equation of the robot, and by setting the last joints as zero always, we can define a general equation that allows us to use PUMA robot as a 3-DOF robot.

To find the kinematics of the 3-DOF robot, a new D-H coordinate system is established, and a homogenous transformation matrix relating the 3^{rd} coordinate frame to the first coordinate frame is developed.

$\ddot{q} = [\ddot{q}_1 ... \ddot{q}_2 ... \ddot{q}_3]^T$,

$[\dot{q}\dot{q}] = [\dot{q}_1\dot{q}_2 ... \dot{q}_1\dot{q}_3 ... 0 ... 0 ... 0 ... \dot{q}_2\dot{q}_3 ... 0]^T$,

$[\dot{q}^2] = [\dot{q}_1^{\,2} ... \dot{q}_2^{\,2} ... \dot{q}_3^{\,2}]^T$,

The angular acceleration is found as to be:

$$\ddot{q} = A^{-1}(q).\left\{\Gamma - \left[B(q).\dot{q}\dot{q} + C(q).\dot{q}^2 + g(q)\right]\right\}$$

Now let $I = \left\{\Gamma - \left[B(q).\dot{q}\dot{q} + C(q).\dot{q}^2 + g(q)\right]\right\} \Rightarrow \ \ddot{q} = A^{-1}(q).I$

$$I_1 = \Gamma_1 - \left[b_{112}.\dot{q}_1\dot{q}_2 + b_{113}.\dot{q}_1\dot{q}_3 + b_{123}.\dot{q}_2\dot{q}_3\right] - \left[c_{12}.\dot{q}_2{}^2 + c_{13}.\dot{q}_3{}^2\right]$$
$$I_2 = \Gamma_2 - \left[b_{223}.\dot{q}_2\dot{q}_3\right] - \left[c_{21}.\dot{q}_1{}^2 + c_{23}.\dot{q}_3{}^2\right] - g_2$$
$$I_3 = \Gamma_3 - \left[c_{31}.\dot{q}_1{}^2 + c_{32}.\dot{q}_2{}^2\right] - g_3$$

1.4 Conclusion

In this chapter we give some background mathematical to modeling robot we talking about geometric description and dynamic modeling and about other modeling we let it in Appendix A same direct model geometric and direct model kinematics.

And next we give some dynamic model description for PUMA560 robot for more detail about this robot see this [1], after we explain how can we using PUMA560 as 3DOF robot for control it by type-1 and type-2 fuzzy logic controller in the next chapters.

Chapter 2

Type-1 Fuzzy logic controller

2.1.1 Introduction

This chapter introduces the basic concepts, notation, and basic operations for the type-1 fuzzy sets that will be needed in the following chapters. Type-2 fuzzy sets as well as their operations will be discussed in the next chapter. For this reason, in this chapter we will focus only on type-1 fuzzy logic. Since research on fuzzy set theory has been underway for over 30 years now, it is practically impossible to cover all aspects of current developments in this area. Therefore, the main goal of this chapter is to provide an introduction to and a summary of the basic concepts and operations that are relevant to the study of type-1 fuzzy sets.

Fuzzy logic controller (FLC) which used in this memory is Mamdani method, or used to call Max-Min method.

2.2.1 Fuzzy set theory

Fuzzy logic was first proposed by Zadeh (1965) and is based on the concept of fuzzy sets[8]. Fuzzy set theory provides a means for representing uncertainty. In general, probability theory is the primary tool for analyzing uncertainty, and assumes that the uncertainty is a random process. However, not all uncertainty is random, and fuzzy set theory is used to model the kind of uncertainty associated with imprecision, vagueness and lack of information.
Conventional set theory distinguishes between those elements that are members of a set and those that are not, there being very clear, or crisp boundaries. Figure 2.1 shows the crisp set 'medium temperature'. Temperatures between 20 and 30'C lie within the crisp set, and have a membership value of one.

The central concept of fuzzy set theory is that the membership function *M*, like probability theory, can have a value of between 0 and 1 [13] [14]. In Figure 2.2, the membership function

has a linear relationship with the *x-axis*, called the universe of discourse *U*. This produces a triangular shaped fuzzy set. Fuzzy sets represented by symmetrical triangles are commonly used because they give good results and computation is simple. Other arrangements include non-symmetrical triangles, trapezoids, Gaussian and bell shaped curves [15] [16].

Let the fuzzy set 'medium temperature' be called fuzzy set *M*. If an element u of the universe of discourse *U* lies within fuzzy set *M*, it will have a value of between 0 and 1. This is expressed mathematically as [11]:

$$\mu_M(u) \in [0,1] \tag{2.1}$$

When the universe of discourse is discrete and finite, fuzzy set *M* may be expressed as [11]:

$$M = \sum_{i=1}^{n} \mu_M(u_i)/u_i \tag{2.2}$$

In equation (2.2) '/' is delimiter. Hence the numerator of each term is the membership value in fuzzy set *M* associated with the element of the universe indicated in the denominator. When *n=11*, equation (2.2) can be written as:

$$\begin{aligned} M = {} & 0/0 + 0/5 + 0/10 + 0.33/15 + 0.67/20 + 1/25 + 0.67/30 + 0.33/35 \\ & + 0/40 + 0/45 + 0/50 \end{aligned} \tag{2.3}$$

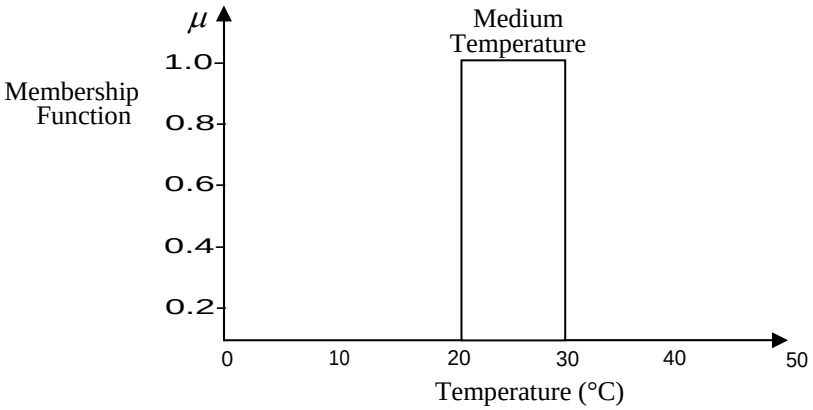

Figure 2.1 Crisp set (medium temperature).

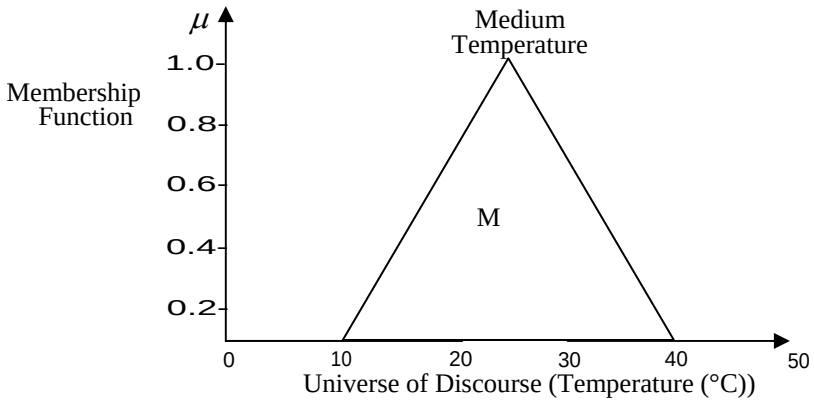

Figure 2.2 Fuzzy set 'medium temperature'

2.2.2 Basic fuzzy set operations

Let A and B be two fuzzy sets within a universe of discourse U with membership functions μ_A and μ_B respectively. The following fuzzy set operations can be defined as:

Equality: Two fuzzy sets A and B are equal if they have the same membership function within a universe of discourse U.

$$\mu_A(u) = \mu_B(u) \qquad \textit{for all } u \in U \tag{2.4}$$

Union: The union of two fuzzy sets A and B corresponds to the Boolean OR function and is given by:

$$\mu_{A\cup B}(u) = \mu_{A+B}(u) = \max\{\mu_A(u), \mu_B(u)\} \qquad \textit{for all } u \in U \tag{2.5}$$

Intersection: The intersection of two fuzzy sets A and B corresponds to the Boolean AND function and is given by:

$$\mu_{A\cap B}(u) = \min\{\mu_A(u), \mu_B(u)\} \qquad \textit{for all } u \in U \tag{2.6}$$

Complement: The complement of fuzzy set A corresponds to the Boolean NOT function and is given by:

$$\mu_{\neg A}(u) = 1 - \mu_A(u) \qquad \textit{for all } u \in U \tag{2.7}$$

Example 2.1[8]

Find the union and intersection of fuzzy set low temperature *L* and medium temperature *M* shown in Figure 2.3. Find also the complement of fuzzy set *M*. using equation (2.2) the fuzzy sets for *n=11* are:

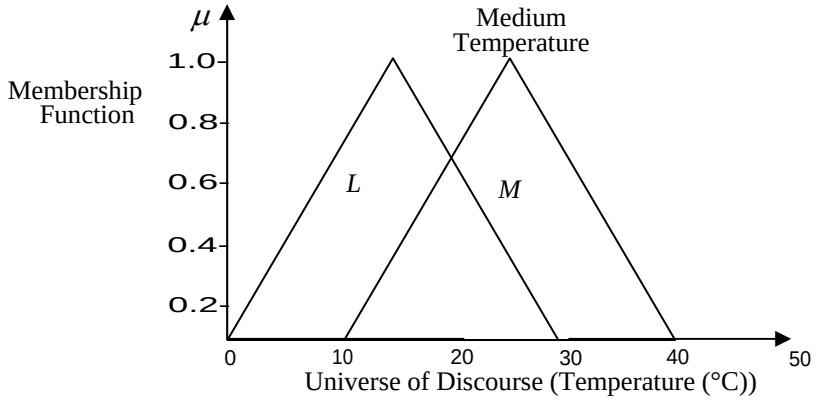

Figure 2.3 Overlapping sets 'low' and 'medium temperature'.

$$\begin{aligned} L &= 0/0 + 0.33/5 + 0.67/10 + 1/15 + 0.67/20 + 0.33/25 \\ &+ 0/30 + 0/35 + \cdots\cdots + 0/50 \\ M &= 0/0 + 0/5 + 0/10 + 0.33/15 + 0.67/20 + 1/25 + 0.67/30 \\ &+ 0.33/35 + 0/40 + \cdots + 0/50 \end{aligned} \tag{2.8}$$

a - Union: Using equation (2.5)

$$\begin{aligned} \mu_{L+M}(u) &= \max(0,0)/0 + \max(0.33,0)/5 + \max(0.67,0)/10 \\ &+ \max(1,0.33)/15 + \max(0.67,0.67)/20 + \max(0.33,1)/25 \\ &+ \max(0,0.67)/30 + \max(0,0.33)/35 + \max(0,0)/40 + \cdots \\ &+ \max(0,0)/50 \end{aligned} \tag{2.9}$$

$$\begin{aligned} \mu_{L+M}(u) &= 0/0 + 0.33/5 + 0.67/10 + 1/15 + 0.67/20 + 1/25 + 0.67/30 \\ &+ 0.33/35 + 0/40 + \cdots + 0/50 \end{aligned} \tag{2.10}$$

b- Intersection: Using equation (2.6) and replacing 'max' by 'min' in equation (2.9) gives:

$$\begin{aligned} \mu_{L\cap M}(u) &= 0/0 + 0/5 + 0/10 + 0.33/15 + 0.67/20 + 0.33/25 \\ &+ 0/30 + \cdots + 0/50 \end{aligned} \tag{2.11}$$

Equations (2.10) and (2.11) are shown in Figure 10. 4.

c- Complement: Using equation (2.7):

$$\begin{aligned}\mu_{\neg M}(u) &= (1-0)/0 + (1-0)/5 + (1-0)/10 + (1-0.33)/15 \\ &+ (1-0.67)/20 + (1-1)/25 + (1-0.67)/30 + (1-0.33)/35 \\ &+ (1-0)/40 + \cdots + (1-0)/50\end{aligned} \tag{2.12}$$

Equation (2.12) is illustrated in Figure 2.5.

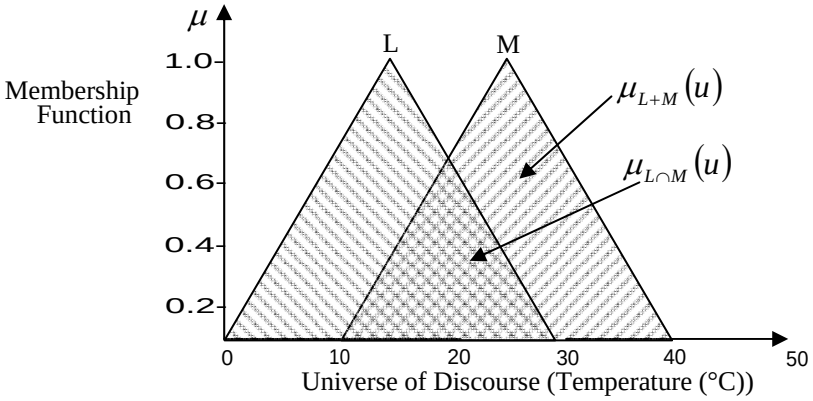

Figure 2.4 'Union' and 'intersection' functions.

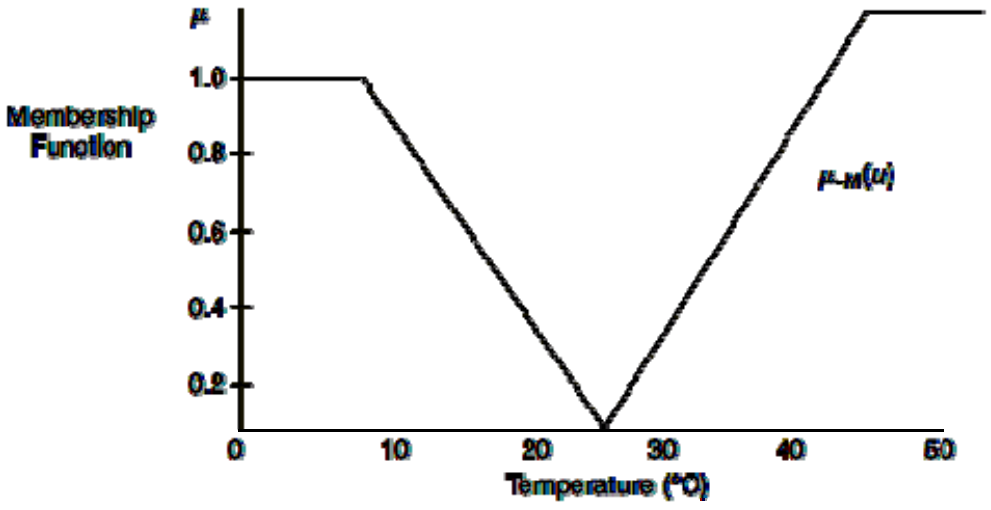

Figure 2.5 The complement of fuzzy set M.

2.2.3 Fuzzy relations

An important aspect of fuzzy logic is the ability to relate sets with different universes of discourse. Consider the relationship:

IF L THEN M (2.13)

In equation (2.13) L is known as the antecedent and *M* as the consequent. The relationship is denoted by:

$$A = L \times M \tag{2.14}$$

Or:

$$L \times M = \begin{bmatrix} \min\{\mu_L(u_1), \mu_M(v_1)\} & \cdots & \min\{\mu_L(u_1), \mu_M(v_k)\} \\ \min\{\mu_L(u_j), \mu_M(v_1)\} & \cdots & \min\{\mu_L(u_j), \mu_M(v_k)\} \end{bmatrix} \tag{2.15}$$

Where $u_1 \to u_j$ and $v_1 \to v_k$ are the discretized universe of discourse. Consider the statement:

IF L is low THEN M is medium (2.16)

Then for the fuzzy sets *L* and *M* defined by equation (2.8), for U from 5 to 35 in steps of 5

$$L \times M = \begin{bmatrix} \min(0.33,0) & \cdots & \min(0.33,1) & \cdots & \min(0.33,0.33) \\ \min(0.67,0) & \cdots & \min(0.67,1) & \cdots & \min(0.67,0.33) \\ \vdots & \vdots & \vdots & \vdots & \vdots \\ \min(0,0) & \cdots & \min(0,1) & \cdots & \min(0,0.33) \end{bmatrix} \tag{2.17}$$

Which gives:

$$L \times M = \begin{bmatrix} 0 & 0 & 0.33 & 0.33 & 0.33 & 0.33 & 0.33 \\ 0 & 0 & 0.33 & 0.67 & 0.67 & 0.67 & 0.33 \\ 0 & 0 & 0.33 & 0.67 & 1 & 0.67 & 0.33 \\ 0 & 0 & 0.33 & 0.67 & 0.67 & 0.67 & 0.33 \\ 0 & 0 & 0.33 & 0.33 & 0.33 & 0.33 & 0.33 \\ 0 & 0 & 0 & 0 & 0 & 0 & 0 \\ 0 & 0 & 0 & 0 & 0 & 0 & 0 \end{bmatrix} \tag{2.18}$$

Several such statements would form a control strategy and would be linked by their union

$$A = A_1 + A_2 + A_3 + \cdots\cdots A_n \tag{2.19}$$

2.2.4 Fuzzy logic control [8]

The basic structure of a Fuzzy Logic Control (FLC) system is shown in Figure 2.6. Fuzzy logic controller (FLC) which used in this memory is Mamdani.

The fuzzification process

Fuzzification is the process of mapping inputs to the FLC into fuzzy set membership values in the various input universes of discourse. Decisions need to be made regarding
(a) Number of inputs
(b) Size of universes of discourse
(c) Number and shape of fuzzy sets.

A FLC that emulates a PD controller will be required to minimize the error *e(t)* and the rate of change of error *de/dt*, or *ce*.

The size of the universes of discourse will depend upon the expected range (usually up to the saturation level) of the input variables. Assume for the system about to be considered that e has a range of ± 6 and *ce* a range of ± 1.

The number and shape of fuzzy sets in a particular universe of discourse is a trade- off between precision of control action and real-time computational complexity. In this example, seven triangular sets will be used.

Each set is given a linguistic label to identify it, such as Positive Big (PB), Positive Medium (PM), Positive Small (PS), About Zero (Z), Negative Small (NS), Negative Medium (NM) and Negative Big (NB). The seven set fuzzy input windows for e and ce are shown in Figure 2.7. If at a particular instant, *e(t)*= 2.5 and *de/dt* =*ce* = -0.2, then, from Figure 2.7, the input fuzzy set membership values are:

$$\mu_{PS}(e) = 0.7 \quad \mu_{PM}(e) = 0.4$$
$$\mu_{NS}(ce) = 0.6 \quad \mu_{z}(ce) = 0.3 \tag{2.20}$$

The fuzzy rulebase

The fuzzy rule base consists of a set of antecedent-consequent linguistic rules of the form

$$IF\ e\ is\ PS\ AND\ ce\ is\ NS\ THEN\ u\ is\ PS \tag{2.21}$$

This style of fuzzy conditional statement is often called a 'Mamdani'-type rule, after Mamdani (1976) who first used it in a fuzzy rulebase to control steam plant.

The rulebase is constructed using a priori knowledge from either one or all of the following sources:
(a) Physical laws that govern the plant dynamics
(b) Data from existing controllers.
(c) Imprecise heuristic knowledge obtained from experienced experts.

If (c) above is used, then knowledge of the plant mathematical model is not required. The two seven set fuzzy input windows shown in Figure 2.7 gives a possible 7 x 7 set of control rules of the form given in equation (2.21). It is convenient to tabulate the two-dimensional rulebase as shown in Figure 2.8.

Fuzzy inference

Figure 2.8 assumes that the output window contains seven fuzzy sets with the same linguistic labels as the input fuzzy sets. If the universe of discourse for the control signal *u(t)* is ±9, then the output window is as shown in Figure 2. 9.

Assume that a certain rule in the rulebase is given by equation (2.22)

$$IF\ e\ is\ A\ AND\ ce\ is\ B\ THEN\ u = C \tag{2.22}$$

From equation (2.5) the Boolean OR function becomes the fuzzy max operation, and from equation (2.6) the Boolean AND function becomes the fuzzy min operation. Hence equation (2.22) can be written as

$$\mu_C(u) = \max\left[\min\left(\mu_A(e), \mu_B(ce)\right)\right] \tag{2.23}$$

Equation (2.23) is referred to as the max-min inference process or max-min fuzzy reasoning.

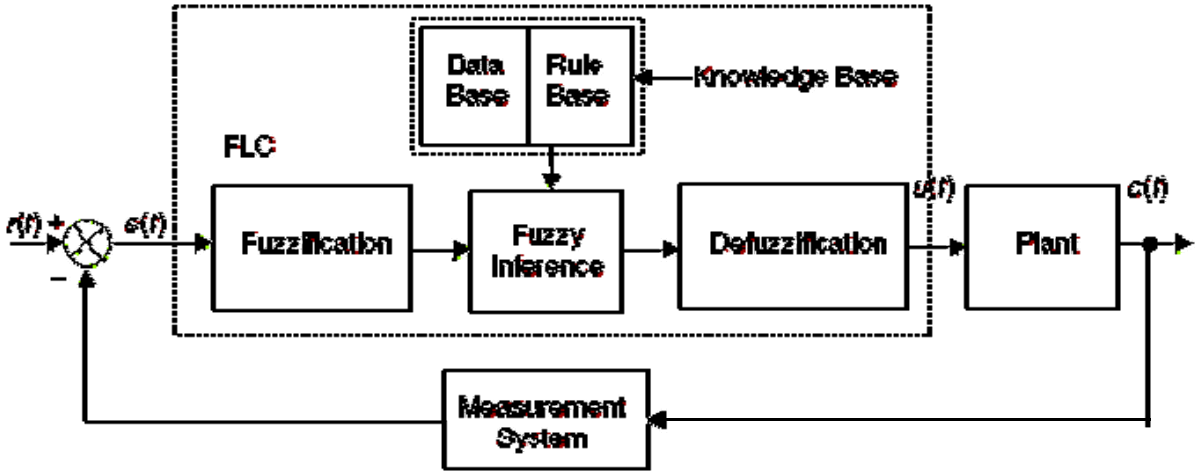

Figure 2.6 Fuzzy Logic Control

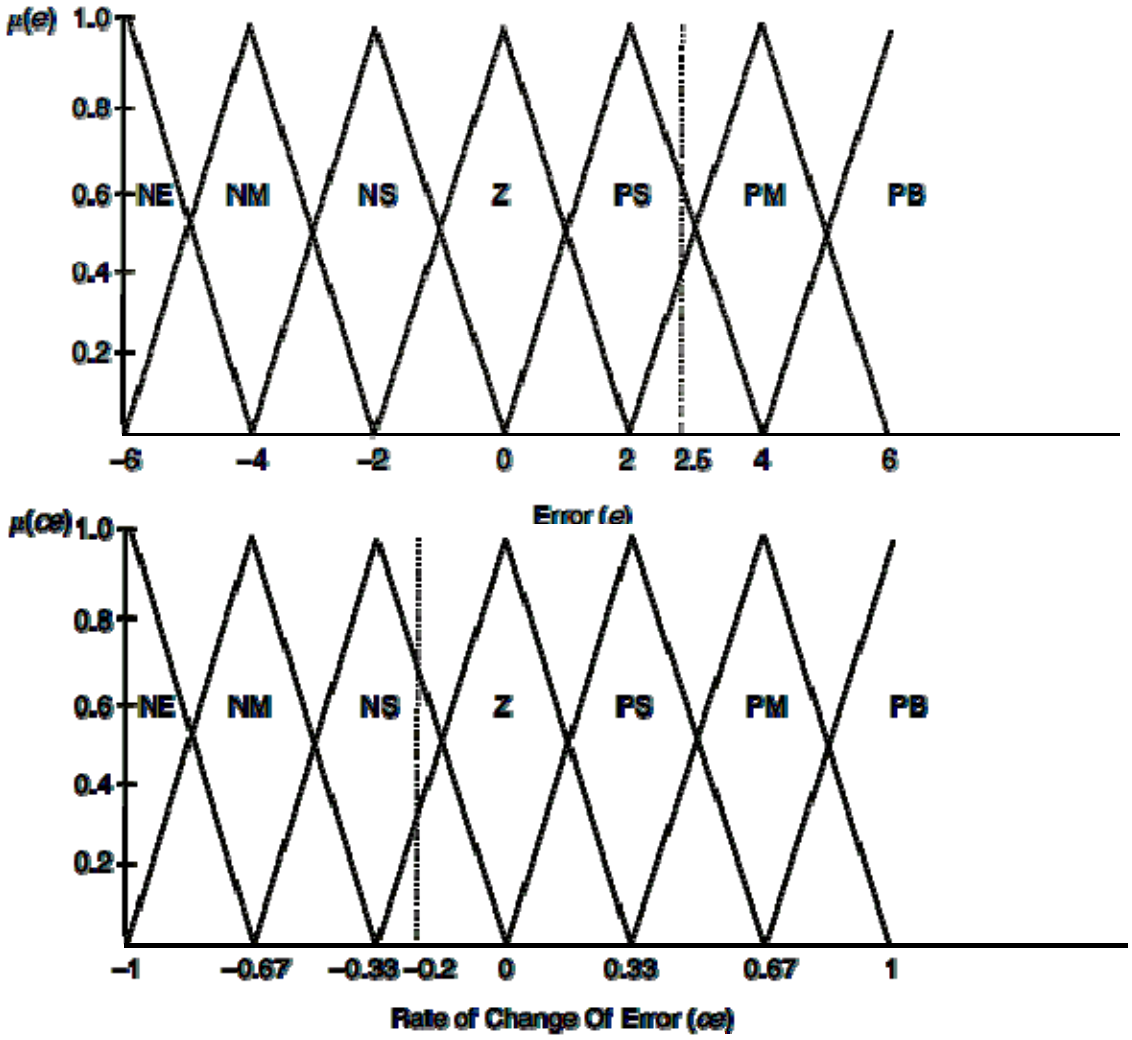

Figure 2.7 Seven set fuzzy input windows for error (*e*) and rate of change of error (*ce*).

ce \ e	NB	NM	NS	Z	PS	PM	PB
NB	NB	NB	NB	NM	Z	PM	PB
NM	NB	NB	NB	NM	PS	PM	PB
NS	NB	NB	NM	NS	PS	PM	PB
Z	NB	NM	NS	Z	PS	PM	PB
PS	NB	NM	NS	PS	PM	PB	PB
PM	NB	NM	NS	PM	PB	PB	PB
PB	NB	NM	Z	PM	PB	PB	PB

Figure2.8 Tabular structure of a linguistic fuzzy rulebase.

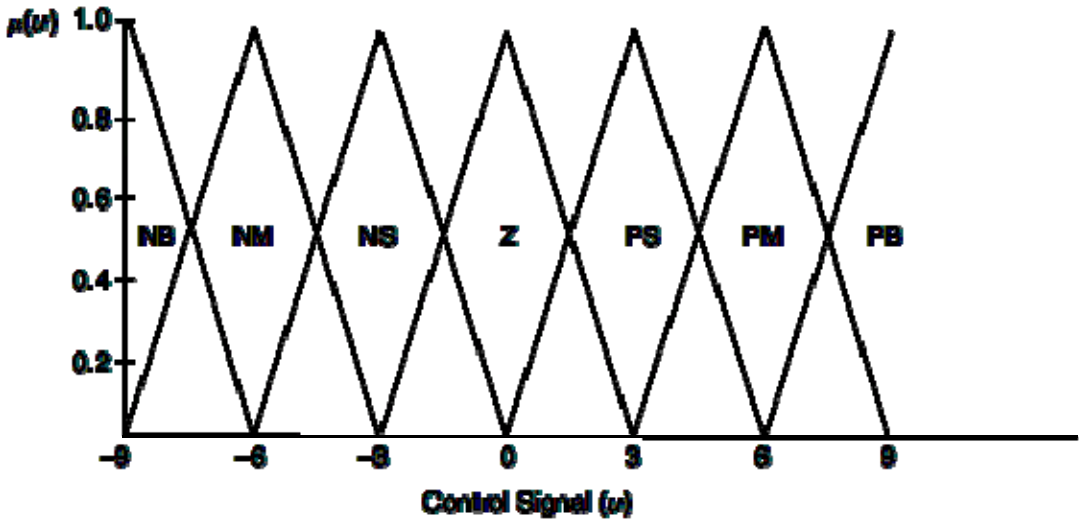

Figure2.9 Seven set fuzzy output window for control signal (u).

In Figure 2.7 and equation (2.20) the fuzzy sets that were 'hit' in the error input window when $e(t)$ = 2.5 were PS and PM. In the rate of change input window when ce = -0.2, the fuzzy sets to be 'hit' were NS and Z. From Figure 2.8, the relevant rules that correspond to these 'hits' are:

$$\begin{aligned} &\cdots OR\ IF\ e\ is\ PS\ AND\ ce\ is\ NS \\ &\quad OR\ IF\ e\ is\ PS\ AND\ ce\ is\ Z \\ &\quad THEN\ u = PS \end{aligned} \tag{2.24}$$

$$\begin{aligned} &\cdots OR\ IF\ e\ is\ PM\ \ AND\ ce\ is\ NS \\ &OR\ IF\ e\ is\ PM\ \ AND\ ce\ is\ Z \\ &THEN\ u = PM \end{aligned} \tag{2.25}$$

Applying the max-min inference process to equation (2.24)

$$\mu_{PS}(u) = \max\left[\min\left(\mu_{PS}(e), \mu_{NS}(ce)\right), \min\left(\mu_{PS}(e), \mu_{Z}(ce)\right)\right] \tag{2.26}$$

Inserting values from equation (2.20)

$$\begin{aligned} \mu_{PS}(u) &= \max\left[\min(0.7,0.6), \min(0.7,0.3)\right] \\ &= \max\left[0.6,0.3\right] = 0.6 \end{aligned} \tag{2.27}$$

Applying the max-min inference process to equation (2.25)

$$\mu_{PM}(u) = \max\left[\min\left(\mu_{PM}(e), \mu_{NS}(ce)\right), \min\left(\mu_{PM}(e), \mu_{Z}(ce)\right)\right] \tag{2.28}$$

Inserting values from equation (2.20)

$$\begin{aligned} \mu_{PS}(u) &= \max\left[\min(0.4,0.6), \min(0.4,0.3)\right] \\ &= \max\left[0.4,0.3\right] = 0.4 \end{aligned} \tag{2.29}$$

Fuzzy inference is therefore the process of mapping membership values from the input windows, through the rulebase, to the output window(s).

The defuzzification

Defuzzification is the procedure for mapping from a set of inferred fuzzy control signals contained within a fuzzy output window to a non-fuzzy (crisp) control signal. The centre of area [9, 10, 11] method is the most well known defuzzification technique, which in linguistic terms can be expressed as:

$$Crisp\ control\ signal = \frac{Sum\ of\ \ first\ moments\ of\ \ area}{Sum\ of\ \ areas} \tag{2.30}$$

For a continuous system, equation (2.30) becomes:

$$u(t) = \frac{\int u\mu(u)du}{\int \mu(u)du} \tag{2.31}$$

Or alternatively, for a discrete system, equation (2.30) can be expressed as:

$$u(kT) = \frac{\sum_{i=1}^{n} u_i \mu(u_i)}{\sum_{i=1}^{n} \mu(u_i)} \tag{2.32}$$

For the case when *e(t)* = 2.5 and *ce* = -0 .2, as a result of the max-min inference process (equations (2.27) and (2.29)), the fuzzy output window in Figure 2.9 is 'clipped', and takes the form shown in Figure 2.10.

From Figure 2.10, using the equation for the area of a trapezoid:

$$\begin{aligned} Area_{PS} &= \frac{0.6(6+2.4)}{2} = 2.52 \\ Area_{PS} &= \frac{0.2(6+3.6)}{2} = 0.96 \end{aligned} \tag{2.33}$$

From equation (2.30)

$$u(t) = \frac{(2.52 \times 3) + (0.96 \times 6)}{2.52 + 0.96} = 3.83 \tag{2.34}$$

Hence, for given error of 2.5, and a rate of change of error of -0.2, the control signal from the fuzzy controller is 3.83.

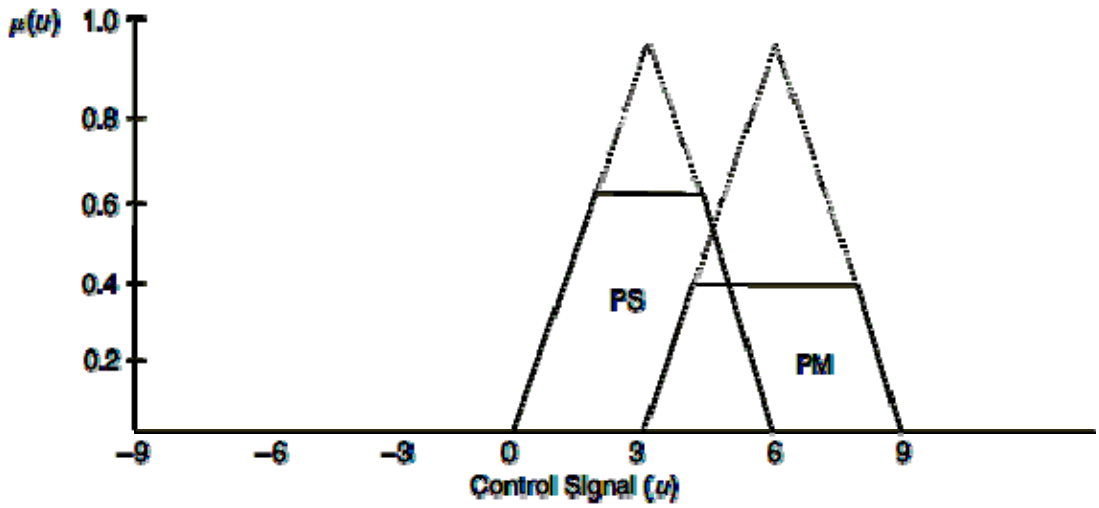

Figure 2.10 Clipped fuzzy output window due to fuzzy inference.

Example 2.2 [8]

For the input and output fuzzy windows given in Figure 2.7 and 2.9, together with the fuzzy rulebase shown in Figure 2.8, determine:

(a) The membership values of the input windows *e* and *ce*.
(b) The max-min fuzzy inference equations.
(c) The crisp control signal *u(t)*.
when *e* = -3 and *ce* = 0

Solution

(a) When *e* = -3 and *ce* = 0 .3 are mapped onto the input fuzzy windows, they are referred to as fuzzy singletons. From Figure 2.7

$$e = -3 \quad \mu_{NS}(e) = 0.5 \quad \mu_{NM}(e) = 0.5 \tag{2.35}$$

ce = 0 .3, using similar triangles:

$$\frac{1}{0.33} = \frac{\mu_Z(ce)}{(0.33 - 0.3)} \tag{2.36}$$

$$\mu_Z(ce) = 0.09$$

And

$$\frac{1}{0.33} = \frac{\mu_{PS}(ce)}{0.3}$$
$$\mu_{PS}(ce) = 0.91 \tag{2.37}$$

(b) The rules that are 'hit' in the rulebase in Figure 2.8 are

$$\begin{aligned} &\cdots OR\ IF\ e\ is\ NS\ AND\ ce\ is\ Z \\ &OR\ IF\ e\ is\ NS\ AND\ ce\ is\ PS \\ &THEN\ u = NS \end{aligned} \tag{2.38}$$

$$\begin{aligned} &\cdots OR\ IF\ e\ is\ NM\ AND\ ce\ is\ Z \\ &OR\ IF\ e\ is\ NM\ AND\ ce\ is\ PS \\ &THEN\ u = NM \end{aligned} \tag{2.39}$$

Applying max-min inference to equation (2.38):

$$\mu_{NS}(u) = \max[\min(\mu_{NS}(e), \mu_Z(ce)), \min(\mu_{NS}(e), \mu_{PS}(ce))] \tag{2.40}$$

Inserting values into (2.40):

$$\begin{aligned} \mu_{NS}(u) &= \max[\min(0.5,0.09), \min(0.5,0.91)] \\ &= \max[0.09,0.5] = 0.5 \end{aligned} \tag{2.41}$$

and similarly with equation (2.39)

$$\begin{aligned} \mu_{NM}(u) &= \max[\min(\mu_{NM}(e), \mu_Z(ce)), \min(\mu_{NM}(e), \mu_{PS}(ce))] \\ \mu_{PS}(u) &= \max[\min(0.5,0.09), \min(0.5,0.91)] \\ &= \max[0.09,0.5] = 0.5 \end{aligned} \tag{2.42}$$

Using equations (2.41) and (2.42) to 'clip' the output window in Figure 2.9, the output window is now as illustrated in Figure 2.11.

(c) Due to the symmetry of the output window in Figure 2.11, from observation,
the crisp control signal is:

$$u(t) = -4{,}5$$

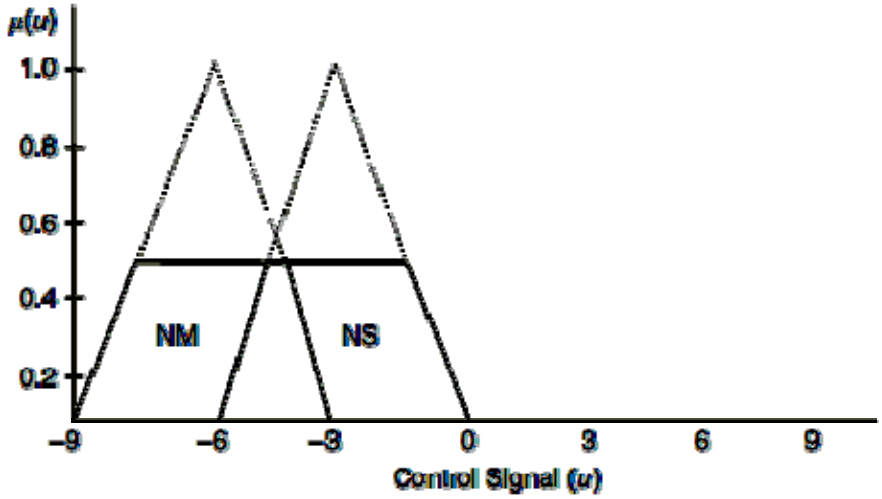

Figure 2.11 Fuzzy output window for Example 2.2.

2.3 Trajectory generation

The dynamics of the robot requires the imposition of a realizable trajectory of reference in order to ensure the displacement of the end effector of the robot from an initial point q_0 to the end point q_{end} with acceptable control on the articulation. The choice of this trajectory is connected to the evolution of the position, the speed and the acceleration desired of each articulation.

Then in this memory (FLC) which used is Mamdani and for testing this controller we use tow trajectory first a circle in space and second LEAHY trajectory.

First circle in space:

$$\begin{cases} \theta_1 = 0 \\ \theta_2 = 2*t \\ \theta_3 = -2*t \end{cases} \tag{2.43}$$

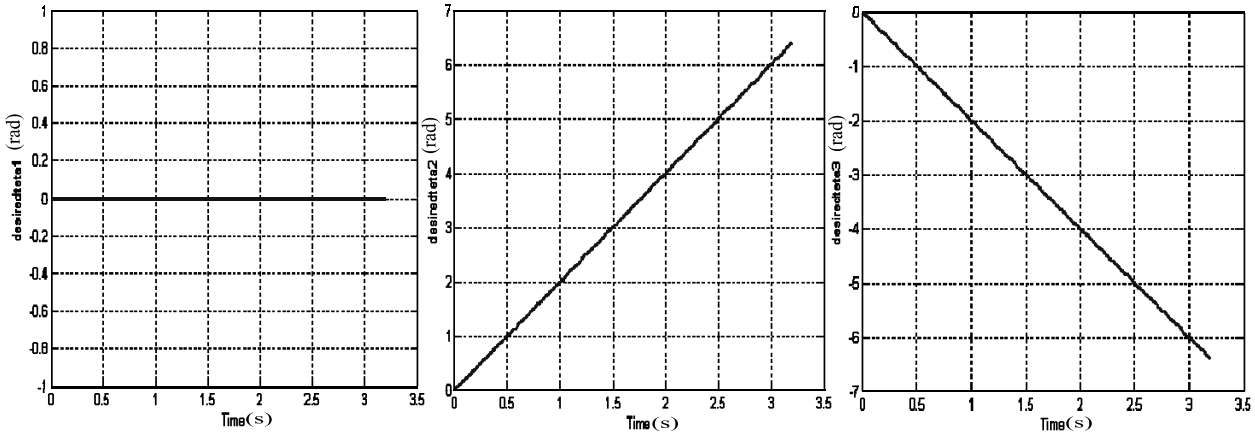

Figure 2.12 Circle in space

Second LEAHY trajectory:

For the robot of the PUMA type there exists a cycloid trajectory test Figure 2.13 proposed by LEAHY[17]. The different articulation move respectively from position {-50°, -135°, 135°} to the position {45,-85°,30°} in a time of movement equal to 1,5 seconds.

This trajectory is selected because it excites all the dynamics of this arm manipulator.

$$\theta_{di} = \begin{cases} \theta_{di}(0) + \dfrac{D_i}{2\pi}\left[2\pi\dfrac{t}{t_{end}} - \sin\left(2\pi\dfrac{t}{t_{end}}\right)\right] & for \quad 0 \le t \le t_{end} \\ \theta_{di}(t_{end}) & for \quad t_{end} \prec t \\ D_i = \theta_{di}(t_{end}) - \theta_{di}(0) & \end{cases} \tag{2.44}$$

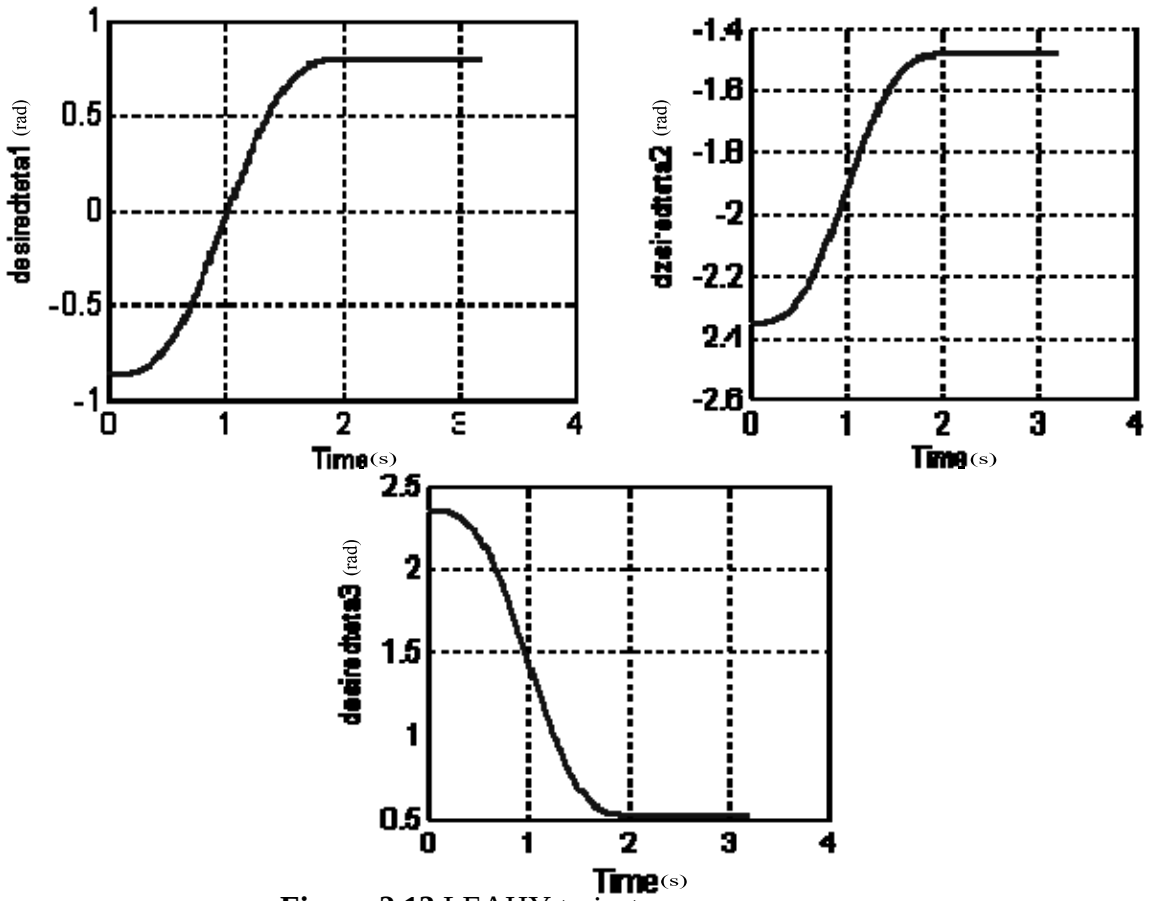

Figure 2.13 LEAHY trajectory

2.4 Type-1 Fuzzy control of PUMA560 with 3DOF

In Figure 2.14 we show the structure type-1 FLC of PUM560 with 3DOF, the regulator which we use is five classes, do mean has 25 rule bases, the rule base table in Figure 2.15 and in Figure2.16 fuzzy sets for error and change error and out put of control *T*. All the gains of type-1 fuzzy controller we do tuning until get good positions with lower error in ideal case.

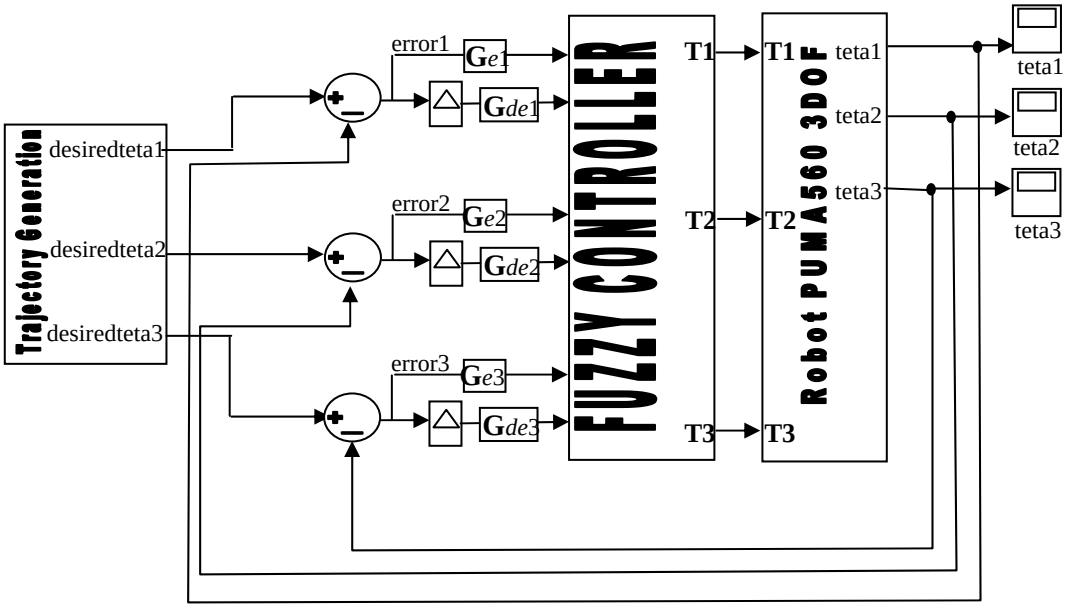

Figure 2.14 Structure type-1 FLC of PUMA560 3DOF

Velocity error						
Position error		**LN**	**SN**	**Ze**	**SP**	**LP**
	LN	LN	LN	LN	SN	Ze
	SN	LN	LN	SN	Ze	SP
	Ze	LN	SN	Ze	SP	LP
	SP	SN	Ze	SP	LP	LP
	LP	Ze	SP	LP	LP	LP

Figure 2.15 Rule Base table[39]

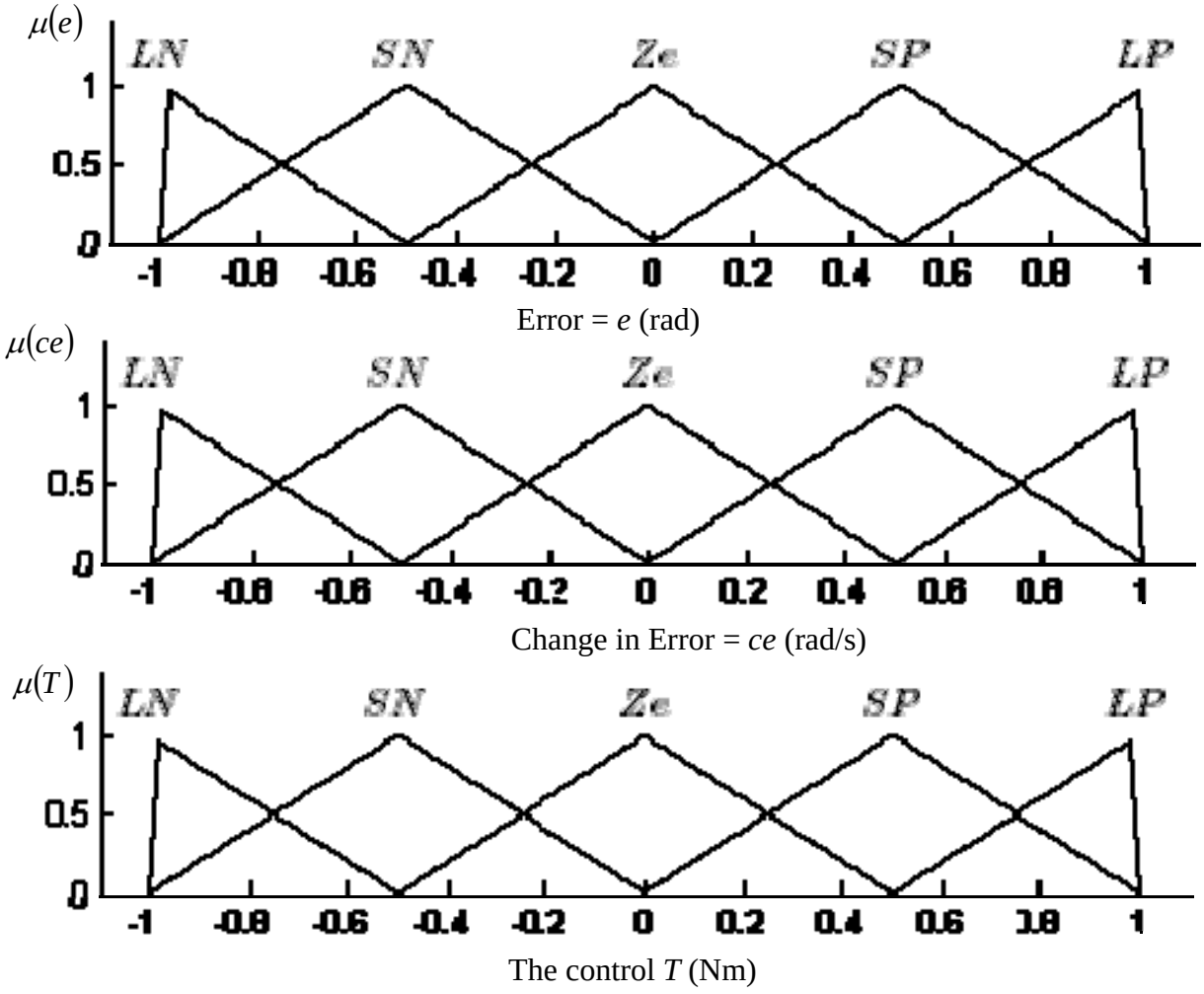

Figure 2.16 Fuzzy set for each articulation.

2.4.1 Result of simulation with circle trajectory

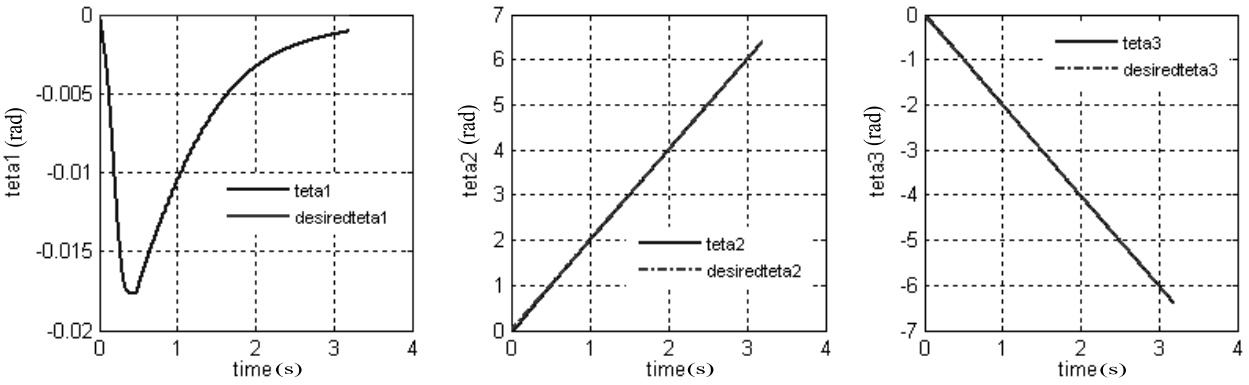

Figure 2.17 Position of joints 1,2,3 (rad)

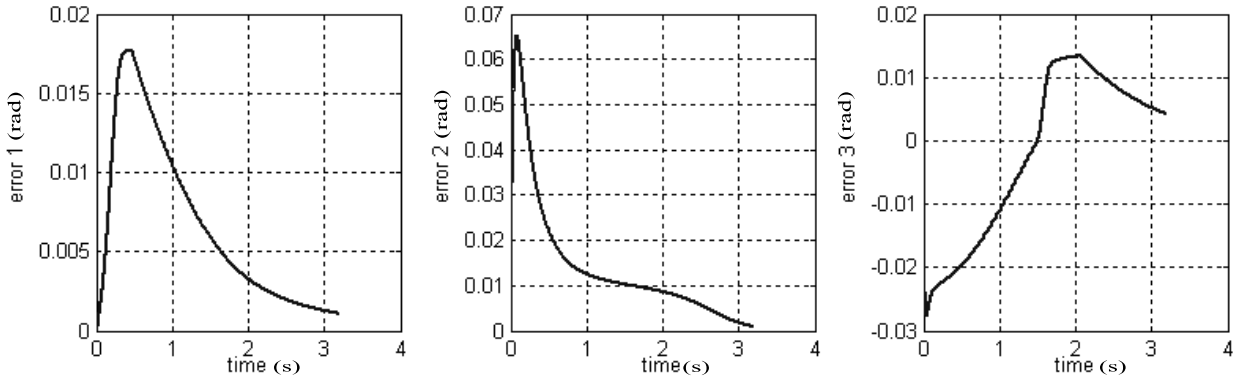

Figure 2.18 Position error of joints 1,2,3 (rad)

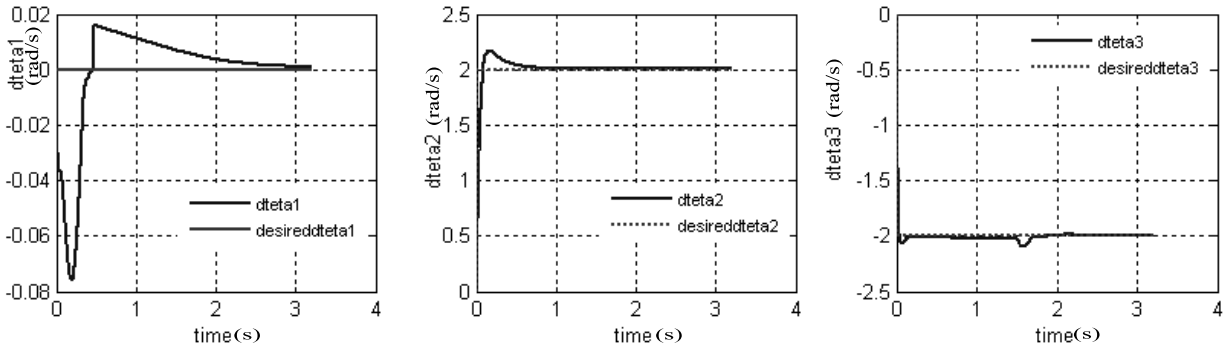

Figure 2.19 Velocity of joints 1,2,3 (rad/s)

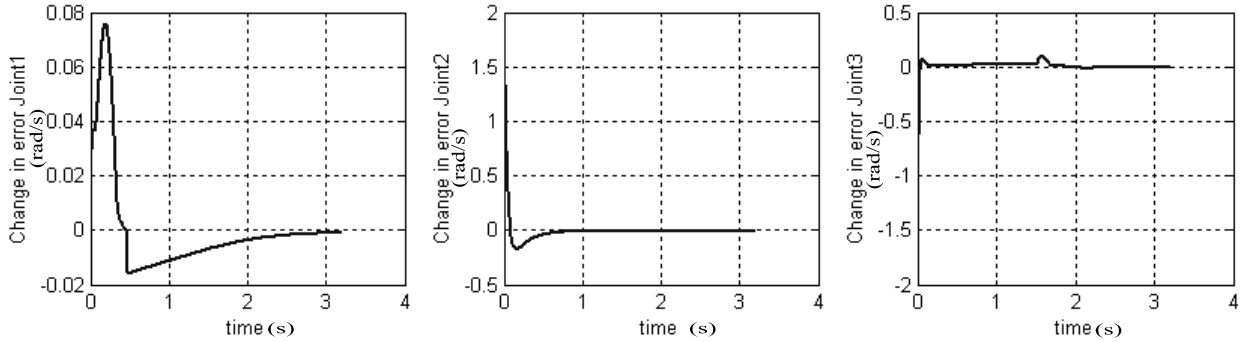

Figure 2.20 Velocity error of joints 1,2,3 (rad/s)

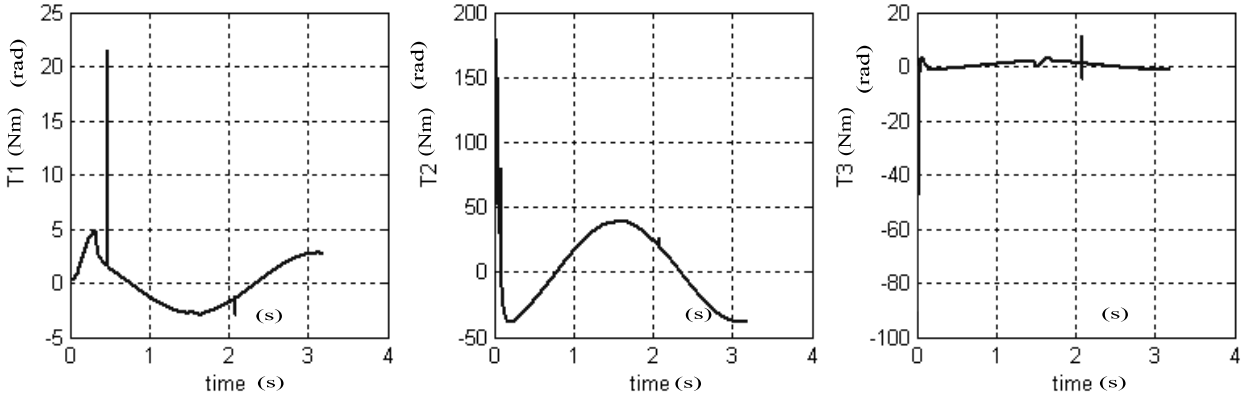

Figure 2.21 Torque inputs of the robot joints 1,2,3 (Nm).

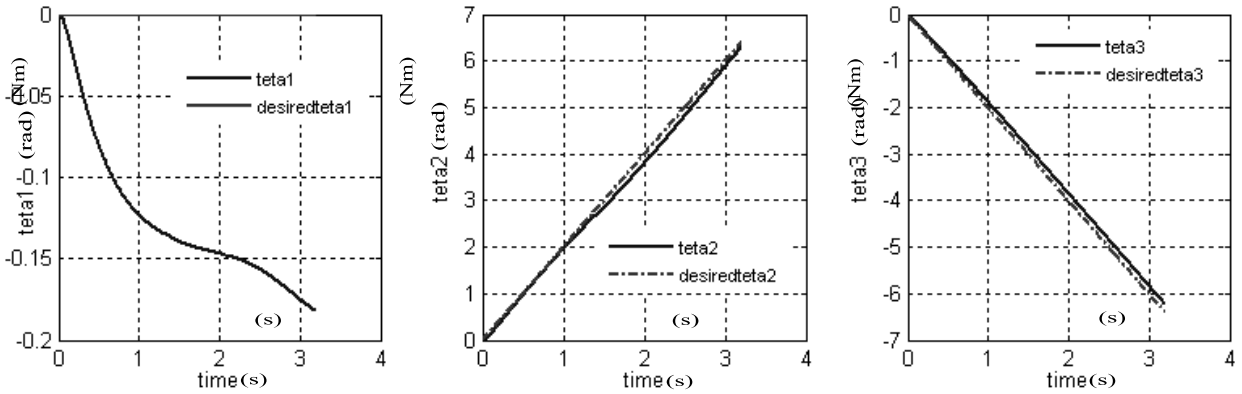

Figure 2.22 Position of joints 1,2,3 (rad) with white noisy in measure of position.

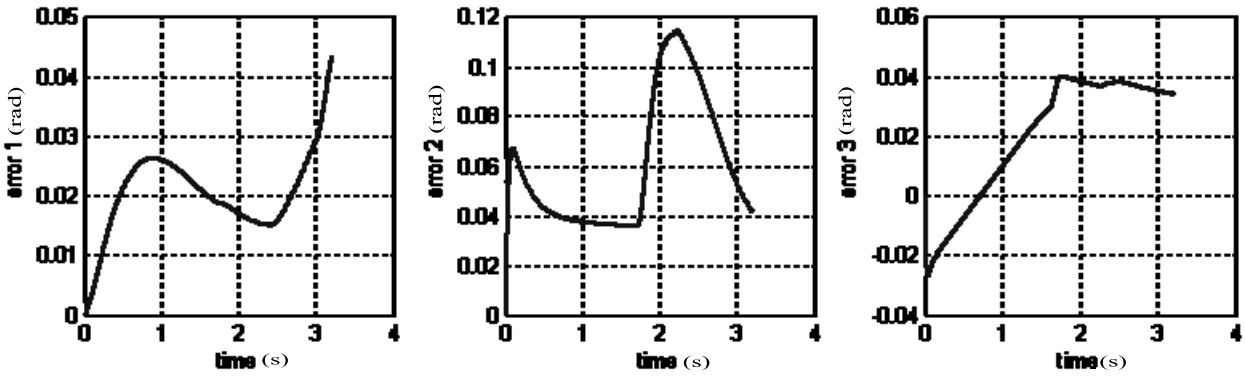

Figure 2.23 Position error of joints 1,2,3 (rad) with white noisy.

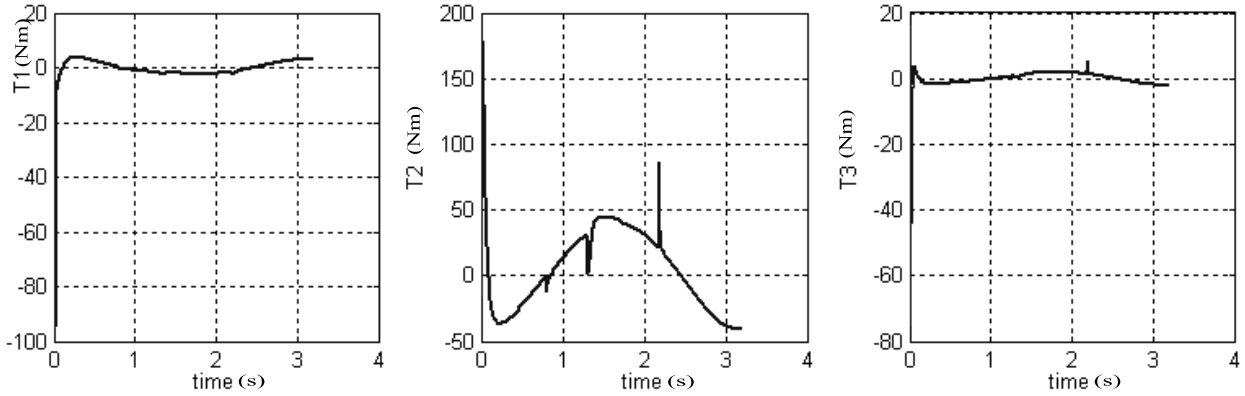

Figure 2.24 Torque inputs of the robot joints 1,2,3 (Nm) with white noisy.

2.4.2 Result of simulation with LEAHY trajectory

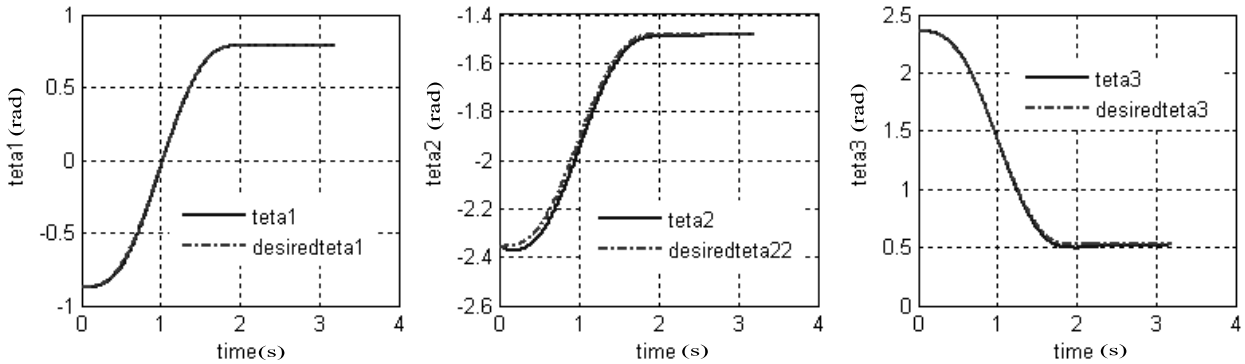

Figure 2.25 Position of joints 1,2,3 (rad).

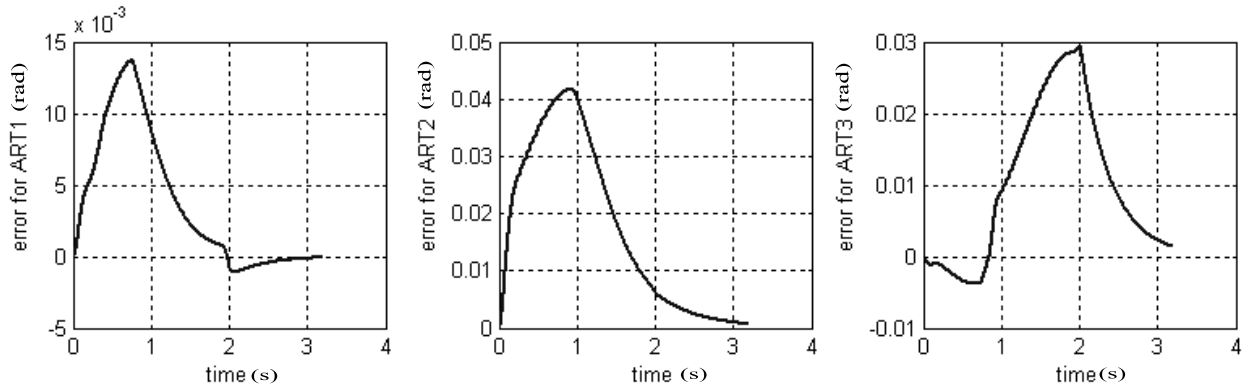

Figure 2.26 Position error of joints 1,2,3 (rad).

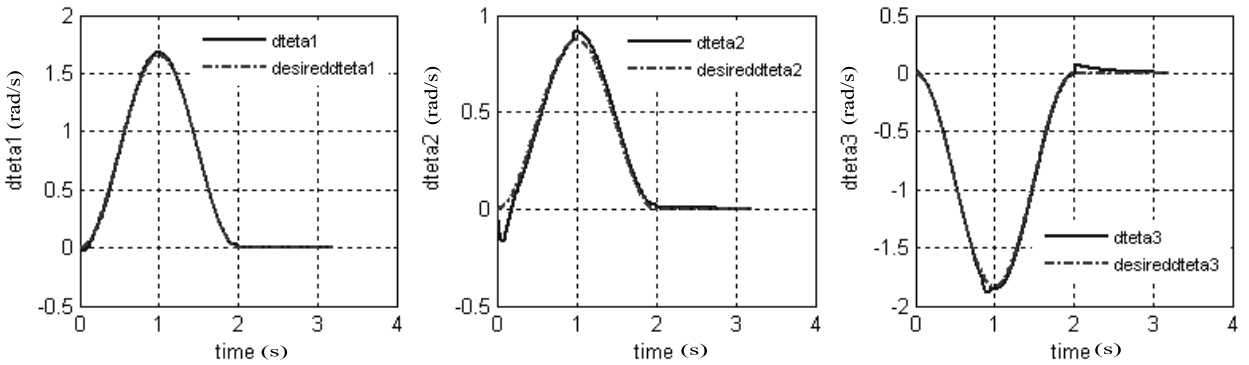

Figure 2.27 Velocity of joints 1,2,3 (rad/s).

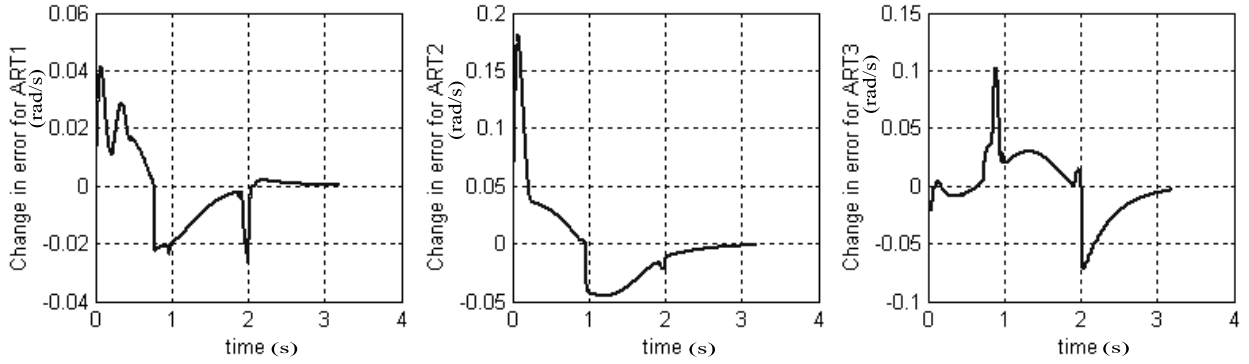

Figure 2.28 Velocity change error of joints 1,2,3 (rad/s).

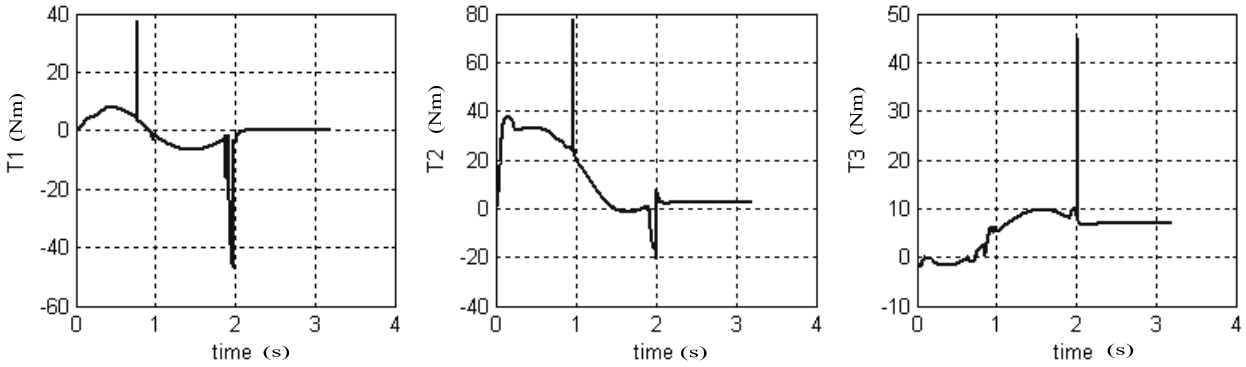

Figure 2.29 Torque inputs of the robot joints 1,2,3 (Nm).

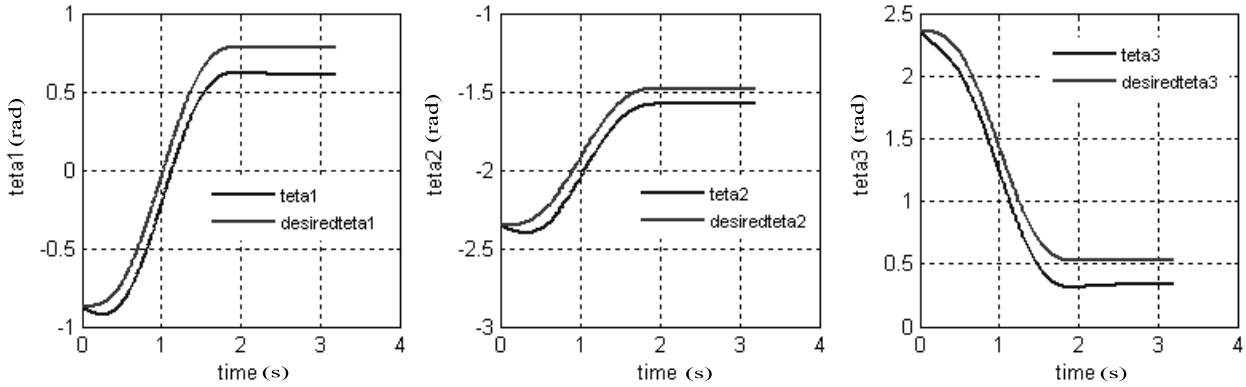

Figure 2.30 Position of joints 1,2,3 (rad) with white noisy.

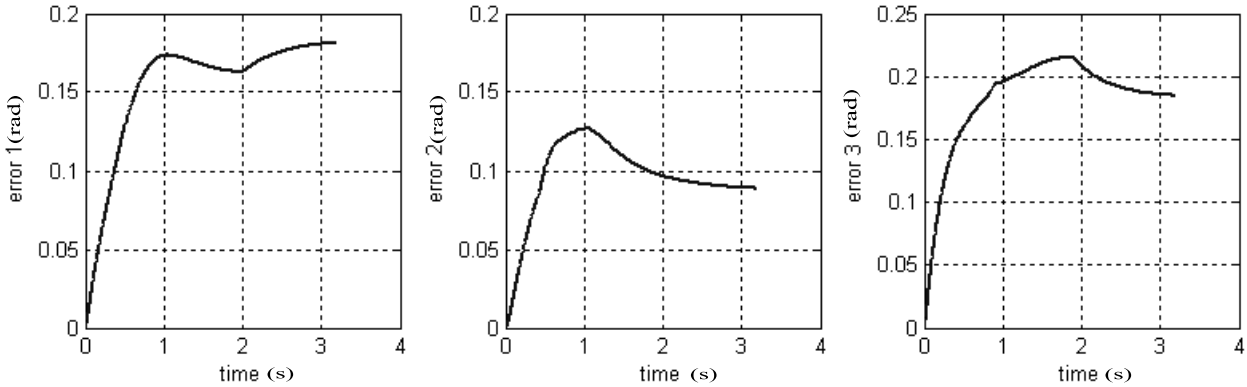

Figure 2.31 Position error of joints 1,2,3 (rad) with white noisy.

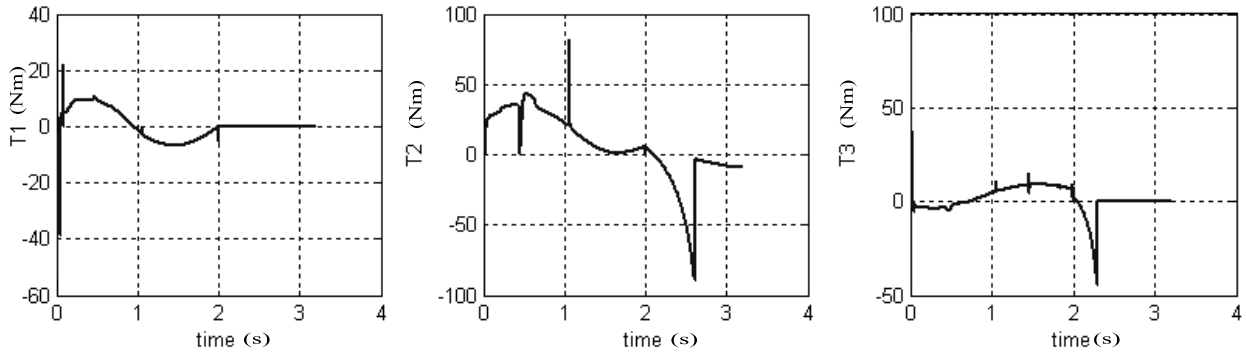

Figure 2.32 Torque inputs of the robot joints 1,2,3 (Nm) with white noisy.

By visual inspection from from Figures 2.17 to Figure 2.32 we can show that:

- Good position in ideal case and with low position error.
- Bad position in presence of uncertainty big position error.
- The positions and velocities of joints are continuous.
- The control torques of the joints 1,2,3 are limited and don't pass the maximum torque for each joints.

2.5 Conclusion

In this chapter, we have studies and developed type-1 fuzzy controller applies to the problem of the following of trajectory of robots manipulators we have tests two trajectory rings and trajectory of LEAHY, the experience and knowledge of human experts are needed to decide both the membership functions and the rules based on the available linguistic or numeric information. The simulation effectuated on the robot manipulator PUMA560 with 3DOF. The results of simulations prove that type-1 FLC have good position with low error in ideal case (In uncertainty absence) but with uncertainty presence have bad position. In the following chapters, we will perform and analysis of the interval type-2 FLC responses with same robot.

Chapter 3

Type-2 Fuzzy logic controller

3.1.1 Introduction

We introduce in this chapter a new area in fuzzy logic, which is called type-2 fuzzy logic were initially defined by Zadeh [21][24]. Basically, a type-2 fuzzy set is a set in which we also have uncertainty about the membership function. Of course, type-2 fuzzy systems consist of fuzzy if-then rules, which contain type-2 fuzzy sets. We can say that type-2 fuzzy logic is a generalization of conventional fuzzy logic (type-1) in the sense that uncertainty is not only limited to the linguistic variables but also is present in the definition of the membership functions.

Fuzzy Logic Systems are comprised of rules. Quite often, the knowledge that is used to build these rules is uncertain. Such uncertainty leads to rules whose antecedents or consequents are uncertain, which translates into uncertain antecedent or consequent membership functions [22]. Type-1 fuzzy systems (like the ones seen in the previous chapter), whose membership functions are type-1 fuzzy sets, are unable to directly handle such uncertainties. We describe in this chapter, type-2 fuzzy systems, in which the antecedent or consequent membership functions are type-2 fuzzy sets. Such sets are fuzzy sets whose membership grades themselves are type-1 fuzzy sets; they are very useful in circumstances where it is difficult to determine an exact membership function for a fuzzy set [22].

In what follows, we shall first introduce t is characterized by a type-2 membership function he basic concepts of type-2 fuzzy sets, and type-2 fuzzy reasoning after we explain how we can apply it on PUMA560 manipulator robot with simulation result.

3.2 Notations and terminologies

3.2.1 Type-2 Fuzzy sets

A type-2 fuzzy set, denoted X , is characterized by a type-2 membership function $\mu_{\tilde{A}}(x,u)$, where $x \in X$ and $u \in J_x \subseteq [0,1]$ can write it same as[27] [30]:

$$\tilde{A} = \{ (x,u), 0 \le \mu_{\tilde{A}}(x,u) \le 1 \,|\, \forall x \in X, \forall u \in J_x \subseteq [0,1] \} \tag{3.1}$$

With:

$x \in X$: Primary variable.

$u \in J_x$: Secondary variable.

The equations (3.1) show that the membership function of type-2 fuzzy set $\mu_{\tilde{A}}(x,u)$ is three-dimensional.

$\tilde{A}$ Can also be expressed as:

$$\tilde{A} = \int_{x \in X} \int_{u \in J_x} \mu_{\tilde{A}}(x,u)/(x,u); \quad J_x \in [0,1] \tag{3.2}$$

Where $\iint$ denotes union over all admissible x and u . For discrete universes of discourse $\int$ is replaced by $\sum$.

3.2.2 Representation type-2 membership function

A two-dimensional graphic of type-2 membership function is shown on figure 3.1. [28]

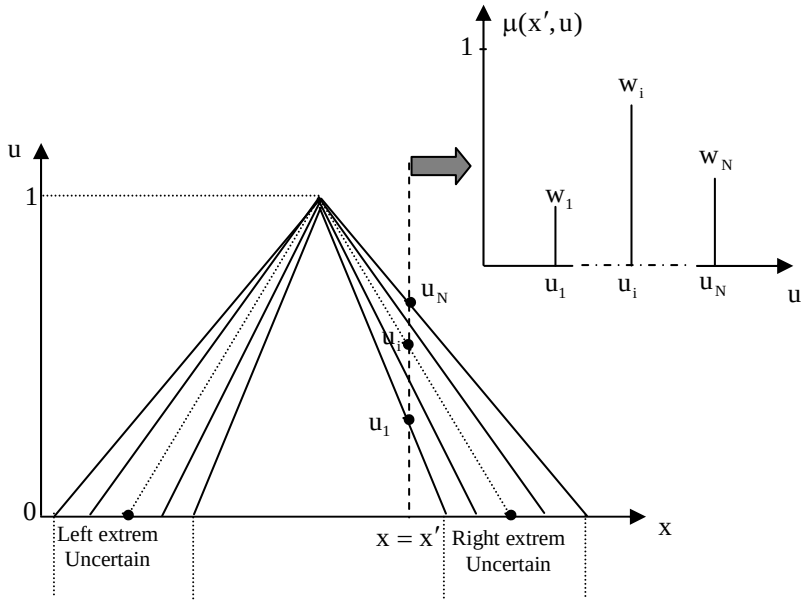

Figure 3.1 Triangular membership function

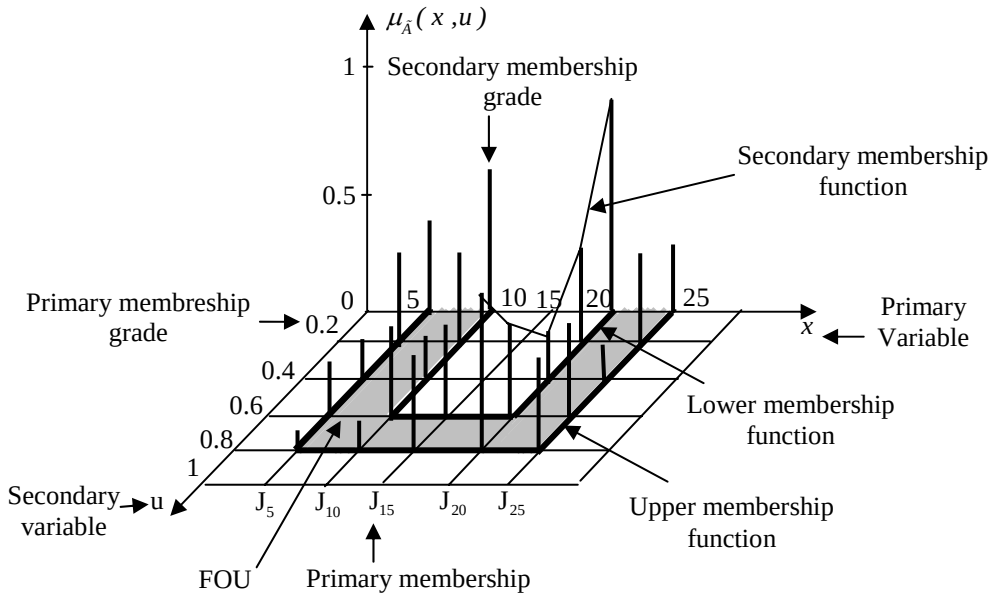

Figure 3.2 is a three-dimensional representation the of type-2 membership function. In this case x and u are as discrete [27]**.**

3.2.3 vertical-slice

At each value of x, say $x = x'$, the 2D plane whose axes are u and $\mu_{\tilde{A}}(x',u)$is called a vertical slice [27] [30] of $\mu_{\tilde{A}}(x,u)$. A secondary membership function is a vertical slice of $\mu_{\tilde{A}}(x,u)$. It is It $\mu_{\tilde{A}}(x=x',u)$ for $x' \in X$ and $\forall u \in J_{x'} \subseteq [0,1]$.

The figure 3.3 has five vertical slices associated with it. The secondary membership function at x = 20, is in figure 3.4

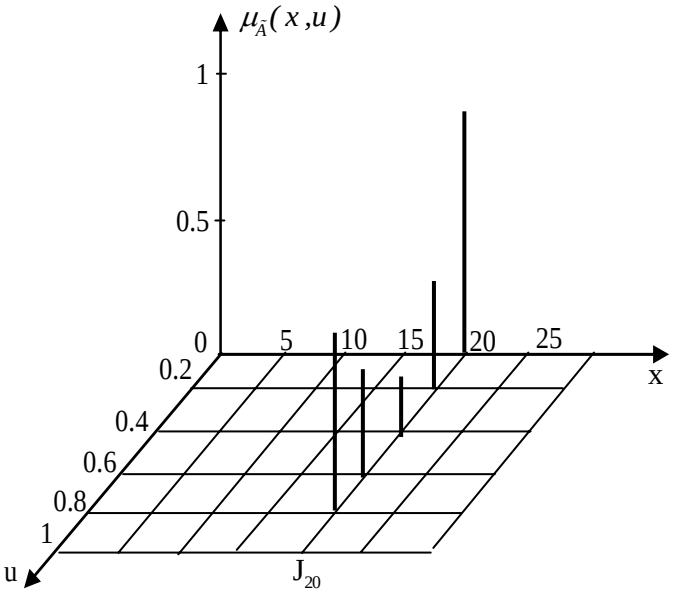

Figure 3.3 Fuzzy set for *x*=20.

3.2.4 Secondary membership function

It represents a secondary set of type-1. For all $x' \in X$ and $\forall u \in J_{x'} \subseteq [0,1]$, secondary membership function is given by [27] [29]:

$$\mu_{\tilde{A}}(x',u) \equiv \mu_{\tilde{A}}(x') = \int_{u \in J_{x'}} f_{x'}(u)/u \quad \text{---} \quad J_{x'} \in [0,1] \ \ et \ \ 0 \le f_{x'}(u) \le 1 \tag{3.3}$$

Since $\forall x' ; x' \in X$, we can omit dot in $\mu_{\tilde{A}}(x')$ and adopt the notation $\mu_{\tilde{A}}(x)$ for the secondary membership function, which is a type-1 fuzzy membership function.

While being based on the concept of the secondary sets, it is possible to reinterpret a type-2 fuzzy set as being the union of all the secondary sets, as follows:

$$\tilde{A} = \{ (x, \mu_{\tilde{A}}(x)) \,|\, \forall x \in X \} \tag{3.4}$$

Or same as:

$$\tilde{A} = \int_{x \in X} \mu_{\tilde{A}}(x) \Big/ x = \int_{x \in X} \left[\int_{u \in J_x} f_x(u)/u \right] \Big/ x \qquad J_x \subseteq [0,1] \tag{3.5}$$

In the case X and J_x are discrete, the equation (3.5) becomes:

$$\tilde{A} = \sum_{x_i \in X} \mu_{\tilde{A}}(x_i)/x_i = \sum_{x_i \in X} \left[\sum_{u_i \in J_x} f_x(u_i) \Big/ u \right] \Big/ x_i \qquad J_x \subseteq [0,1] \tag{3.6}$$

3.2.5 Primary membership

The domain of a secondary membership function is called the primary membership of x [27] [29]. In (3.5), J_x is the primary membership of x, where for $\forall x \in X$, $J_x \subseteq [0,1]$.

3.2.6 Secondary membership grade

The amplitude of a secondary membership function is called a secondary grade[30], denote by $f_x(u)$.

3.2.7 Footprint of uncertainty (FOU)

Uncertainty in the primary memberships of a type-2 fuzzy set $\tilde{A}$ consists of a bounded region that we call the footprint of uncertainty (FOU) [27] [30]. It is the union of all primary memberships.

$$FOU(\tilde{A}) = \bigcup_{x \in X} J_x \tag{3.7}$$

The shaded region in Figure 3.2 is the FOU. Other examples of FOUs are given in (3.4). The term footprint of uncertainty is very useful, because it not only focuses our attention on the uncertainties inherent in a specific type-2 membership function, whose shape is a direct consequence of the nature of these uncertainties, but it also provides a very convenient verbal description of the entire domain of support for all the secondary grades of a type-2 membership function. It also lets us depict a type-2 fuzzy set graphically in two-dimensions instead of three dimensions, and in so doing lets us overcome the first difficulty about type-2 fuzzy sets-their three-dimensional nature which makes them very difficult to draw. The shaded FOUs imply that there is a distribution that sits on top of it-the new third dimension of type-2 fuzzy sets.

What that distribution looks like depends on the specific choice made for the secondary grades. When they all equal one, the resulting type-2 fuzzy sets are called interval type-2 fuzzy sets. Such sets are the most widely used type-2 fuzzy sets to date.

3.2.8 Upper and lower membership function

An “upper membership function” and a “lower membership functions” are two type-1 membership functions that are bounds for the FOU of a type-2 fuzzy set $\tilde{A}$. The upper membership function is associated with the upper bound of $FOU\left(\tilde{A}\right)$ and denote by $\overline{u}_{\tilde{A}}(x)$. The lower membership function is associated with the lower bound of $FOU\left(\tilde{A}\right)$ and denote by $\underline{u}_{\tilde{A}}(x)$ [27] [30].

$$\begin{aligned} \overline{u}_{\tilde{A}}(x) &= \overline{FOU(\tilde{A})} \qquad \forall x \in X \\ \underline{u}_{\tilde{A}}(x) &= \underline{FOU(\tilde{A})} \qquad \forall x \in X \end{aligned} \tag{3.8}$$

3.2.9 Principal membership function

The principal membership function of type-2 fuzzy set, denote $\mu_{\tilde{A}}^{prin}(x)$ is defined as the union of all the points which satisfied the following condition[27] [30]:

$$\mu_{\tilde{A}}^{prin}(x) = \int_{x \in X} u/x \ , \ \forall x \in X \ , u \in J_x \subseteq [0,1], \ f_x(u) = 1 \tag{3.9}$$

3.3 Operations of type-2 fuzzy sets

In this section we describe the set theoretic operations of type-2 fuzzy sets [19] [20]. We are interested in the case of type-2 fuzzy sets, whose secondary membership functions are type-1 fuzzy sets. To compute the union, intersection, and complement of type-2 fuzzy sets, we need to extend the binary operations of minimum (or product) and maximum, and the unary operation of negation, from crisp numbers to type-1 fuzzy sets. The tool for computing the union, intersection, and complement of type-2 fuzzy sets is Zadeh’s extension principle [18].

3.3.1 Extension principle

$A_1,...,A_n$, n type-1 fuzzy sets whose universe of discourses are $X_1,...,X_n$ respectively. The principle of extension of Zadeh announces that the image of the sets $A_1,...,A_n$ by a relation f is a type-1 fuzzy set defined as [18]:

$$f(A_1,\cdots,A_n) = \int_{x_1 \in X_1} \cdots \int_{x_n \in X_n} \mu_{A_1}(x_1) * \cdots * \mu_{A_n}(x_n) / f(x_1,\cdots,x_n) \tag{3.10}$$

* denote T-norm, $\mu_{A_i}(x_i)$ is grade membership of x_i in set A_i .

3.3.2 Union of type-2 fuzzy sets (JOIN operation)

Consider two type-2 fuzzy sets $\tilde{A}$ and $\tilde{B}$ defined on universe of discourse X and their secondary membership function $\mu_{\tilde{A}}(x)$ and $\mu_{\tilde{B}}(x)$ respectively.

Union of $\tilde{A}$ and $\tilde{B}$, denote by $\tilde{A} \cup \tilde{B}$ is type-2 fuzzy set its membership function $\mu_{\tilde{A}\cup\tilde{B}}(x,v)$ is defined by[27] [30]:

$$\tilde{A} \cup \tilde{B} \Leftrightarrow \mu_{\tilde{A}\cup\tilde{B}}(x,v) = \int_{x \in X} \mu_{\tilde{A}\cup\tilde{B}}(x) / x = \int_{x \in X} \left[\int_{v \in J_x^{\tilde{A}\cup\tilde{B}} \subseteq [0,1]} h_x(v) / v \right] \Big/ x \tag{3.11}$$

$h_x(v)$: Secondary membership grade of the union set.

$J_x^{\tilde{A}\cup\tilde{B}}$: Primary membership of the type-2 fuzzy set $\tilde{A} \cup \tilde{B}$.

Secondary membership function of the union set:

$$\int_{v \in J_x^{\tilde{A}\cup B}} h_x(v) / v = f\left(\int_{u \in J_x^{\tilde{A}} \subseteq [0,1]} f_x(u) / u , \int_{w \in J_x^{\tilde{B}} \subseteq [0,1]} g_x(w) / w \right) \equiv f(\mu_{\tilde{A}}(x), \mu_{\tilde{B}}(x)) \tag{3.12}$$

$f_x(u)$ and $g_x(w)$ are secondary membership grade of the sets $\tilde{A}$ and $\tilde{B}$.

$J_x^{\tilde{A}}$ and $J_x^{\tilde{B}}$ primary membership $\tilde{A}$ and $\tilde{B}$ respectively.

By the principle of extension in the equation (3.17), it comes:

$$f\Big(\int_{u\in J_x^{\tilde{A}}\subseteq[0,1]} f_x(u)/u\,,\ \int_{w\in J_x^{\tilde{B}}\subseteq[0,1]} g_x(w)/w\Big)=\int_{u\in J_x^{\tilde{A}}}\int_{w\in J_x^{\tilde{B}}} f_x(u)*g_x(w)/f(u,w)\equiv\mu_{\tilde{A}}(x)\cup\mu_{\tilde{B}}(x) \quad (3.13)$$

$\cup$ Denote union, if f is maximum operation denote it by $\vee$, secondary membership function of union set is:

$$\mu_{\tilde{A}\cup\tilde{B}}(x)=\int_{u\in J_x^{\tilde{A}}}\int_{w\in J_x^{\tilde{B}}} f_x(u)*g_x(w)/(u\vee w);\ \ x\in X \quad (3.14)$$

In the discrete case, the equation (3.19) is same as:

$$\mu_{\tilde{A}\cup\tilde{B}}(x)=\sum_{u_i\in J_x^{\tilde{A}}}\sum_{w_j\in J_x^{\tilde{B}}} f_x(u_i)*g_x(w_j)/(u_i\vee w_j) \quad (3.15)$$

3.3.3 Intersection of type-2 fuzzy sets (MEET operation)

the intersection of the $\tilde{A}$ and $\tilde{B}$, denote by $\tilde{A}\cap\tilde{B}$, is type-2 fuzzy set their membership function $\mu_{\tilde{A}\cap\tilde{B}}(x,v)$ defined by [27] [30]:

$$\tilde{A}\cap\tilde{B}\Leftrightarrow\mu_{\tilde{A}\cap\tilde{B}}(x,v)=\int_{x\in X}\mu_{\tilde{A}\cap\tilde{B}}(x)/x \quad (3.16)$$

The secondary membership function of the intersection set is:

$$\mu_{\tilde{A}\cap\tilde{B}}=\int_{u\in J_x^{\tilde{A}}}\int_{w\in J_x^{\tilde{B}}} f_x(u)*g_x(w)/(u\wedge w)\equiv\mu_{\tilde{A}}(x)\cap\mu_{\tilde{B}}(x) \quad (3.17)$$

$\cap$: MEET operation.
$\wedge$: MIN operation.

In the discrete case the equation (3.17) it becomes same as:

$$\mu_{\tilde{A}\cap\tilde{B}}(x)=\sum_{u_i\in J_x^{\tilde{A}}}\sum_{w_j\in J_x^{\tilde{B}}} f_x(u_i)*g_x(w_j)/(u_i\wedge w_j) \quad (3.18)$$

3.3.4 Complement of type-2 fuzzy set

The complement of the $\tilde{A}$, denote $\bar{\tilde{A}}$, is a type-2 fuzzy set associated with membership function $\mu_{\bar{\tilde{A}}}(x,v)$ defined by[27]:

$$\bar{\tilde{A}} \Leftrightarrow \mu_{\bar{\tilde{A}}}(x,v) = \int_{x \in X} \mu_{\bar{\tilde{A}}}(x) / x \tag{3.19}$$

By applying the extension principle, the secondary membership function of the complement set is:

$$\mu_{\bar{\tilde{A}}}(x) = \int_{u \in J_x^{\bar{\tilde{A}}}} f_x(u) / (1-u) \equiv \neg \mu_{\tilde{A}}(x) \; ; \; x \in X \tag{3.20}$$

$\neg$: NEGATION operation.

In the discrete case the equation (3.20) becomes:

$$\mu_{\bar{\tilde{A}}}(x) = \sum_{u_i \in J_x^{\bar{\tilde{A}}}} f_x(u_i) / (1-u_i) \tag{3.21}$$

Example 3.1 Type-2 fuzzy set operations:

In this example we illustrate the union, intersection and complement operations for two type-2 fuzzy sets $\tilde{A}$ and $\tilde{B}$, and for a particular element *x* for which the secondary membership functions in these two sets are $\mu_{\tilde{A}}(x) = 0.5/0.1 + 0.8/0.2$ and $\mu_{\tilde{B}} = 0.4/0.5 + 0.9/0.9$. Using in the operations the minimum t-norm and the maximum t-conorm, we have the following results:

$$\begin{aligned}
\mu_{\tilde{A} \cup \tilde{B}}(x) = \mu_{\tilde{A}}(x) \cup \mu_{\tilde{B}}(x) &= (0.5/0.1 + 0.8/0.2) \cup (0.4/0.5 + 0.9/0.9) \\
&= (0.5 \wedge 0.4)/(0.1 \vee 0.5) + (0.5 \wedge 0.9)/(0.1 \vee 0.9) + \\
&(0.8 \wedge 0.4)/(0.2 \vee 0.5) + (0.8 \wedge 0.9)/(0.2 \vee 0.9) \\
&= 0.4/0.5 + 0.5/0.9 + 0.4/0.5 + 0.8/0.9 \\
&= \max\{0.4, 0.4\}/0.5 + \max\{0.5, 0.8\}/0.9 \\
&= 0.4/0.5 + 0.8/0.9
\end{aligned}$$

$$\begin{aligned}\mu_{\tilde{A}\cap\tilde{B}}(x) = \mu_{\tilde{A}}(x) \cap \mu_{\tilde{B}}(x) &= (0.5/0.1 + 0.8/0.2) \cap (0.4/0.5 + 0.9/0.9) \\ &= (0.5 \wedge 0.4)/(0.1 \wedge 0.5) + (0.5 \wedge 0.9)/(0.1 \wedge 0.9) + \\ &(0.8 \wedge 0.4)/(0.2 \wedge 0.5) + (0.8 \wedge 0.9)/(0.2 \wedge 0.9) \\ &= 0.4/0.1 + 0.5/0.1 + 0.4/0.2 + 0.8/0.2 \\ &= \max\{0.4,0.5\}/0.1 + \max\{0.4,0.8\}/0.2 \\ &= 0.5/0.1 + 0.8/0.2\end{aligned}$$

$$\mu_{\tilde{\tilde{A}}}(x) = 0.5/(1-0.1) + 0.8/(1-0.2) = 0.5/0.9 + 0.8/0.8$$

3.4 General type-2 fuzzy system

The basics of fuzzy logic do not change from type-1 to type-2 fuzzy sets, [22]. A higher-type number just indicates a higher “degree of fuzziness”. Since a higher type changes the nature of the membership functions, the operations that depend on the membership functions change; however, the basic principles of fuzzy logic are independent of the nature of membership functions and hence, do not change. Rules of inference like Generalized Modus Ponens or Generalized Modus Tollens continue to apply.

The structure of the type-2 fuzzy rules is the same as for the type-1 case because the distinction between type-2 and type-1 is associated with the nature of the member-ship functions. Hence, the only difference is that now some or all the sets involved in the rules are of type-2. In a type-1 fuzzy system, where the output sets are type-1 fuzzy sets, we perform defuzzification in order to get a number, which is in some sense a crisp (type-0) representative of the combined output sets. In the type-2 case, the output sets are type-2, so we have to use extended versions of type-1 defuzzification methods. Since type-1 defuzzification gives a crisp number at the output of the fuzzy system, the extended defuzzification operation in the type-2 case gives a type-1 fuzzy set at the output. Since this operation takes us from the type-2 output sets of the fuzzy system to a type-1 set, we can call this operation “type reduction” and call the type-1 fuzzy set so obtained a “type-reduced set”. The type-reduced fuzzy set may then be defuzzified to obtain a single crisp number; however, in many applications, the type-reduced set may be more important than a single crisp number[22] [29].

Type-2 sets can be used to convey the uncertainties in membership functions of type-1 fuzzy sets, due to the dependence of the membership functions on available linguistic and numerical

information. Linguistic information, in general, does not give any information about the shapes of the membership functions. When membership functions are determined or tuned based on numerical data, the uncertainty in the numerical data, e.g., noise, translates into uncertainty in the membership functions. In all such cases, any available information about the linguistic/numerical uncertainty can be incorporated in the type-2 framework. However, even with all of the advantages that fuzzy type-2 systems have, the literature on the applications of type-2 sets is scarce. We think that more applications of type-2 fuzzy systems will come in the near future as the area matures and the theoretical results become more understandable for the general public in the fuzzy arena [30].

The general structure of a type-2 fuzzy controller (type-2 fuzzy controller: T2FC) is represented in figure 3.4

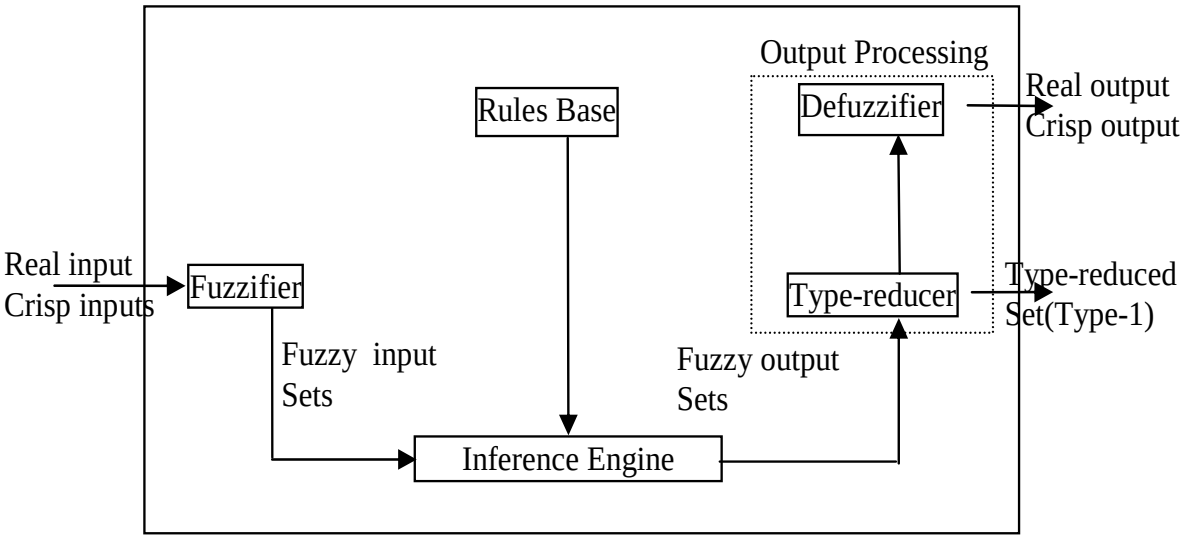

Figure 3.4 Type-2 Fuzzy Controller structure [29]

This structure is similar to that of the type-1 fuzzy controller. However, their differences in:

- The type of the membership function used.
- Procedure of adopted defuzzifier. In a T2FC, a block of reduction of the type is essential to convert the type-2 fuzzy set to a type-1fuzzy set.

3.4.1 Fuzzification

In this memory, we will consider only singleton fuzzification(Crisp input), in the input fuzzy set.

3.4.2 Rules

In the type-1 case, we generally have "IF-THEN" rules, where the *l*th rule has the form

$$"R^l : IF\ x_1\ is\ F_1^l\ and\ x_2\ is\ F_2^l\ and \ldots and\ x_p\ is\ F_p^l\ THEN\ y\ is\ G^l" \tag{3.22}$$

Where x_i's are inputs, F_i^l's are antecedent sets $(i = 1, \ldots\ldots, p)$, y is the output, and G^l are consequent sets.

The distinction between type-1 FLS and type-2 FLS is associated with the nature of the membership function, which is not important while forming rules, hence, the structure of the rules remains exactly the same in the type-2 FLS case, the only difference being that now some or all of the sets involved are of type-2, so, the *l*th rule in a type-2 FLS has the form

$$"R^l : IF\ x_1\ is\ \tilde{F}_1^l\ and\ x_2\ is\ \tilde{F}_2^l\ and \ldots and\ x_p\ is\ \tilde{F}_p^l\ THEN\ y\ is\ \tilde{G}^l" \tag{3.23}$$

Where x_i's are inputs, $\tilde{F}_i^l$'s are antecedent sets $(i = 1, \ldots\ldots, p)$, y is the output, and $\tilde{G}^l$ are consequent sets, It is not necessary that all the antecedents and the consequent be type-2 fuzzy sets. As long as one antecedent or the consequent set is type-2, we will have a type-2 FLC.

3.4.3 Inference Engine

In general, the Rules we use will have multiple antecedents connected by ands. Just as in the type-1 case, we can connect these multiple antecedents by the meet operation (corresponding to t-norm in the type-1 case).Different rules can be combined using the join operation (corresponding to t-conorm in the type-1 case), or during defuzzification.

The output of the inference engine [22] [29] consists of the fired consequent fuzzy sets. Each one of which is modified from a consequent fuzzy set by a degree of firing. This degree of firing is

obtained, in general, as a result of t-norm (meet) and t-conorm (join) operations on membership grades of the inputs.

The relation (3.23) is interpreted as a fuzzy implication type-2 defined by:

$$R^l : \tilde{F}_1^l \times ... \times \tilde{F}_p^l \rightarrow \tilde{G}^l \tag{3.24}$$

This relation is described by the membership function same as:

$$\mu_{R^l}(x_1,...,x_p,y) = \mu_{\tilde{F}_1^l \times ... \times \tilde{F}_p^l \rightarrow \tilde{G}^l}(x_1,...,x_p,y) = \left[\bigcap_{i=1}^{p} \mu_{\tilde{F}_i^l}(x_i) \right] \cap \mu_{\tilde{G}^l}(y) \tag{3.25}$$

$\tilde{F}_1^l \times ... \times \tilde{F}_p^l$ Denote the Cartesian product of $\tilde{F}_1^l,...,\tilde{F}_p^l$.

3.4.4 Type-Reduction

Observe, from figure 3.4, that the defuzzifier block in the type-1 FLC is replaced by two blocks: type-reducer and defuzzifier. We consider type-reduction in this subsection.

In a type-1 FLC, where the output sets are type-1 fuzzy sets, we perform defuzzification in order to get a number which is in some sense a crisp (type-0) representative of the combined output sets. In the type-2 case, the output sets are type-2, so we have to use "extended principle" of type-1 defuzzification methods. Since type-1 defuzzification gives a crisp number at the output of the FLS, the extended defuzzification operation in the type-2 case gives a type-1 fuzzy set at the output. Since this operation takes us from the type-2 output sets of the FLC to a type-1 set, we call this operation "type-reduction" [22] [30] and call the type-1 set so obtain a single crisp number, however, in many application, the type reduced set may be more important than a single crisp number.

There exist many kinds of type-reduction, such as centroid, center-of-sets, height and modified height, the details of which are given in [22][30]. In this memory, for illustrative purposes, we focus on center-of-sets type-reduction.

Center-of-sets type-reduction

In this method[30], each set of the consequence $\tilde{G}^l$ is replaced by its centroid. If the set of output $\tilde{G}^l$ is of type-2, its centroid $C_{\tilde{G}^l}$ is a type-1 fuzzy set. Then the weighted average of all the centroid is calculated, associating with each centroid $C_{\tilde{G}^l}$ a weight equal the degree of activation of the *l*th rule is given by $E_l(x) = \bigcap_{i=1}^{p} \mu_{\tilde{F}_i^l}(x)$. Procedure of calculation of the type-reduced set $Y_{ce}(x)$ is:

1. Discretize the output space *Y* into a suitable number of points, and compute the centroid $C_{\tilde{G}^l}$ of each consequent set on the discretized output space. These consequent centroid sets can be computed ahead of time and stored for future use.
2. Compute the degree of firing, $E_l(x)$ associated with the *l*th consequent.
3. Discretize the domain of each $C_{\tilde{G}^l}$ into a suitable number of M_l points, $l = 1,...,M$.
4. Discretize the domain of each $E_l(x)$ into a suitable number of points, say N_l $l = 1,...,M$.
5. Enumerate all the possible combinations $\{c_1,...,c_M, e_1,...,e_M\}$ such that $c_l \in C_{\tilde{G}^l}$ and $e_l \in E_l$.

   The total number of combinations will be $\prod_{l=1}^{M} M_l N_l$
6. Compute the center-of-sums type-reduced set using (3.26).

$$Y_{ce}(x) = \int_{c_1}\cdots\int_{c_M}\int_{e_1}\cdots\int_{e_M} Sup\left[\Im_{l=1}^{M}\mu_{C_{\tilde{G}^l}}(c_l) * \Im_{l=1}^{M}\mu_{E_l}(e_l)\right] \Big/ \frac{\sum_{l=1}^{M} c_l e_l}{\sum_{l=1}^{M} e_l} \tag{3.26}$$

Where $\Im$ and $*$ indicate the T-norm chosen.

3.4.5 Defuzzification

To obtain a crisp output from the type-2 FLS, we can defuzzifiy the type-reduced set[22] [30]. The most natural way of doing this seems to be by finding the centroid of the type-reduced set, however, there exist other possibilities, like choosing the unity membership point in the type-reduced set.

The defuzzification makes to transform the linguistic output of the type-reduction to numeric valued. Several methods of defuzzification were proposed in the literature [32]. But the most used method is:

Centre of area

The defuzzification determines the X-coordinate of the center of gravity y_{CG}^{*} [22] [30] of the fuzzy function:

$$y_{CG}^{*} = \frac{\int_{y} y\,\mu_Y(y)\,dy}{\int_{y} \mu_Y(y)\,dy} \tag{3.27}$$

In the discrete case:

$$y_{CG}^{*} = \frac{\sum_{i} y_i\,\mu_Y(y_i)}{\sum_{i} \mu_Y(y_i)} \tag{3.28}$$

3.5 Interval type-2 Fuzzy controller

3.5.1 Interval type-2 fuzzy set

An interval type-2 fuzzy set $\tilde{A}$ in X is defined as:

$$\tilde{A} = \int_{x\in X} \int_{u\in J_x \subseteq [0,1]} 1/(x,u) = \int_{x\in X} \left[\int_{u\in J_x \subseteq [\grave{a},1]} 1/u \right] \Big/ x \tag{3.29}$$

Where x is the primary variable with domain X, u is the secondary variable, which has domain J_x at each $x \in$ X, J_x [22] is called the primary membership of x. For interval type-2 sets, the secondary grades of $\tilde{A}$ all equal 1 [22][25] [26].

3.5.2 MEET and JOIN for Interval set

- The meet under minimum or product t-norms of *n* interval type-1 sets $A_1,...,A_n$ having domains $[l_1,r_1],...,[l_n,r_n]$ respectively, where $[l_i,r_i]\subseteq[0,1]$, $i=1,..,n$ is an interval set with domain $[l_1*...*l_n, r_1*...*r_n]$ such as[26] [31]:

$$\bigcap_{i=1}^{n} A_i = \int_{w\in[l_1*...*l_n, r_1*...*r_n]} 1/w \tag{3.30}$$

* Chosen t-norms.

- The join under maximum t-norms of *n* interval type-1 sets $A_1,...,A_n$ $A_1,...,A_n$ having domains $[l_1,r_1],...,[l_n,r_n]$ respectively, where $[l_i,r_i]\subseteq[0,1]$, $i=1,..,n$ is an interval set with domain $[l_1\vee...\vee l_n, r_1\vee...\vee r_n]$ such as:

$$\bigcup_{i=1}^{n} A_i = \int_{w\in[l_1\vee...\vee l_n, r_1\vee...\vee r_n]} 1/w \tag{3.31}$$

$\vee$ Denote max operation.

3.5.3 Inference

In interval type-2 fuzzy system using the minimum or product t-norms operations, the *l*th activated rule $\bigcap_{i=1}^{p} \mu_{\tilde{F}_i^l} = F^l(x_1,...,x_p)$ gives us interval determined by tow extreme $\underline{f}^l(x_1,...,x_n)$ and $\overline{f}^l(x_1,...,x_n)$ same as[26]:

$$F^l(x_1,...,x_n) = \left[\underline{f}^l(x_1,...,x_n), \overline{f}^l(x_1,...,x_n)\right] \equiv \left[\underline{f}^l, \overline{f}^l\right] \tag{3.32}$$

With $\underline{f}^l$ and $\overline{f}^l$ are given as:

$$\begin{aligned} \underline{f}^l &= \underline{\mu}_{\tilde{F}_1^l}(x_1) *...* \underline{\mu}_{\tilde{F}_p^l}(x_p) \\ \overline{f}^l &= \overline{\mu}_{\tilde{F}_1^l}(x_1) *...* \overline{\mu}_{\tilde{F}_p^l}(x_p) \end{aligned} \tag{3.33}$$

The output set $\mu_{\tilde{B}^l}(y)$ of the *l*th activated rule R^l is type-2 fuzzy set:

$$\mu_{\tilde{B}^l}(y) = \int_{b^l \in \left[\underline{f}^l * \underline{\mu}_{\tilde{G}^l}(y),\ \overline{f}^l * \overline{\mu}_{\tilde{G}^l}(y)\right]} 1 \Big/ b^l \quad , \quad y \in Y \tag{3.34}$$

$$\mu_{\tilde{B}}(y) = \bigcup_{l=1}^{N} \mu_{\tilde{B}^l}(y) \tag{3.35}$$

$\underline{\mu}_{\tilde{G}^l}(y)$ and $\overline{\mu}_{\tilde{G}^l}(y)$ represent upper and lower membership function of the set $\mu_{\tilde{G}^l}(y)$.

3.5.4 Type-reduction and Defuzzification

After fuzzification, fuzzy inference, type-reduction and defuzzification [26] [31] [33], we obtain a crisp output. For an interval type-2 FLC, this crisp output is the center of the type-reduced set, we know that for an interval type-2 FLC, regardless of singleton or non-singleton fuzzification, and minimum or product t-norm, the result of input and antecedent operations (firing strength) is an interval type-1 set which is determined by its left-most and right-most points $\underline{f}^l$ and $\overline{f}^l$. The fired output consequent set $\mu_{\tilde{B}^l}(y)$ of rule R^l can be obtained from the fired interval strength using (3.33). Then the fired combined output consequent set $\mu_{\tilde{B}^l}(y)$ can be computed using (3.35).

There exist many kinds of type-reduction, such as centroid, center-of-sets, height and modified height, the details of which are given in [22] and [33]. In this memory, for illustrative purposes, we focus on center-of-sets type-reduction, which can be expressed as:

$$y_{\cos}\left(W^1,\ldots,W^M,F^1,\ldots F^M\right) = \left[y_l, y_r\right] = \iint_{w^l \in \left[w_l^1, w_r^1\right], w^M \left[w_l^M, w_r^M\right]} \iint_{f^1 \in \left[\underline{f}^1, \overline{f}^1\right], f^M \in \left[\underline{f}^M, \overline{f}^M\right]} 1 \Big/ \frac{\sum_{i=1}^{M} f^i w^i}{\sum_{i=1}^{M} f^i} \tag{3.36}$$

Where y_{COS} an interval set is determined by two end points $(y_l \text{ and } y_r)$, $f^i \in \left[\underline{f}^i, \overline{f}^i\right], w^i \in W^i = \left[w_l^i, w_r^i\right], W^i$ is the centroid of the interval type-2 consequent set $\tilde{G}$ (the centroid of a type-2 fuzzy set is described in Appendix C).

Observe that $y_{COS}\left(W^1,\ldots,W^M,F^1\ldots F^M\right)$ is an interval type-1 set. So, to find $y_{COS}\left(W^1,\ldots,W^M,F^1\ldots F^M\right)$ we just need to compute the two end-points of this interval. Unfortunately, no closed-form formula is available for y_{COS}.

$$y = \frac{\sum_{i=1}^{M} f^i w^i}{\sum_{i=1}^{M} f^i} \tag{3.37}$$

The maximum value of y is y_r, and the minimum value of y is y_l. From (3.37), we see that y is a monotonic increasing function with respect to w^i, so, y_r is only associated with w_r^i, and similarly y_l is only associated with w_l^i. In the COS type-reduction method, the two end-points of $y_{COS}, (y_l \text{ and } y_r)$ depend on a mixture of $\underline{f}^i \text{or} \overline{f}^i$ values. In this case, $(y_l \text{ and } y_r)$ can be represented as:

$$y_l = \frac{\sum_{i=1}^{M} f_l^i w_l^i}{\sum_{i=1}^{M} f_l^i} \tag{3.38}$$

Where f_l^i denotes the firing strength membership grade either $\left(\underline{f}^i \text{or} \overline{f}^i\right)$ contributing to the right-most point y_l, similarly to y_r.

$$y_r = \frac{\sum_{i=1}^{M} f_r^i w_r^i}{\sum_{i=1}^{M} f_r^i} \tag{3.39}$$

Where f_r^i denotes the firing strength membership grade either $\left(\underline{f}^i \text{or} \overline{f}^i\right)$ contributing to the right-most point y_r.

In order to compute $(y_l \text{ and } y_r)$, we need to compute $\{f_l^i, i = 1,2,\ldots,M\}$ and $\{f_r^i, i = 1,2,\ldots,M\}$. This can be done using the exact computational procedure given in [31] [33]. Here we briefly provide the computation procedure for y_r. Without loss of generality, assume the w_r^is are arranged in ascending order $w_r^1 \le w_r^2 \ldots \le w_r^M$.

1. Compute y in (3.39) by initially setting $f_r^i = \frac{\overline{f}^i + \underline{f}^i}{2}$ $for\ i = 1,\ldots,M$ where $\left(\underline{f}^i \text{ and } \overline{f}^i\right)$ have been previously computed using (3.33) and let $y' = y$.
2. Find $R(1 \le R \le M-1)$ such that $w_r^R \le y_r' \le w_r^{R+1}$.
3. Compute y in (3.37) when $f_r^i = \underline{f}^i$ $for\ i \le R, and\ f_r^i = \overline{f}^i$ $for\ i \succ R, then\ set\ y_r'' = y_r$.
4. If $y'' \ne y'$ then go to step 5. If $y'' = y'$ then stop, and set $y_r = y''$.
5. Set y' equal to y'', and return to step 2.

This 5 step computation procedure has been proven to converge to the exact solution in no more than M iterations [31] [33]. Observe that in this procedure, the number R is very important. For $i \le R$, $f_r^i = \underline{f}^i$ and $for\ i \succ R$, $f_r^i = \overline{f}^i$, so y_r can be represented as:

$$y_r = y_r\left(\underline{f}^1,\ldots,\underline{f}^R,\overline{f}^{R+1},\ldots,\overline{f}^M,w_r^1,\ldots,w_r^M\right) \tag{3.40}$$

The procedure for computing y_l is very similar. Just replace w_r^i by w_l^i, and in step 2, find $L(1 \le L \le M-1)$, such that $w_l^L \le y_l' \le w_l^{L+1}$, and in step 3 $f_l^i = \overline{f}^i$ $for\ i \le L, and\ f_l^i = \underline{f}^i$ $for\ i \succ L$. Then y_l can be represented as:

$$y_r = y_r\left(\overline{f}^1,\ldots,\overline{f}^R,\underline{f}^{R+1},\ldots,\underline{f}^M,w_l^1,\ldots,w_l^M\right) \tag{3.41}$$

Because y_{COS} is an interval set, we defuzzify it using the average of $(y_l \text{ and } y_r)$, and hence, the defuzzified output of an interval type-2 FLC is:

$$output\quad of\quad Centroid = \frac{y_l + y_r}{2} \tag{3.42}$$

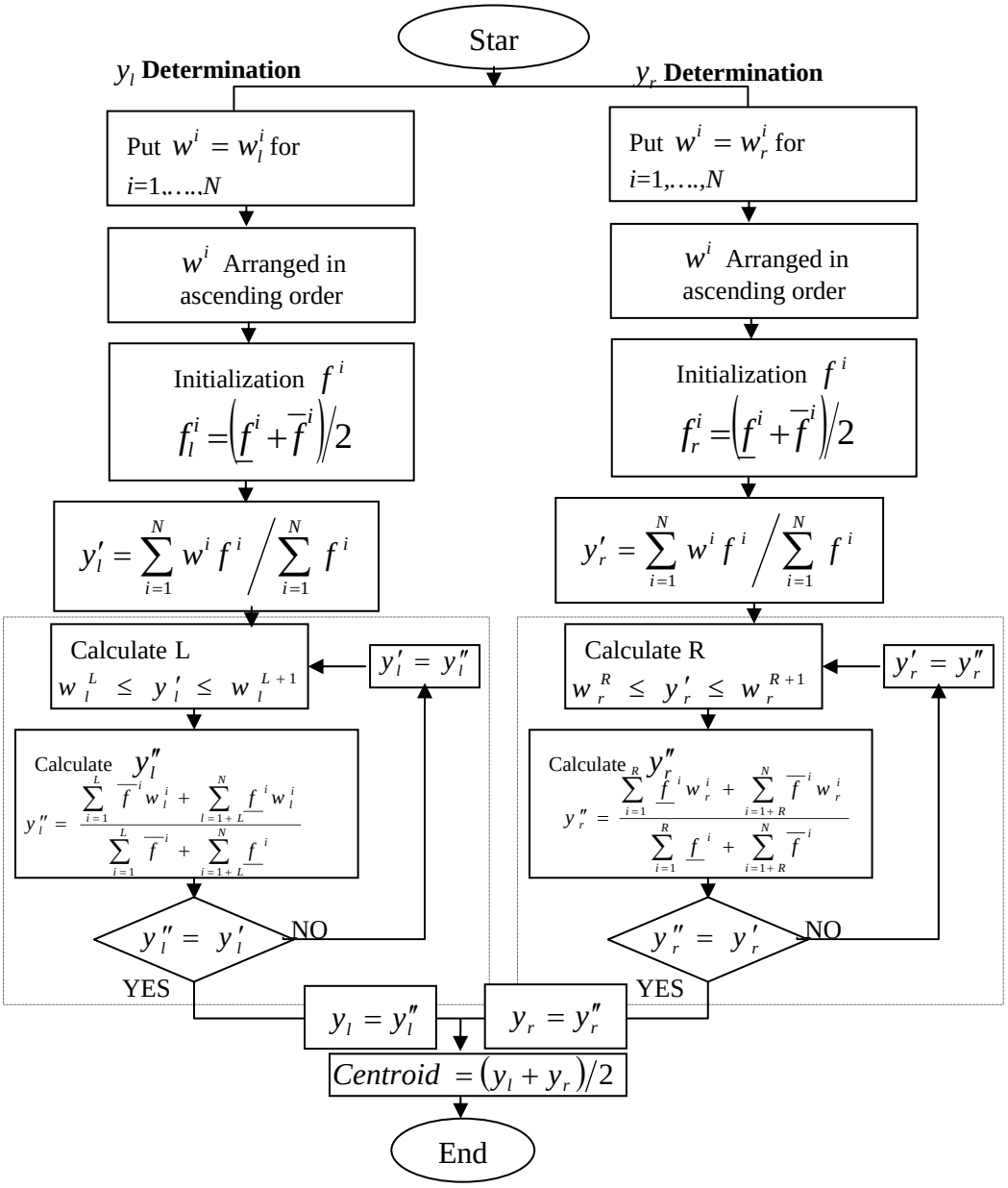

Figure 3.5 Karnik-Mendel Algorithms to locate Centroid on Interval type-2 set [31].

3.6 Interval type-2 Fuzzy control with PUMA560 3DOF

In Figure 3.6 we show the structure interval type-2 FLC with PUM560 3DOF, the regulator which we use is five classes, do mean has 25 rule bases, the rule base table in Figure 3.7 and in Figure3.8 fuzzy sets for error and change error and out put of control *T*. All the gains of Interval type-2 fuzzy controller we do tuning until get good positions with lower error in ideal case.

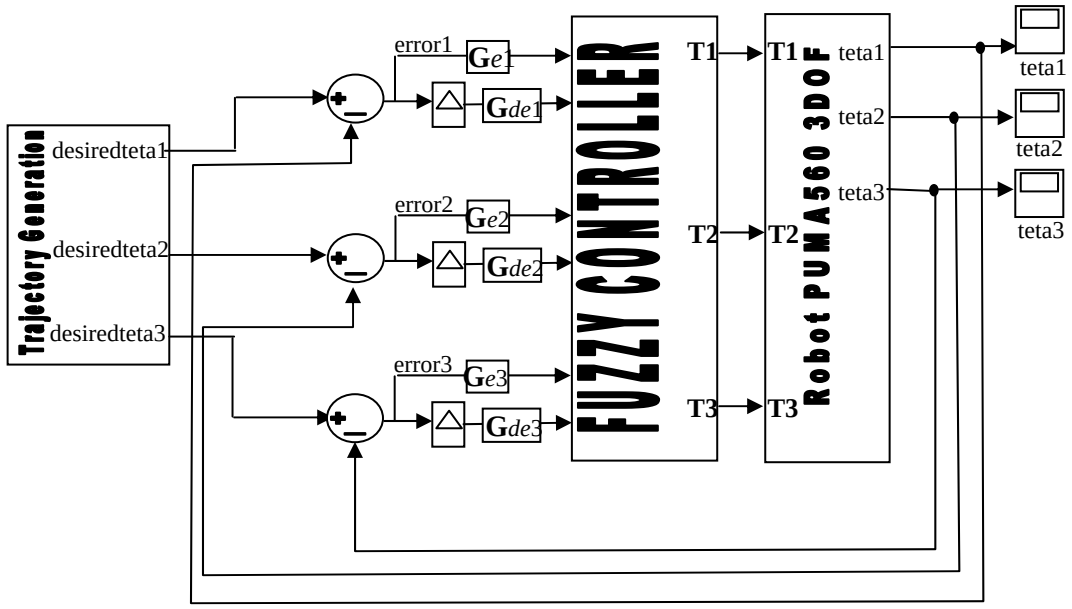

Figure 3.6 Structure Interval type-2 FLC with PUMA560 3DOF

Velocity error						
Position error		**LN**	**SN**	**Ze**	**SP**	**LP**
	LN	LN	LN	LN	SN	Ze
	SN	LN	LN	SN	Ze	SP
	Ze	LN	SN	Ze	SP	LP
	SP	SN	Ze	SP	LP	LP
	LP	Ze	SP	LP	LP	LP

Figure 3.7 Rule Base table[39]

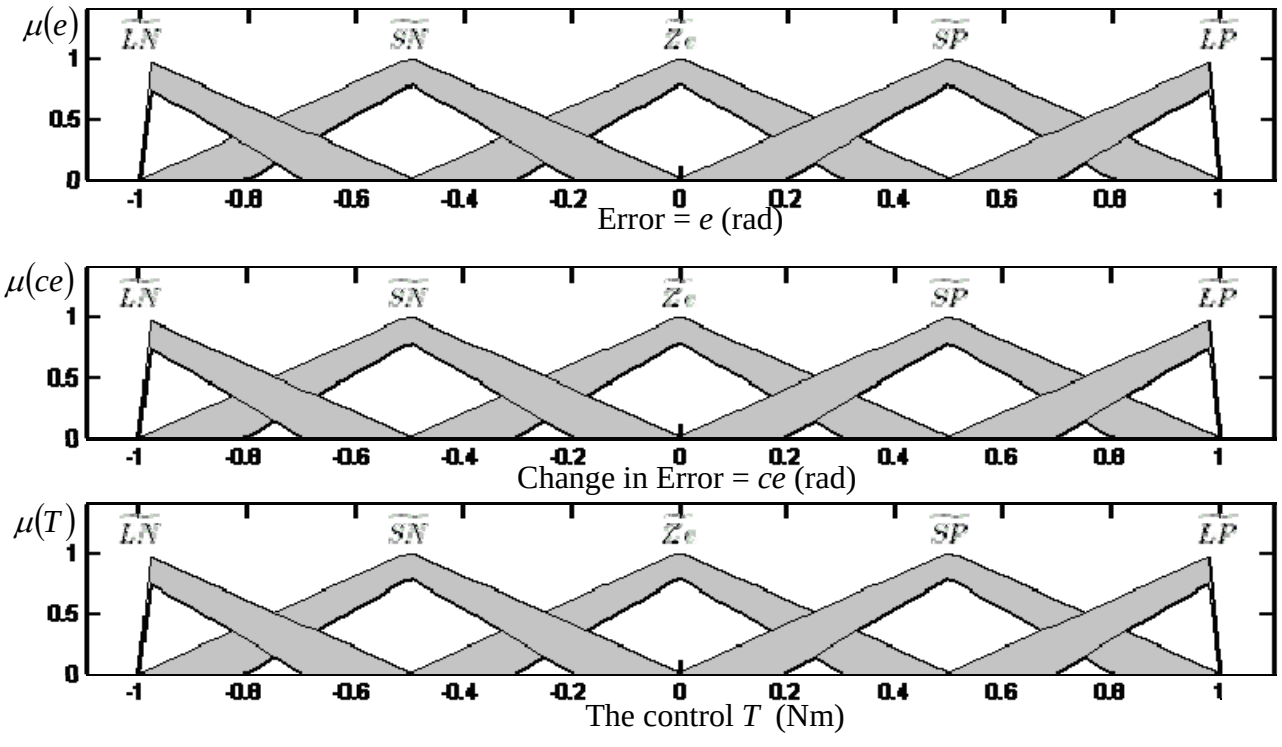

Figure 3.8 Fuzzy set type-2 for each articulation.

3.7 Result of simulation with tow trajectory

We use same trajectory which used in chapter 2, a circle in space and LEAHY trajectory.

3.7.1 Result of simulation with circle trajectory

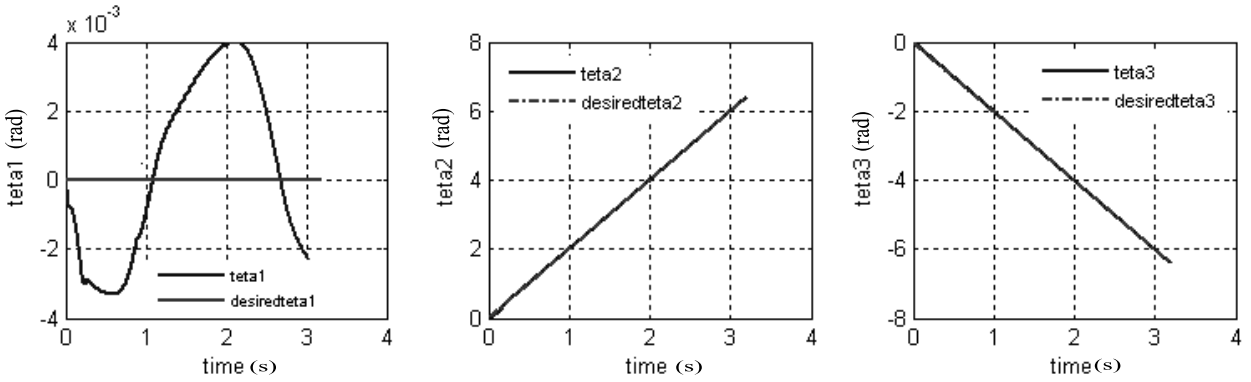

Figure 3.9 Position of joints 1,2,3 (rad).

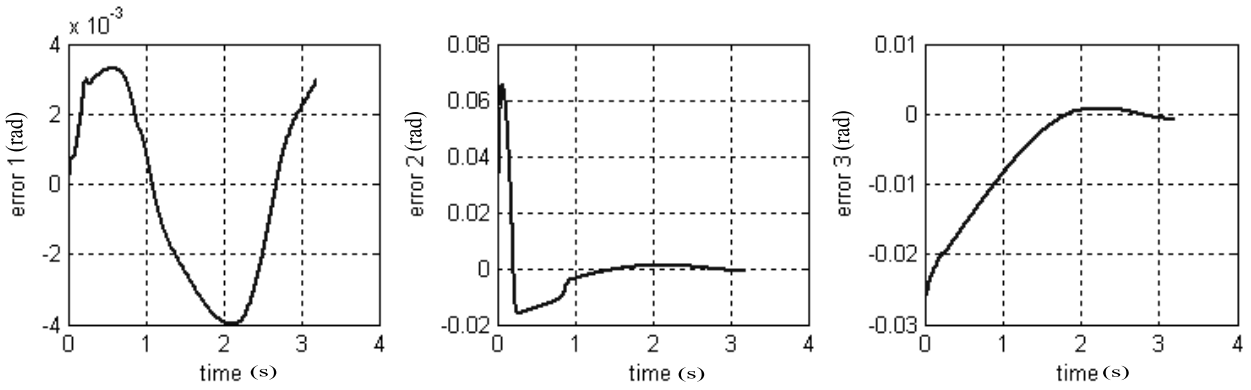

Figure 3.10 Position error of joints 1,2,3 (rad).

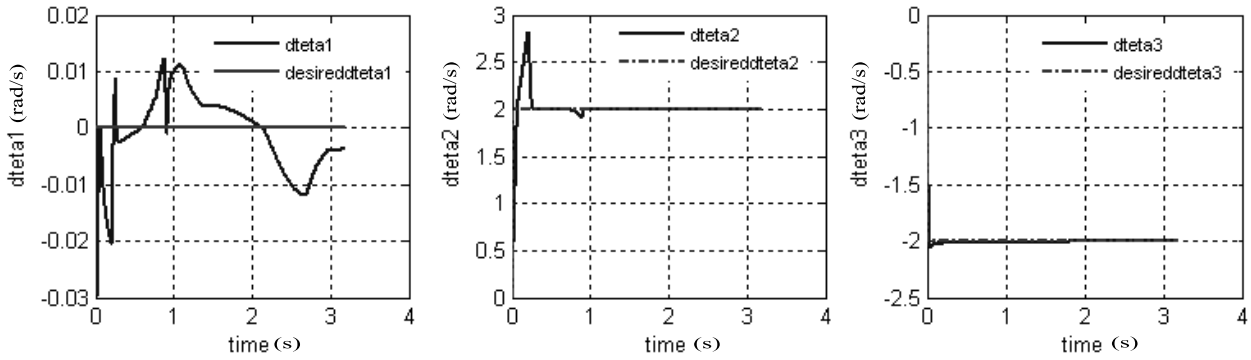

Figure 3.11 Velocity of joints 1,2,3 (rad/s).

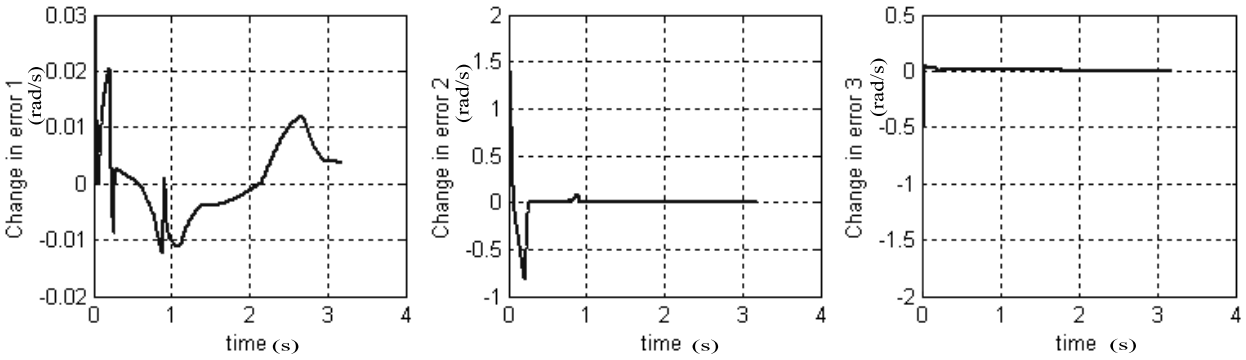

Figure 3.12 Velocity error of joints 1,2,3 (rad/s).

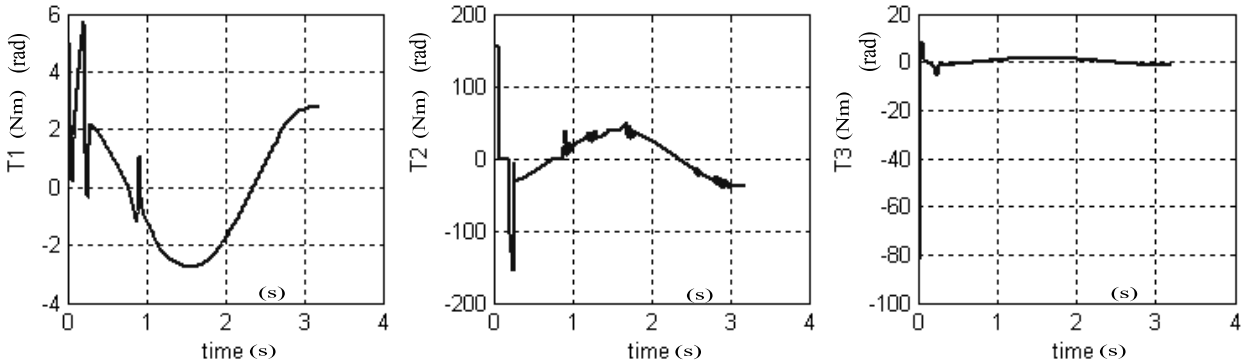

Figure 3.13 Torque inputs of the robot joints 1,2,3 (Nm).

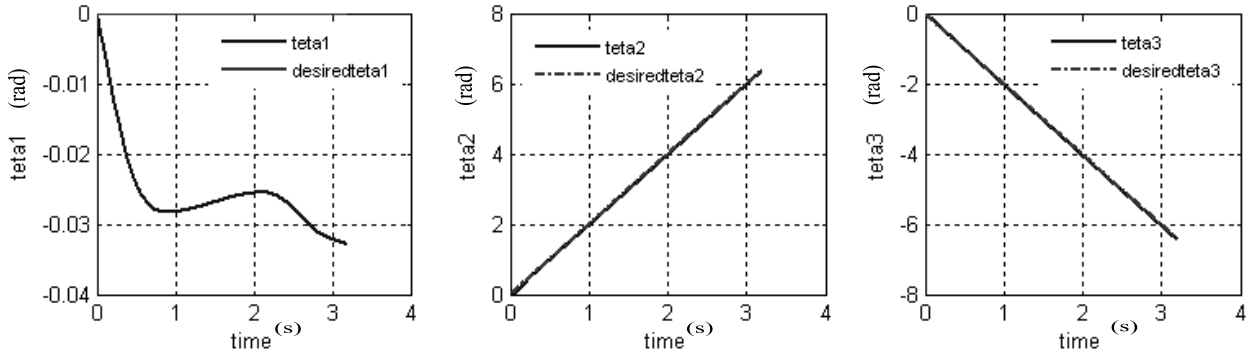

Figure 3.14 Position of joints 1,2,3 (rad) with white noisy in measure of position.

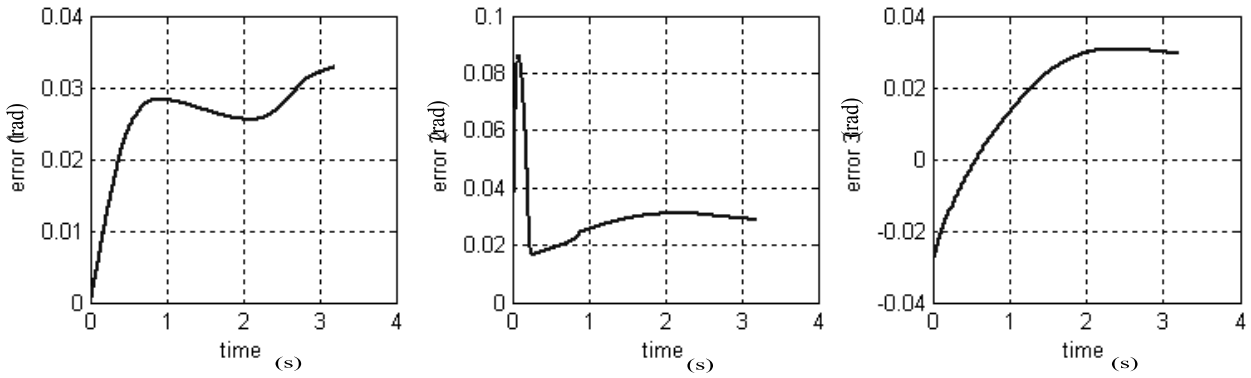

Figure 3.15 Position error of joints 1,2,3 (rad) with white noisy.

3.7.2 Result of simulation with LEAHY trajectory

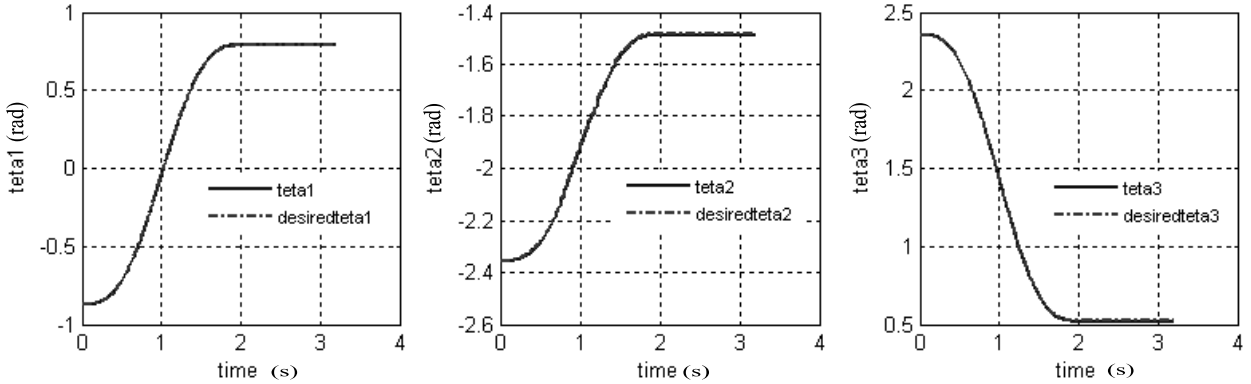

Figure 3.16 Position of joints 1,2,3 (rad).

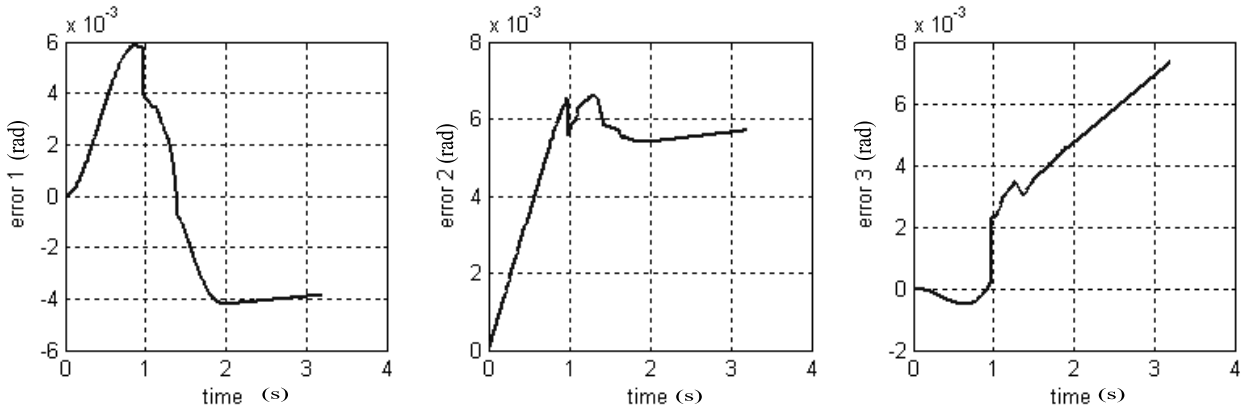

Figure 3.17 Position error of joints 1,2,3 (rad).

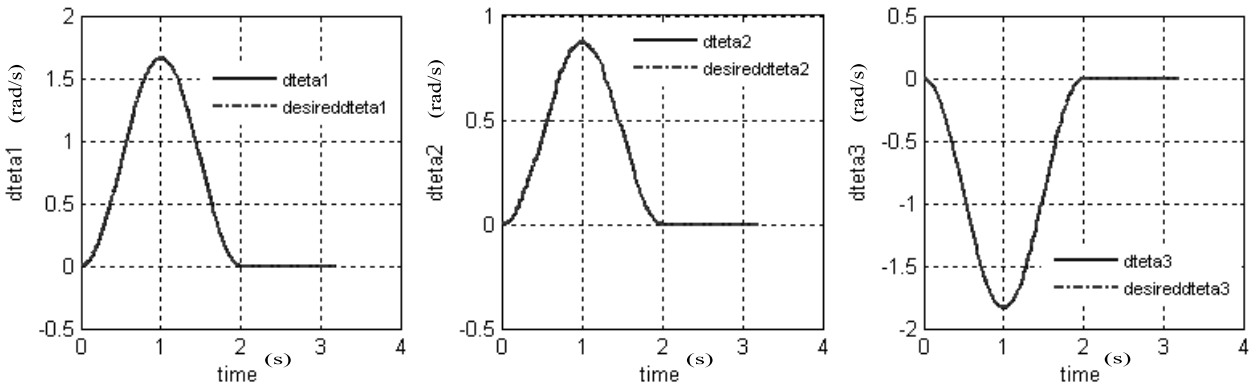

Figure 3.18 Velocity of joints 1,2,3 (rad/s).

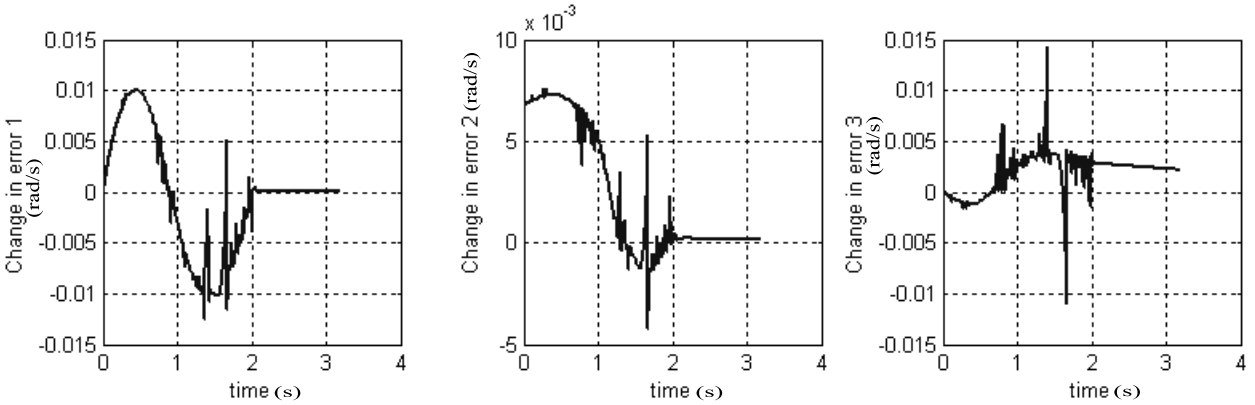

Figure 3.19 Velocity change error of joints 1,2,3 (rad/s).

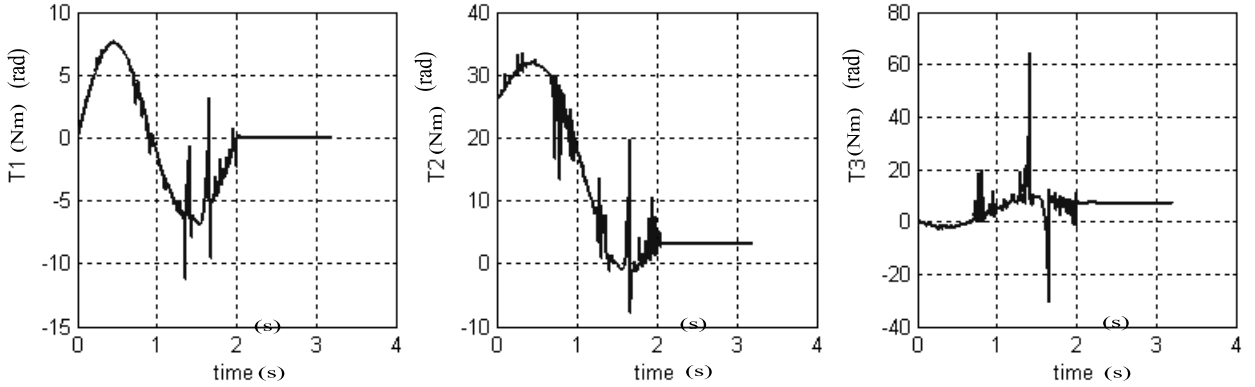

Figure 3.20 Torque inputs of the robot joints 1,2,3 (Nm).

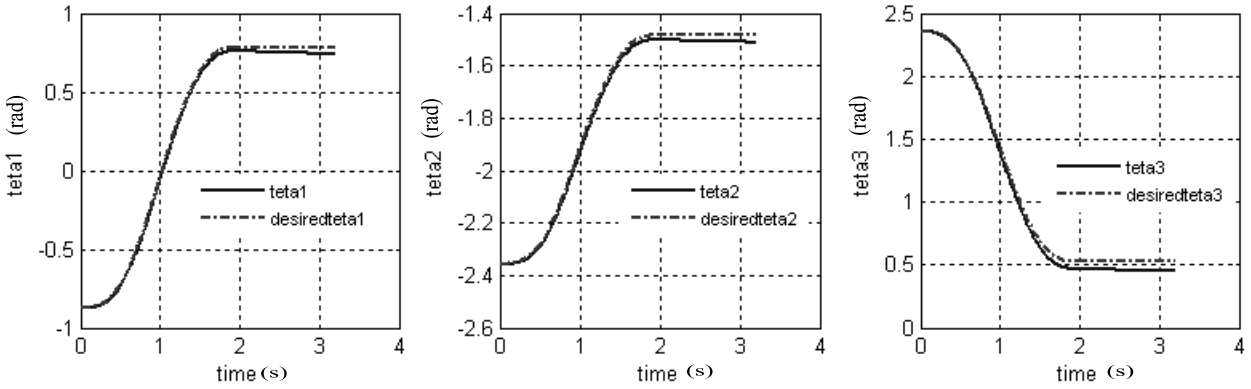

Figure 3.21 Position of joints 1,2,3 (rad) with white noisy.

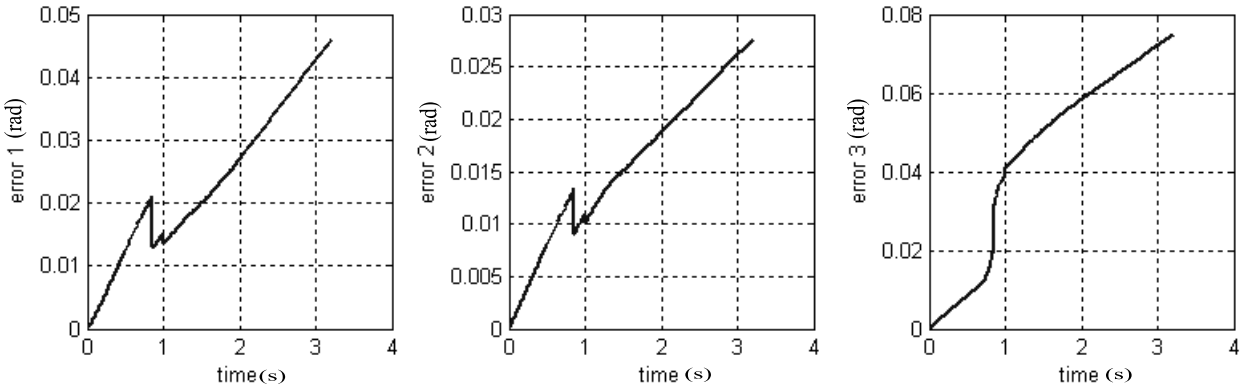

Figure 3.22 Position error of joints 1,2,3 (rad) with white noisy.

By visual inspection from Figure 3.9 to Figure 3.22 we can show that:

- Good position in ideal case and with white noisy.
- The positions errors in tow case approximately are equals and are both low.
- The positions and velocities of joints are continuous.
- The control torques of the joints 1,2,3 are limited and don't pass the maximum torque for each joints.
- The good performances are with trajectory of LEAHY because it excites all the dynamics of robot PUMA560.

3.8 Conclusion

In this chapter, we have presented the main ideas underlying type-2 fuzzy logic and we have only started to point out the many possible applications of this powerful computational theory.

We have discussed in some detail type-2 fuzzy set theory, fuzzy reasoning and fuzzy inference systems. At the end, we apply type-2 fuzzy modeling with the Mamdani approaches on PUMA560 3DOF. The results of simulations prove that Interval type-2 FLC have good with low error and accepted control torques of the joints. In the following chapters, we will perform a comparative analysis of the type-1 FLC and interval type-2 FLC responses.

Chapter 4

Comparative study between Type-1 FLC and Type-2 FLC

4.1 Introduction

We describe in this section the comparison of the simulation results of both approaches. As a performance measure we will use the Integral of Square Error (ISE) and Integral of Square Torque (IST)[36].

4.2 Comparative study

We simulated fuzzy logic controller type-1 and type-2 for PUMA560 3DOF with tow trajectory test, with and without noisy.

4.2.1 Comparative study between fuzzy logic controller type-1 and type-2 in theory

Type-1 fuzzy set is a generalization of the crisp set, whose membership grades can only be 0 or 1 Figure 4.3. A type-1 FLC is constructed completely by type-1 fuzzy sets. It contains four components rule base, fuzzifier, inference engine and defuzzifier, as shown in Figure 4.1.
The fuzzy model introduced by Mamdani is also known as the Mamdani model. It is the most widely model used by FLCs. The results reported in this memory assume this model.
Type-l FLC, whose membership functions are type-1 fuzzy sets Figure 4.3, are unable to directly handle fuzzy membership functions. Type-2 FLC, the subject of this research memory, in which antecedent or consequent membership functions are type-2 fuzzy sets Figure 4.4, can handle fuzzy membership functions.

Figure 2.2 shows the schematic diagram of a type-2 FLC. It is similar to its type-1 counterpart, the major difference being that at least one of the fuzzy sets in the rule base is type-2. Hence, the outputs of the inference engine are type-2 sets and a type-reducer is needed to convert them into a type-1 set before defuzzification can be carried out.

Since the outputs of the inference engine are type-2 fuzzy sets, they must be type-reduced before the defuzzifier Figure 4.2 (b) can be used to generate a crisp output. This is the main structural difference between type-1 and type-2 FLCs.

The concept of type-2 fuzzy sets was introduced by Zadeh [21] [24] as an extension of the concept of an ordinary fuzzy set, a type-1 fuzzy set. Type-2 fuzzy sets have grades of membership that are themselves fuzzy [21] [24]. A type-2 membership grade can be any subset in [0,1] - the primary membership, and corresponding to each primary membership, there is a secondary membership (which can also be in [0,1]) that defines the possibilities for the primary membership. A type-1 fuzzy set is a special case of a type-2 fuzzy set; its secondary membership function is a subset with only one element, unity. Type-2 fuzzy sets allow us to handle linguistic uncertainties, as typified by the adage "words can mean different things to different people.

A general formula for the extended sup-star composition of type-2 relations is given by Karnik and Mendel [22] [33]. Based on this formula, Karnik and Mendel [22]-[37] established a complete type-2 FLC theory to handle uncertainties in system parameters.

Similar to a type-1 FLC, a type-2 FLC includes fuzzifier, rule base, fuzzy inference engine, and output processor, as shown in Figure. 4.2a [22]. The output processor includes type-reducer and defuzzifier, as shown in Figure 4.2b; it generates a type-1 fuzzy set output (from the type-reducer) or a crisp number (from the defuzzifier). These type-2 FLC are again characterized by IF-THEN rules, but their antecedent or consequent sets are now type-2. Type-2 FLC can be used when the circumstances are too uncertain to determine exact membership grades, such as when training data is corrupted by noise.

The most commonly used fuzzifier is a singleton; but, such a fuzzifier is not adequate when data is corrupted by measurement noise. In this case, a nonsingleton fuzzifier, that treats each measurement as a fuzzy number, should be used. The theory and applications of a type-1 FLC with nonsingleton fuzzifier are presented in [38].

One major disadvantage of type-2 FLC is that they may not be suitable for real-time applications because they require large computational power, especially when there are many memberships function and the rule base is large.

In Table 4.1 we resume some differences characteristics between type-1 FLC and type-2 FLC.

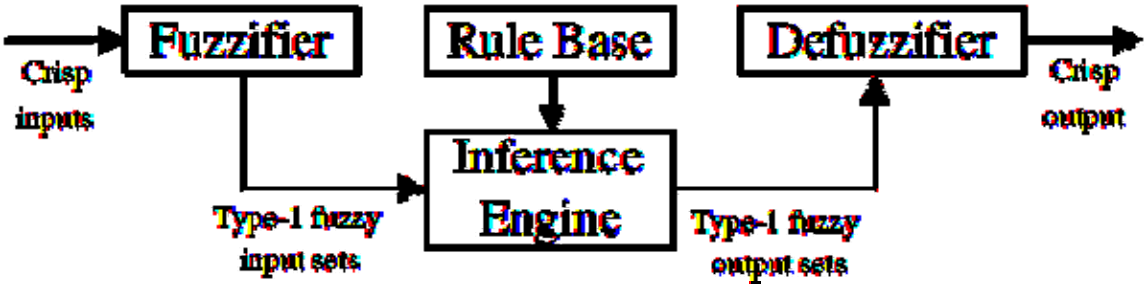

Figure 4.1 A type-1 FLC

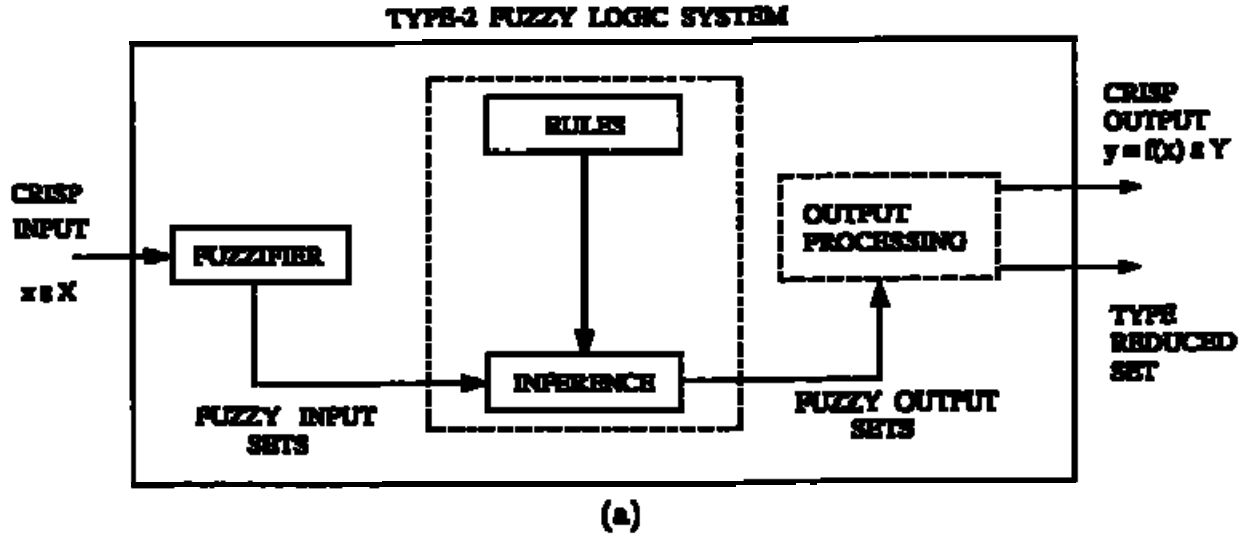

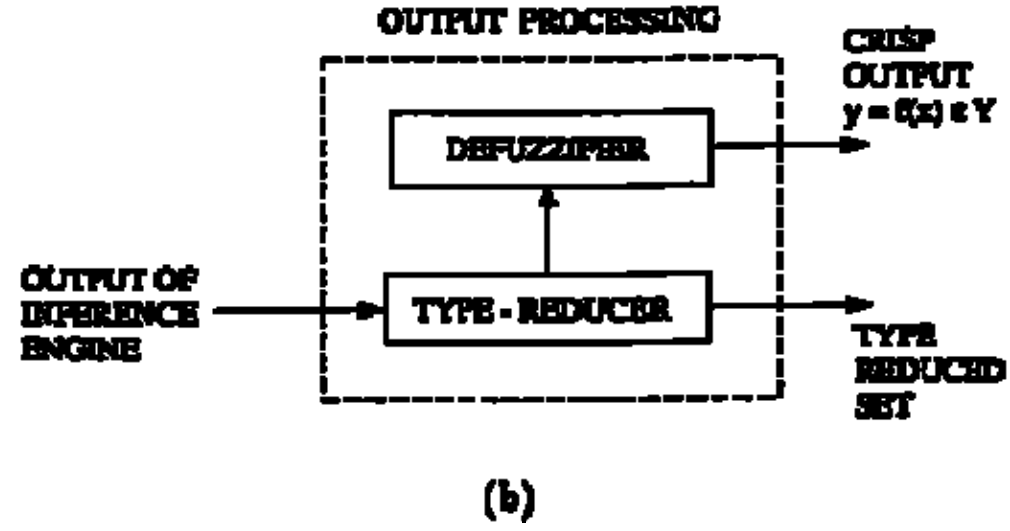

Figure 4.2 the structure of a type-2 FLC. The structure of the output processing block is shown in Figure (b).

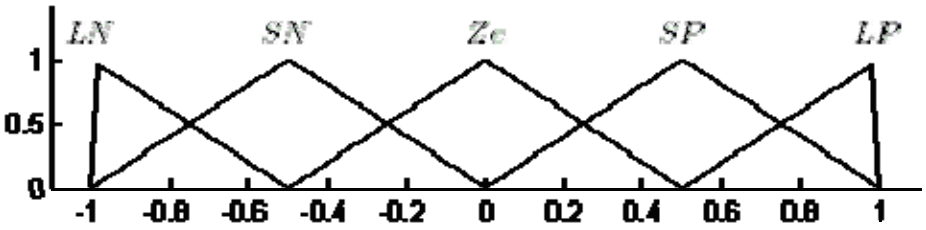

Figure 4.3 Membership function type-1 fuzzy set.

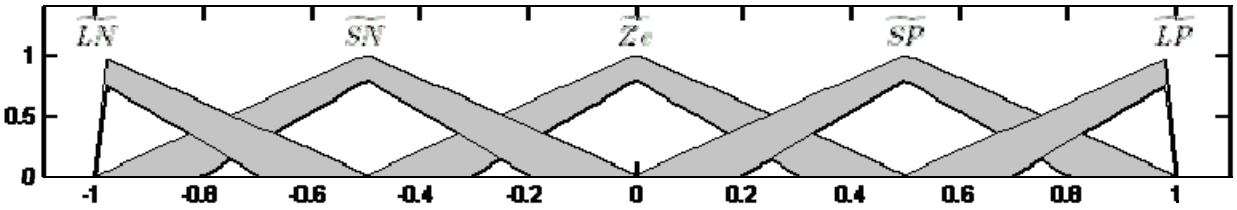

Figure 4.4 Membership function interval type-2 fuzzy set.

FLC	Type-1	Type-2
Grades of membership	Crisp	Fuzzy
Type-reducer	Don't need	need
Computational	Small	Large
Program	Easy	Hard

Table 4.1 Some differences characteristics between type-1 FLC and interval type-2 FLC.

4.2.2 Comparative study simulation response of PUMA560 3DOF

The comparison between type-1 FLC and type-2 FLC by using simulated result for Chapter 2 and chapter 3, In almost all the cases the results for type-2 FLC are better than type-1 FLC. The noise witch use is white noise it's integral of square in Table 4.2, noisy energy represent around 6% from maximum magnitude of position joint for LEAHY trajectory and 2% from maximum magnitude of position joint for Circle trajectory.

Integral of Square Error (ISE)[36]

$$ISE = \int_0^{t_{end}} [e(t)]^2 \, dt$$

Integral of Square Torque (IST)

$$IST = \int_0^{t_{end}} [T(t)]^2 \, dt$$

	Joint 1	**Joint 2**	**Joint 3**
Energy of Noise	0.1075	0.0244	0.1075

Table 4.2 Energy of Noise

4.2.2.a Comparative study for a circle trajectory

Simulation 1a: Ideal case using a type-1 FLC

In this simulation, we did not add uncertainty data (Noise) to the joints, the joints response is illustrated in Figure 4.5. In Table 4.3, we listed the obtained values of ISE and IST for this simulation.

Simulation 2a: Ideal case using a type-2 FLC

Here, we used the same test conditions of simulation 1a, but in this case, we use the controller's algorithm with type-2 fuzzy logic, its output sequence is illustrated in Figure 4.5, and the corresponding the obtained values of ISE and IST are listed in Table 4.3.

The results of Simulation 1a and Simulation 2a obtained are summarized in same figure, by visual inspection; we can observe that:

- In Figure 4.5 shows the joint's response to a circle trajectory. Note, that both responses are very similar.
- In Figure 4.6 shows the position error of joints 1,2,3 for a circle trajectory. Note, in this case the lower errors were obtained with type-1 FLC.
- In Figure 4.7 shows the joint's input torque (Control). Note that both controls are very similar but in type-1 FLC we can see there is some pick and interval type-2 FLC without pick.

Using the ISE and IST in ideal case we can get a quantitative comparison in Table 4.3, where we can observe small differences favoring the results obtained using a type-1 FLC. We can observe in Table 4.3 that using a type-1 FLC we got the lower errors, but with higher torque.

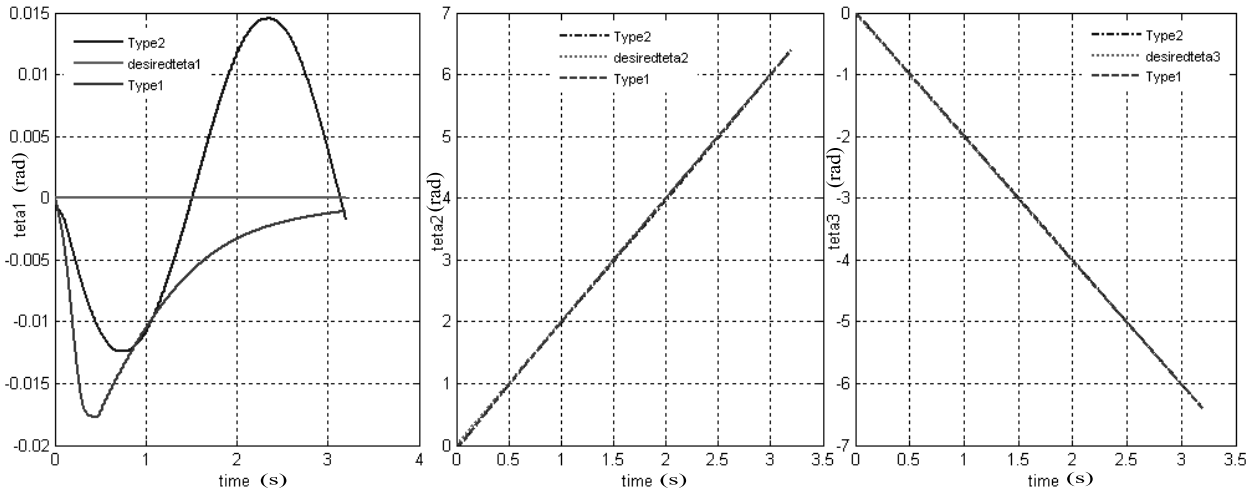

Figure 4.5 This graphic shows the joint's response to a circle trajectory.

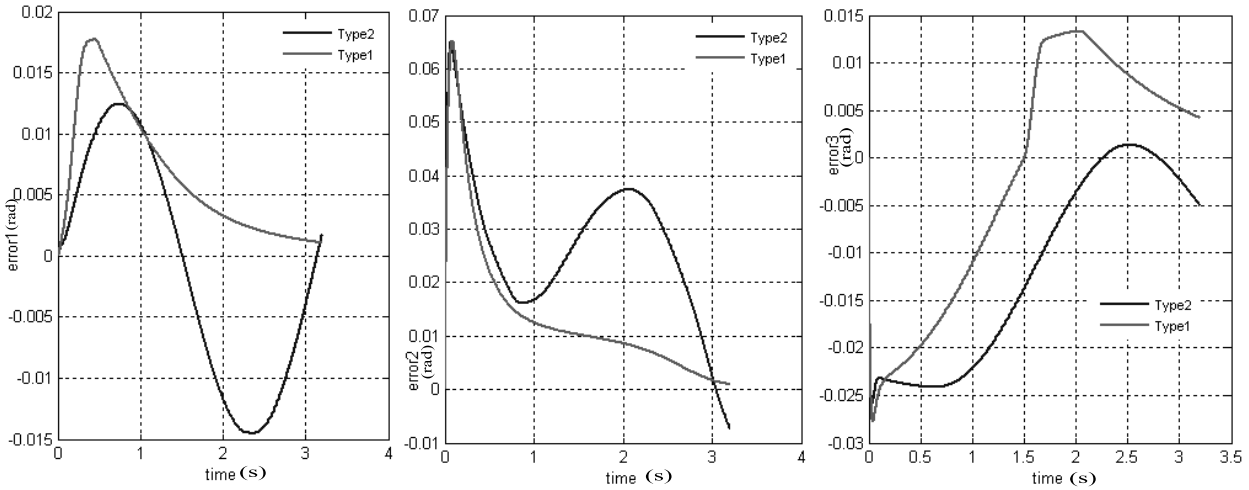

Figure 4.6 This graphic shows the position error of joints 1,2,3 for a circle trajectory.

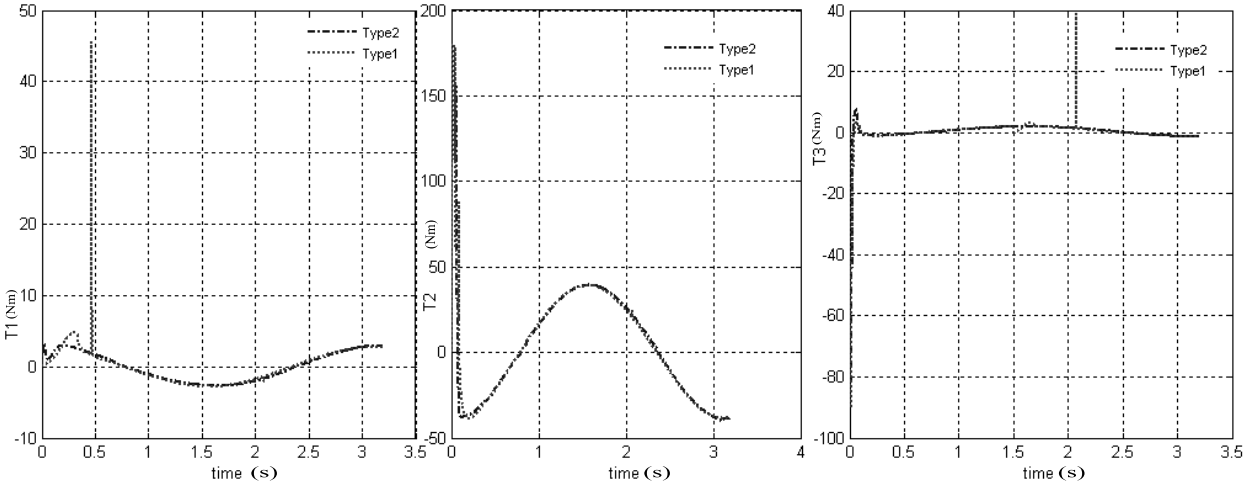

Figure 4.7 This graphic shows the joint's input torque (Control).

Simulation 3a: PUMA560 with uncertainty (White noisy) uses a type-1 FLC.

In this case, we simulated with white noise in measurement joints position the energy of these noisy in Table 4.2. We are showing in Figure 4.8, the joint's position, Figure 4.9 the position error, and Figure 4.10 the input torque (the input control).

Simulation 4a: PUMA560 with uncertainty using a type-2 FLC.

In this simulation, we introduced uncertainty in the joint, in the same way as in Simulation 3a.

We can easily appreciate in Figure 4.8 and Figure 4.9 and 4.10, we can observe that the lower errors are obtained using a type-2 FLC but with little higher torque.

By visual inspection; we can observe that:

- In Figure 4.8 This response was obtained with uncertainty presence (White noise), compare the joint's position produced by type-1 and type-2 FLCs. Note that quite the opposite of Figure 4.5, a type-2 FLC works much better than a type-1 FLC when the

system has uncertainty. The overshoot error is lower for a type-2 FLC this note is clear in Figure 4.9.

- In Figure 4.9 This response was obtained with uncertainty presence (White noise), compare the position errors produced by type-1 and type-2 FLCs. The overshoot error is very lower for a type-2 FLC.
- In Figure 4.10 This response shows the joint's input torque (Control) with uncertainty presence (White noise). Note that both controls are very similar but in type-1 FLC we can see there is some pick and type-2 FLC without pick.

Using the ISE and IST with uncertainty presence (White noise) we can get a quantitative comparison in Table 4.3, where we can observe better response simulation 4a, the results obtained using a type-2 FLC with uncertainty presence (White noise). We can observe in Table 4.3 that using a type-2 FLC we got the lower errors, but with higher torque.

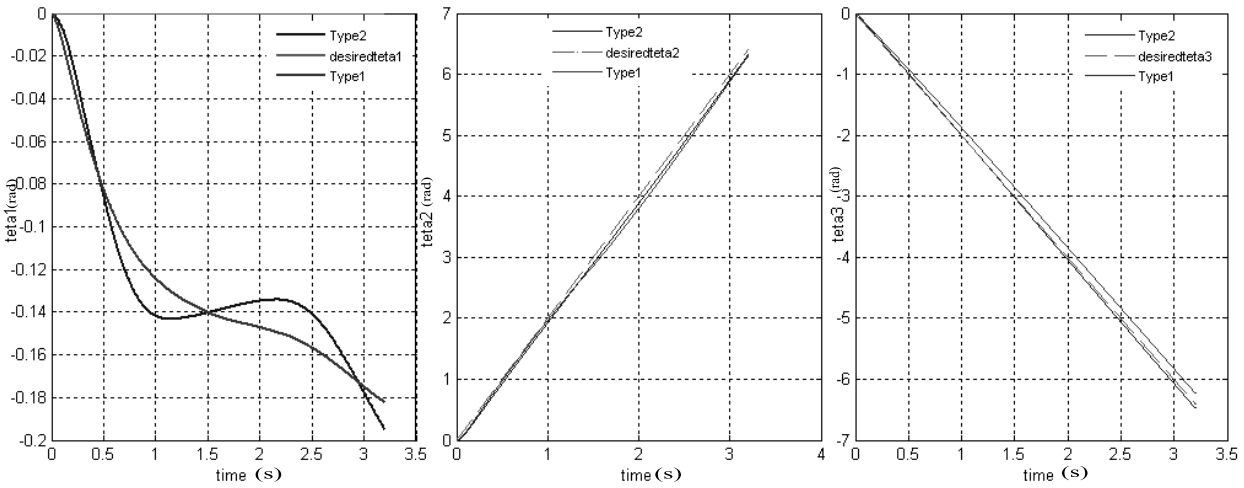

Figure 4.8 This graphic was obtained with uncertainty presence (White noise), compare the joint's position produced by type-1 and type-2 FLCs.

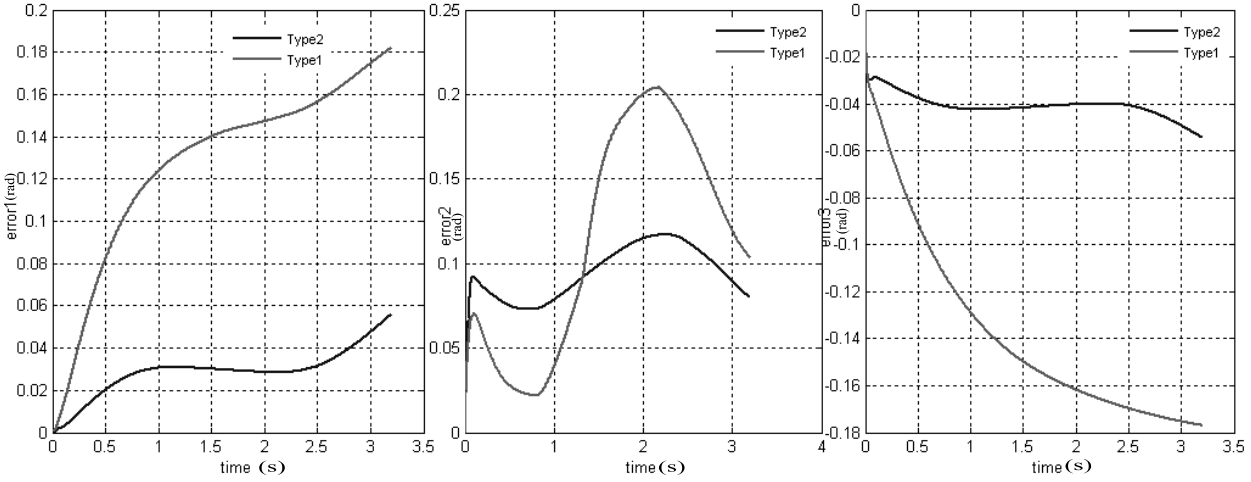

Figure 4.9 This graphic was obtained with uncertainty presence (White noise), compare the position errors produced by type-1 and type-2 FLCs.

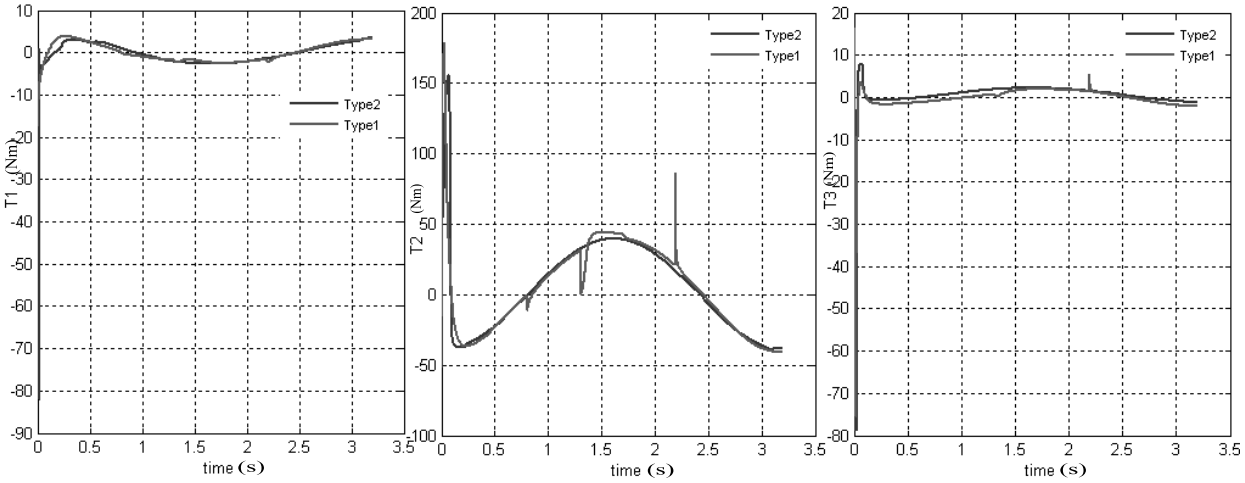

Figure 4.10 This graphic shows the joint's input torque (Control) with uncertainty presence (White noise).

		Type-1		Type-2	
		Ideal case	**Case with Noise**	**Ideal case**	**Case with Noise**
ISE	**Joint 1**	7.1513e-005	0.0180	9.0242e-005	9.54E-004
	Joint 2	3.8241e-004	0.0173	8.9158e-004	0.0091
	Joint 3	1.7454e-004	0.0204	2.4183e-004	0.0016
IST	**Joint 1**	4.6148	5.5391	3.9309	3.6299
	Joint 2	1167.3	1179.4	1236.5	1112.7
	Joint 3	41.2833	34.3775	49.2460	47.5294

Table 4.3 The integral square error and torque for each joint

4.2.2.b Comparative study for LEAHY trajectory

Simulation 1b: Ideal case using a type-1 FLC

In this simulation, we did not add uncertainty data (Noise) to the joints, the joints response is illustrated in Figure 4.11. In Table 4.4, we listed the obtained values of ISE and IST for this simulation.

Simulation 2b: Ideal case using a type-2 FLC

Here, we used the same test conditions of simulation 1b, but in this case, we use the controller's algorithm with type-2 fuzzy logic, its output sequence is illustrated in Figure 4.11, and the corresponding the obtained values of ISE and IST are listed in Table 4.4. By visual inspection, we can observe that the output system responses of the simulation 1b, and this one, are very similar, they are almost overlapped, also we can observe that:

- In Figure 4.11 shows the joint's response to LEAHY trajectory. Note, that both responses are similar.
- In Figure 4.12 shows the position error of joints 1,2,3 for a LEAHY trajectory. Note, in this case the lower errors were obtained with type-2 FLC the opposite of Figure 4.5 and 4.6.
- In Figure 4.13 shows the joint's input torque (Control). Note that both controls are very similar but in type 1 we can see there is pick with big magnitude and type 2 little pick with small magnitude.

Using the ISE and IST in ideal case we can get a quantitative comparison in Table 4.4, where we can observe better response in simulation 2b, the results obtained using a type-2 FLC, the opposite result of simulation with a circle trajectory in ideal case. We can observe in Table 4.4 that using a type-2 FLC we got the lower errors, but with higher torque.

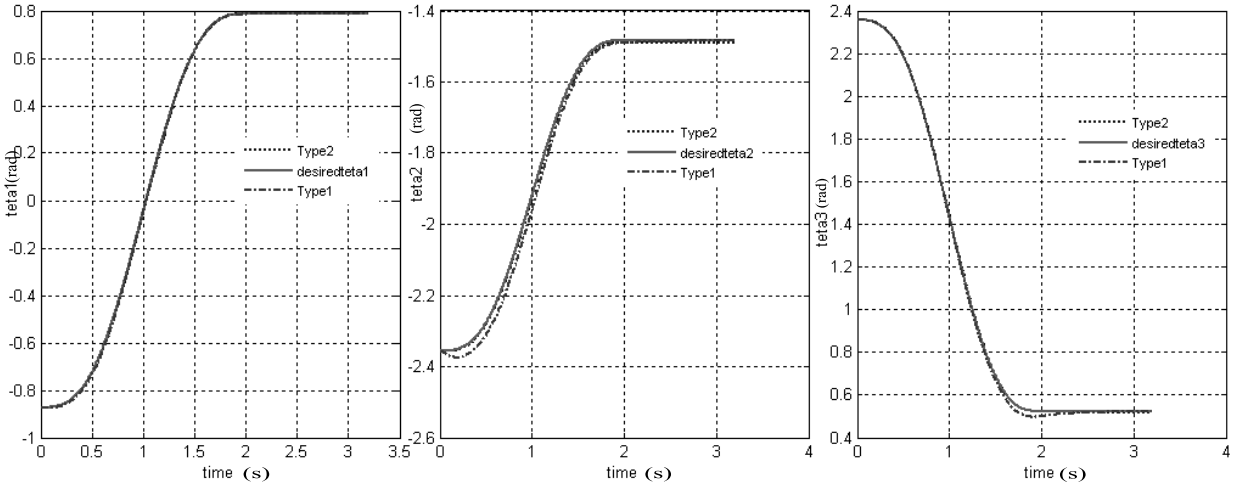

Figure 4.11 This graphic shows the joint's response to LEAHY trajectory.

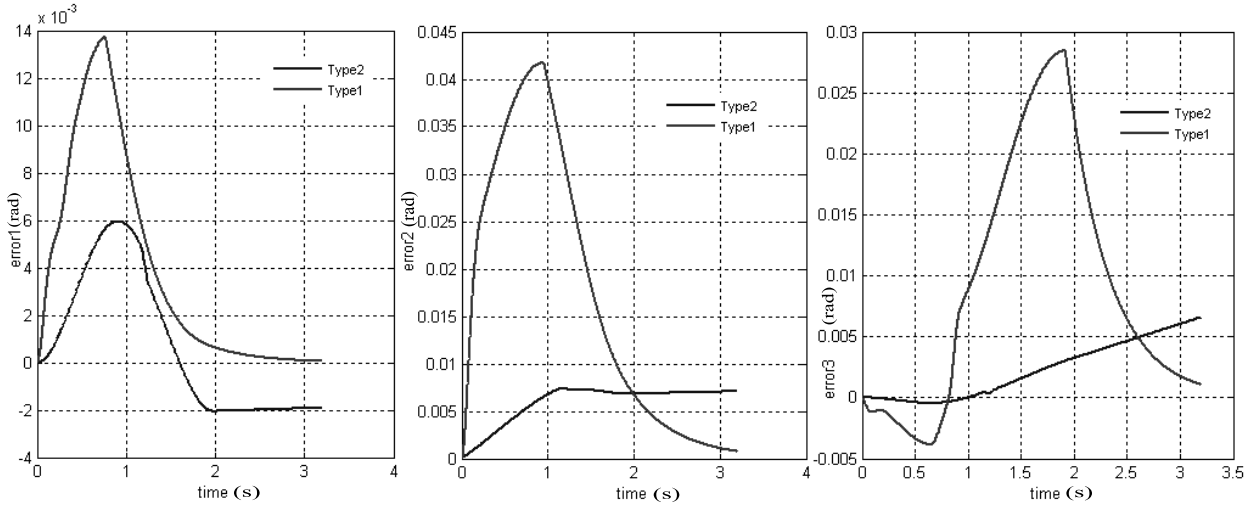

Figure 4.12 This graphic shows the position error of joints 1,2,3.

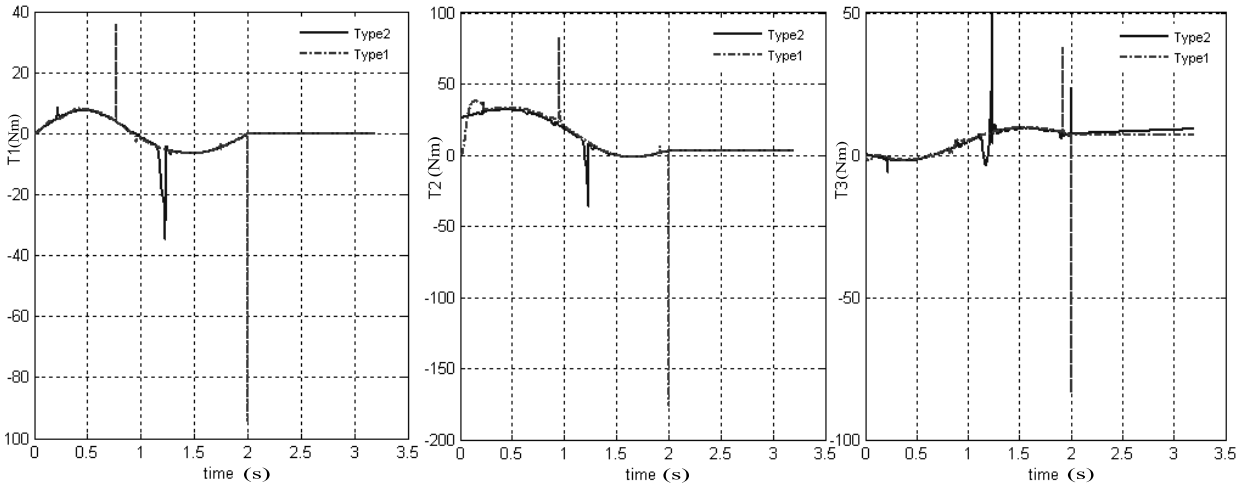

Figure 4.13 This graphic shows the joint's input torque (Control).

Simulation 3b: PUMA560 with uncertainty (White noisy) uses a type-1 FLC.

In this case, we simulated with white noise in measurement joints position the energy of these noisy in Table 4.2. We are showing in Figure 4.14, the joint's position, Figure 4.15 the position error, and Figure 4.16 the input torque (the input control).

Simulation 4b: PUMA560 with uncertainty using a type-2 FLC

In this simulation, we introduced uncertainty in the joint, in the same way as in Simulation 3b.

By visual inspection; we can observe that:

- In Figure 4.14 This graphic was obtained with uncertainty presence (White noise), compare the joint's position produced by type-1 and type-2 FLCs. Note type-2 FLC works much better than a type-1 FLC when the system has uncertainty. The overshoot error is lower for a type-2 FLC.
- In Figure 4.15 This graphic was obtained with uncertainty presence (White noise), compare the position errors produced by type-1 and type-2 FLCs. The overshoot error is very lower for a type-2 FLC.
- In Figure 4.16 shows the joint's input torque (Control) with uncertainty presence (White noise), the control of Type-2 FLC has higher torque than control of Type-1 FLC in this case.

Using the ISE and IST with uncertainty presence (White noise) we can get a quantitative comparison in Table 4.4, where we can observe better response simulation 4b, the results obtained using a type-2 FLC with uncertainty presence (White noise). We can observe in Table 4.4 that using a type-2 FLC we got the lower errors, but with higher torque.

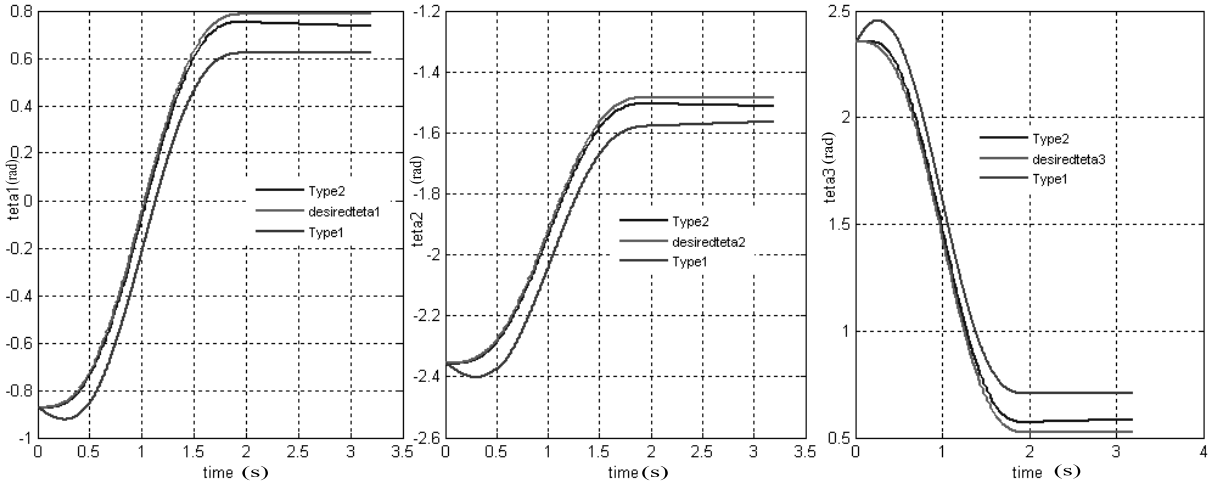

Figure 4.14 This graphic was obtained with uncertainty presence (White noise), compare the joint's position produced by type-1 and type-2 FLCs.

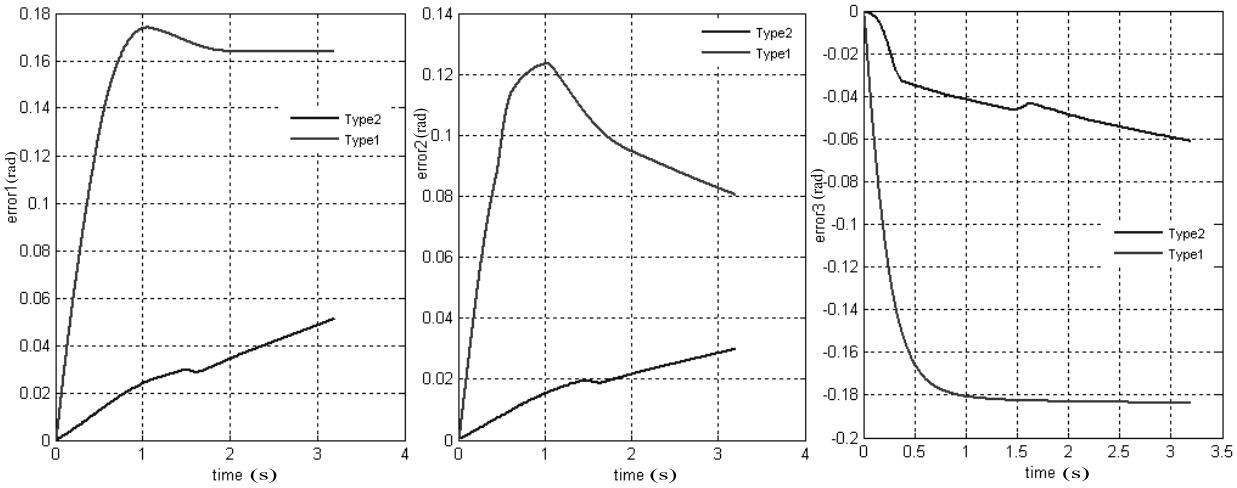

Figure 4.15 This graphic was obtained with uncertainty presence (White noise), compare the position errors produced by type-1 and type-2 FLCs.

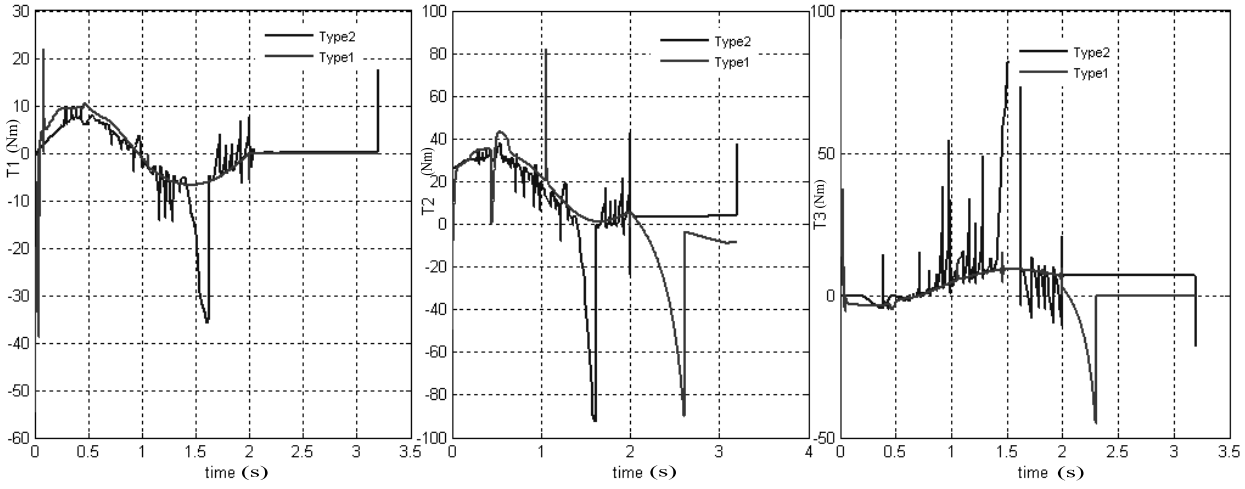

Figure 4.16 This graphic shows the joint's input torque (Control) with uncertainty presence (White noise).

		Type-1		Type-2	
		Ideal case	**Case with Noise**	**Ideal case**	**Case with Noise**
ISE	**Joint 1**	3.5049e-005	0.0233	8.3459e-006	6.1410e-004
	Joint 2	5.0374e-004	0.0090	3.1026e-005	2.4411e-004
	Joint 3	1.8468e-004	0.0294	7.2785e-006	0.0015
IST	**Joint 1**	19.5889	56.1187	33.8643	69.1709
	Joint 2	324.6382	603.4121	361.2606	520.5616
	Joint 3	45.6840	94.5778	52.6138	359.4308

Table 4.4 The integral square error and torque for each joint

4.2.3 Comparison simulation result for a circle and LEAHY trajectory

From section 4.2.2 with using Table 4.3 and Table 4.4 we can resume our result comparative in error and energy about type-1 and type-2 FLC for PUMA560 with 3DOF in Table 4.5 it is clearly type-2 FLC is better.

	Circle trajectory				LEAHY trajectory			
	Type-1		Type-2		Type-1		Type-2	
	Ideal	Noisy	Ideal	Noisy	Ideal	Noisy	Ideal	Noisy
Position error	Better	Bad	Good	Good	Good	Bad	Better	Good

Table 4.5 Comparative position error for tow trajectory.

4.3 Conclusion

We observed and quantified using ISE and IST that in systems without uncertainties (ideal robot) is a better choice to select a type-1 FLC since it works similar to type-2 FLC, and it is easier to program and simulate it.

Unfortunately, real robot are inherently noisy and nonlinear, since any element in the system contributes with deviations of the expected measures because of thermal noise, electromagnetic interference, etc., moreover, they add nonlinearities from element to element in the model of robot. In this case, robot with uncertainty is a better choice to select a type-2 FLC since it doesn't affect by uncertainty.

General Conclusion

In this memory, a type-1 and Interval type-2 FLC are developed for the control of PUMA560 3DOF manipulators in the presence of dynamical modeling. To alleviate the naturally inherited high computational complexity of type-2 FLCs, interval membership functions are adopted. The controllers are also compared in similar operating conditions. Numerical simulations showed the superiority of type-2 FLC in compensating for high-magnitude uncertainties. This finding confirms the theoretical credentials associated to type-2 FLCs in their higher tolerance to the imprecise modeling of fuzzy controllers, namely the fuzzy membership functions and knowledge base.

We are concluding that using type-2 FLC in real applications can be a better choice since the amount of uncertainty in real systems, mostly, is difficult to estimate. But when uncertainty in real system is negligible, we can consider it as an ideal system. In this case, it is a better choice to select a type-1 FLC since it works similar to type-2 FLC, and the size of type-1 FLC program is shorter than type-2 FLC, so it is faster and easier to program and simulate it.

Future work:

- ✓ Implementation interval type-2 fuzzy controller with PUMA560 robot.
- ✓ Optimize the structural and parametric of interval type-2 fuzzy controller.
- ✓ Hybridization interval type-2 fuzzy controller with other robust control such as sliding mode and backstepping ... ...

Appendix A

Direct geometric model

The Direct Geometric Model (DGM) is the set of relations that defines the location of the end effector of the robot as a function of its joint coordinates. For a serial structure, it may be represented by the transformation matrix ${}^0T_n$ as:

$$ {}^0T_n = {}^0T_1(q_1)\,{}^1T_2(q_2)\cdots{}^{n-1}T_n \qquad \text{A.01} $$

This relation can be numerically computed using the general transformation matrix ${}^{j-1}T_j$ given by equation [1.2].

The direct geometric model of a robot may also be represented by the relation:

$$ X = f(q) \qquad \text{A.02} $$

Where q is the vector of joint variables such that:

$$ q = [q_1 \;\; q_2 \;\; q_3 \cdots q_n] $$

Inverse Geometric Model

The direct geometric model of a robot provides the location of the end-effector in terms of the joint coordinates. The problem of computing the joint variables corresponding to a specified location of the end-effector is called the inverse geometric problem. This problem is at the center of computer control algorithms for robots. It has in general a multiple solution and its complexity is highly dependent on the geometry of the robot. The model that gives all the possible solutions for this problem is called the Inverse Geometric Model (IGM).

Direct kinematic model

The direct kinematic model of a robot manipulator gives the velocity of the end-effector $\dot{X}$ in terms of the joint velocities $\dot{q}$. It is written as:

$$\dot{X} = J(q)\dot{q} \qquad \text{A.03}$$

Where $J(q)$ denotes the *(mxn)* Jacobian matrix.

Inverse kinematic model

The inverse kinematic model gives the joint velocities $\dot{q}$ for a desired end-effector velocity $\dot{X}$ this model is equivalent to the inverse differential model, which determines the differential variation of the joint variables *dq* corresponding to a given differential displacement of the end-effector coordinates *dX*. We obtain the inverse kinematic model by solving a system of linear equations analytically or numerically.

Appendix B

Membership Functions

Defines the membership function of a fuzzy set in an analytic expression that allows the membership grade for each element in the defined universe of discourse to be calculated Commonly used "shapes" of membership functions are:

Triangular functions, defined as

$$u_A(x) = \begin{cases} 0 & if\ x \le \alpha_{\min} \\ \dfrac{x-\alpha_{\min}}{\beta-\alpha_{\min}} & if\ x \in [\alpha_{\min}, \beta] \\ \dfrac{\alpha_{\max}-x}{\alpha_{\max}-\beta} & if\ x \in [\beta, \alpha_{\max}] \\ 0 & if\ x \ge \alpha_{\max} \end{cases}$$

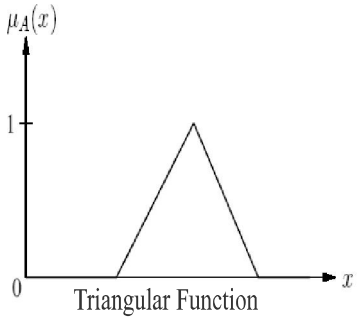

Trapezoidal functions, defined as

$$u_A(x) = \begin{cases} 0 & if\ x \le \alpha_{\min} \\ \dfrac{x-\alpha_{\min}}{\beta_1-\alpha_{\min}} & if\ x \in [\alpha_{\min}, \beta_1] \\ \dfrac{\alpha_{\max}-x}{\alpha_{\max}-\beta_2} & if\ x \in [\beta_2, \alpha_{\max}] \\ 0 & if\ x \ge \alpha_{\max} \end{cases}$$

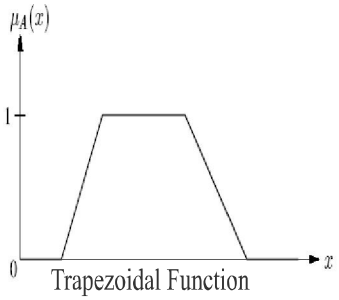

Linguistic Operators

Fuzzy sets are able to deal with **linguistic quantifiers** or '**hedges**'. Hedges such as *more or less, very, not very, slightly*, etc, correspond to modifications in the membership function of the fuzzy set involved.

Linguistic terms are usually used to define each system variable in the fuzzy sets such as **PB** (positive big), **PM** (positive medium), **PS** (positive small), **ZE** (Zero), **NS** (negative small), **NM** (negative medium), **NB** (negative big), etc. Selection of membership functions based on the *range and shape for a variable* is somewhat a subjective design choice.

- **Symmetrically distribute** the fuzzy sets across the defined universe of discourse.
- **Use an odd number of fuzzy sets** for each variable.
- **Overlap adjacent fuzzy sets** to ensure no crisp value fails to correspond to any set.
- **Use triangular or trapezoidal** membership functions as these require less computation.

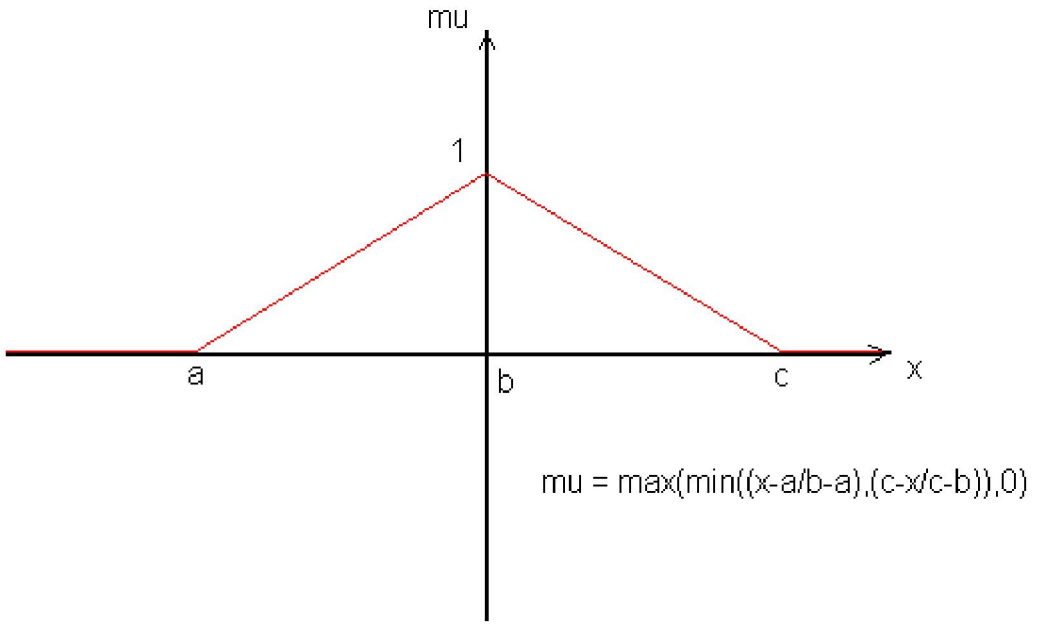

Appendix C

Centroid of an Interval Type-2 Set

Observe, from (C.01), that the centroid of an interval type-2 set $\tilde{A}$, whose domain is discretized into N points, is given as:

$$C_{\tilde{A}} = \int_{\theta_1} \cdots\cdots \int_{\theta_N} 1 \Big/ \frac{\sum_{1}^{N} x_l \theta_l}{\sum_{l=1}^{N} \theta_l} \qquad \text{C.01}$$

Where θ_l belongs to some interval in [0, 1]. Equation (C.01) has the same form as (3.36) except for the fact that x_l in (C.01) are crisp numbers unlike w^i in (3.36), therefore. The same computational procedure described above can be used to compute $C_{\tilde{A}}$ with the x_l and θ_l in (C.01) corresponding to w^i and f^i in (3.36), respectively. Note that in this case, x_l are crisp If N is very large, in Step (4), we can check if $|y'' - y'| \prec \varepsilon$ instead of $y'' = y'$ for some predecided ε.

Bibliography

1. Armstrong B., Khatib O., Burdick J., "*The explicit dynamic model and inertial parameters of the PUMA 560 Arm*", Proc. IEEE Int. Conf on Robotics and Automation, San Francisco, USA, April 1986, p. 510-518.

2. Coelho, L. S., Almeida, O. M. and Coelho, A. R.: "*Design and tuning of intelligent and self-tuning PID controllers*". Available Online: http://www.las.pucpr.br/leandro/artigos_publicados/ paper24_wsc2000.pdf
3. Craig, J.-J.: *Introduction to Robotics – Mechanics and Control,* 2nd edn, Addison-Wesley, Reading, MA, 1982.
4. Etienne Dombre, Wisama Khalil. "*Modeling, identification and control of robots"*, Kogan Page Science, 2004
5. Hu, B.-G., Mann, G. K.-I. and Gosine, R. G.: *A systematic study of fuzzy PID controllers Function-based evaluation approach*, *IEEE Trans. Fuzzy Systems* (2001), 699–7 12.
6. Mark W. Spong, Seth Hutchinson, and M. Vidyasagar: *Robot modeling and control*
7. Mamdani, E. H.: *Application of fuzzy algorithms for control of simple dynamic plant*, in: *Proc. Inst. Elect. Eng. Contr. Sci.*, Vol. 121, 1974, pp. 1585–1588.
8. Roland S. Burns, *ADVANCED CONTROL ENGINEERING*, Butterworth-Heinemann, 2001.
9. L. X. Wang, *Adaptive Fuzzy System and Control: Design and Stability Analysis*, PTR Prentice-Hall, Englewood Cliffs, NJ. 1994.
10. L. X. Wang, *A course in Fuzzy System and Control,* Prentice-Hall, Upper Saddle River, NJ 1997.
11. D. Driankov, H. Hellendoorn and M. Reinfrank, *An Introduction to Fuzzy Control (2nd Ed.),* Springer-Verlag, 1996.
12. Jerry M. Mendel, *Uncertain Rule-Based Fuzzy Logic Systems: Introduction and New Directions.* Prentice Hall, 2001.
13. J. M. Mendel, "*Uncertainty, fuzzy logic, and signal processing,*" Signal Proc., vol. 80, pp.913933, 2000.
14. L. Zadeh, "*Fuzzy logic, Neural networks and soft computing,*" Communications of the

ACM, vol. 37, no. 3, pp. 77-84, 1994.

15. H. J. Zimmermann, "*Fuzzy set theory and its applications*," Kluwer, Boston, 2nd ed., 1993.
16. L. A. Zadeh, "*Fuzzy sets*," Information and Control, vol. 8, pp. 338-353, 1965.
17. Boulahia Abdelmalek, *Commande floue et neuro-floue appliquees a un robot manipulateur*, Mémoire de magister en génie électrique, l'Ecole Militaire Polytechnique, 2000.
18. G. J. Klir and B. Yuan, "*Fuzzy sets, Fuzzy Logic, and Fuzzy Systems: Selected papers by Lotfi A. Zadeh*," Advances in Fuzzy Systems, Applications and theory, vol. 6, 1996.
19. M. Jamshidi, N. Vadiee, and T. J. Ress, "*Fuzzy logic and control*," Upper Saddle River, NJ: Prentice-Hall, 1993.
20. J. M. Mendel, "*Fuzzy logic systems for engineering : A tutorial*," IEEE proceedings, vol. 83, no. 3, pp. 345-377, 1995.
21. L. A. Zadeh, "*The concept of a linguistic variable and its application to approximate reasoning – I*," *Inform. Sci*., vol. 8, pp. 199-249, 1975.
22. N. N. Karnik and J. M. Mendel, "*An introduction to type-2 fuzzy logic Systems*," Univ. Southen California, Rep., Oct. 1998, http://sipi.usc.edu/~mendel/report.
23. J. M. Mendel, *Uncertain Rule-Based Fuzzy Logic Systems: Introduction and New Directions*, Prentice Hall, Upper Saddle River, NJ, 2001.
24. G. J. Klir and B. Yuan, "*Fuzzy sets, Fuzzy Logic, and Fuzzy Systems: Selected papers by Lotfi A. Zadeh*," Advances in Fuzzy Systems, Applications and theory, vol. 6, 1996.
25. N. N. Karnik, J. M. Mendel and and Q. Liang, "*Type-2 fuzzy logic systems*," IEEE Trans. Fuzzy Syst., vol. 7, no. 6, pp. 643-658, Dec. 1999.
26. Q. Liang, and J. M. Mendel, "*Interval type-2 fuzzy logic systems: Theory and design*," IEEE Trans. Fuzzy Syst., vol. 8, no. 5, pp. 535-550, Oct. 2000.
27. Jerry M. Mendel and Robert I. John, "*A Fundamental Decomposition of Type-2 Fuzzy Sets*," Univ. Southen California, Univ.De Montfort UK, 2001.
28. BARKATI Said, " *Modélisation et commande d'un onduleur à sept niveaux à diodes flottantes : Application à la conduite d'une machine asynchrone*", PhD Dissertation in "Ecole National Polytechnique-ALGERIE",2008.
29. Jerry M. Mendel, "*Type-2 fuzzy sets: Some questions and answers*," IEEE Connections, Newsletter of the IEEE Neural Networks Society, Vol. 1, August 2003, pp. 10-13.
30. Nilesh Naval Karnik, *Type-2 fuzzy logic systems*, PhD Dissertation in University of Southern California,1998.
31. Qilian Liang, *Fading channel equalisation and video traffic classification using nonlinear signal pressing techniques*, PhD Dissertation in University of Southern California, 2000.

32. Jerry M. Mendel, "*Fuzzy logic systems for engineering: A tutorial*," IEEE transactions on Fuzzy Systems,Vol. 2, No. 1, 1995, pp.345-377.
33. N. N. Karnik and J. M. Mendel, "*Type-2 Fuzzy Logic Systems: Type-Reduction*", presented at the *1998 IEEE SMC Conference,* San Diego, CA, October.
34. Jerry M. Mendel, "*Advances in type-2 fuzzy sets and systems*," Information Sciences, Vol. 177, 2007, pp. 84–110.
35. Jerry M. Mendel and Hongwei Wu, "*New results about the centroid of an interval type-2 fuzzy set, including the centroid of a fuzzy granule*," Information Sciences, Vol. 177, 2007, pp. 360–377.
36. Roberto Sepuilveda and Oscar Castillo and Patricia Melin and Antonio Rodriguez-Diaz and Oscar Montiel, "*Integrated Development Platform for Intelligent Control based on Type-2 Fuzzy Logic*," presented at the *2005 IEEE*.
37. N. N. Karnik and J. M. Mendel, "*Introduction to Type-2 Fuzzy Logic Systems*", presented at the *1998 IEEE FUZZ Conference,* Anchorage, AK, May.
38. G. C. Mouzouris and J. M. Mendel, "*Nonsingleton fuzzy logic systems: theory and application*," *IEEE Trans. Fuzzy Systems, vol. 5,* no. 1, pp. 56-71, Feb 1997.
39. G. M. Khoury and M.Saad and H.Y.Kanaan," Fuzzy PID Control of a Five DOF Robot Arm" *Journal of Intelligent and Robotic Systems* vol. 40, pp. 299-320, 2004.